

# Effects of External Stimulators on Engineered Skeletal Muscle Tissue Maturation

Claudia Mueller, Mairon Trujillo-Miranda, Michael Maier, Daniel E. Heath, Andrea J. O'Connor, and Sahar Salehi\*

Engineering functional skeletal muscle tissue is an ongoing challenge because of the complexity of the *in vivo* microenvironment and the various factors that contribute to the development and maintenance of the native tissue. However, the growing understanding of the natural skeletal muscle's microenvironment *in vivo*, as well as the ability to successfully reproduce these factors *in vitro*, are contributing to the formation of engineered skeletal muscle tissues (SMTs) with greater biomimetic structure and function. This review first summarizes the structure of skeletal muscle tissue. The role of various hydrogels, biomaterials, and scaffolds as building blocks of complex skeletal muscle structures is then explored. Additionally, the role of external stimuli and regulators that can be applied during *in vitro* culture that lead to the formation of SMT models with higher functionality is examined. These include various physical, biochemical, electrical, mechanical, and magnetic stimulations, as well as biological stimulation through coculture with fibroblasts, endothelial, or neuronal cells. Finally, examples of recently developed functional tissue models that have been developed for *in vitro* and *in vivo* applications and the future outlook for this field are discussed.

This has led to the identification of various factors that are biochemically relevant to the skeletal muscle microenvironment which guide specific cellular behaviors such as targeted cell growth, differentiation, and maturation.<sup>[4]</sup> A wide variety of parameters have been used to effectively guide cell behavior and tissue formation, such as the types of cells that are used, properties of the biomaterials, topography of the cell culture substrate, and methods of stimulations. Furthermore, the combination of the aforementioned parameters can cooperatively lead to the formation of sophisticated skeletal muscle models. This review will first summarize the tissue structure of skeletal muscle, describe the natural maturation process of the tissue, and elucidate the importance of engineering SMT *in vitro*. Next, the technologies used to achieve the tissue engineering of skeletal muscle—from one to four-dimensions—will be reviewed, and the

## 1. Introduction

Skeletal muscle tissue engineering is a field of research focusing on the development of engineered skeletal muscle tissues (SMTs) *in vitro*.<sup>[1]</sup> The field of skeletal muscle tissue engineering has advanced in recent years by moving away from the use of standard 2D culture plates and steadily incorporating new parameters to recapitulate the native tissue's microenvironment.<sup>[2,3]</sup>

level of the maturation and functionality of the engineered SMTs will be compared. Finally, we will discuss the effects of various external stimuli and regulators that are prominent in contemporary SMT engineering, and describe how they influence a tissue model's formation, maturation, and functionality.

## 2. Skeletal Muscle Tissue


Skeletal muscle tissue is a prime example of why anatomy and physiology are traditionally taught in tandem; the form of the SMT is absolutely crucial for the appropriate function of the organ itself. Any damage to this structure will have immediate and detrimental effects on the function of the muscular system. In order to understand how to engineer functional SMT, it is important to understand how the muscle is formed and regulated in the body naturally, including how the body's natural attempts at healing damaged or diseased muscles often fall short in restoring functional muscle tissue.

### 2.1. Structure of Skeletal Muscle Tissue

Skeletal muscle tissue has a highly ordered, hierarchical structure. The highest order of this structure is the muscle itself,

C. Mueller, M. Trujillo-Miranda, Dr. S. Salehi  
Department of Biomaterials  
University of Bayreuth  
Prof.-Rüdiger-Bormann-Str.1, Bayreuth 95447, Germany  
E-mail: sahar.salehi@bm.uni-bayreuth.de

M. Maier, Dr. D. E. Heath, Prof. A. J. O'Connor  
University of Melbourne  
Department of Biomedical Engineering  
Melbourne 3010, Australia

 The ORCID identification number(s) for the author(s) of this article can be found under <https://doi.org/10.1002/admi.202001167>.

© 2020 The Authors. Advanced Materials Interfaces published by Wiley-VCH GmbH. This is an open access article under the terms of the Creative Commons Attribution License, which permits use, distribution and reproduction in any medium, provided the original work is properly cited.

DOI: 10.1002/admi.202001167

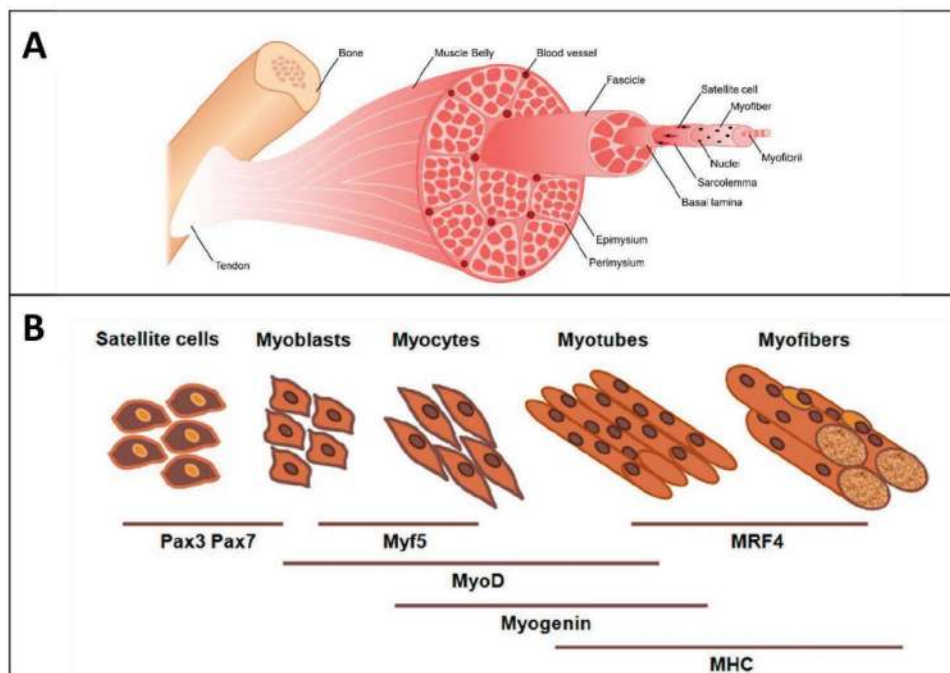


**Figure 1.** The structure and development of skeletal muscle tissue. A) The hierarchical structure of skeletal muscle, wherein fibers are bundled together in increasingly larger fascicles, provide the isotropic form necessary for the specific functions of skeletal muscle. Adapted under the terms of a Creative Commons Attribution 4.0 International License.<sup>[6]</sup> Copyright 2020, MDPI. B) The specialization of myoblasts from satellite cells are characterized by the appearance of paired box 5 (Pax5) and paired box 7 (Pax7). The differentiation of those cells from myoblasts into myotubes are characterized by Myf5, MyoD, and Myogenin. Finally, matured myofibers are characterized as fully functional upon the expression of MHC and Mrf4. Adapted under the terms of a Creative Commons Attribution 4.0 International License.<sup>[7]</sup> Copyright 2018, MDPI.

which consists of a bundle of fascicles combined together under the epimysium, a sheath of connective tissue. Each one of these fascicles are themselves a bundle of muscle fibers, also known as myofibers. A single myofiber is a long, multinucleated muscle cell; it is the muscle cell structure that imbues the skeletal muscle tissues with their ability to contract along a single uniaxial direction. The bundle structure of the organ allows the myofibers to be aligned parallelly in a single direction, thereby maximizing the strength of their contraction (Figure 1A).<sup>[5]</sup>

Importantly, the differentiated adult myofibers are incapable of undergoing mitosis.<sup>[5]</sup> Any fibers that are lost due to damage or disease must be replaced via a precursor cell, known as a myoblast.<sup>[8,9]</sup> Each myofiber has a supportive scaffolding structure around it called the basal lamina. Inside the basal lamina resides a population of progenitor cells, or satellite cells, that maintain the myoblast population through proliferation and subsequent differentiation. Satellite cells are a major component of the body's muscular maintenance system, and are frequently activated to replace any lost myofibers. Myoblasts are mononucleated cells that, under the appropriate external stimuli, will undergo differentiation by fusing with other myoblasts until they form a single, multinucleated myofiber (Figure 1B). During repair, the satellite cell-derived myoblasts typically differentiate by fusing to existent secondary fibers, thereby increasing their size and regaining lost functionality of the tissue.<sup>[8,10]</sup> Through this process, the body can maintain and regulate the size and shape of the skeletal muscles over time.

The functional capabilities of the myofibers are derived from internal structures comprised of specific populations of

specialized proteins.<sup>[11]</sup> These proteins form long parallel fibrils inside the muscle cells, with repeating functional units termed sarcomeres that are arranged along the length of these bands. Each sarcomere starts and ends with a band of proteins known as the Z-disc. In between each Z-disc, thin filaments made up of actin are arranged forming a type of backbone around a core of thick filaments comprised of the protein myosin. As myosin and actin bind together, the thin filaments are dragged across the thick filaments, and the sarcomere itself contracts. With these smallest of actions, these proteins provide the basis for the skeletal muscle's critical functions.<sup>[5,8,11]</sup>

Myofibers utilize mechanotransduction pathways to regulate their functional characteristics. Muscle cells are capable of detecting mechanical signals from their environment through the use of transmembrane proteins known as integrins. Integrins form the attachment points between the intracellular cytoskeleton and the extracellular matrix (ECM). Mechanotransduction is the process by which mechanical signals such as matrix stiffness or shear stress are translated into chemical responses by cells. Integrins can be recruited together to form complex transmembrane bundles known as focal adhesions.<sup>[12]</sup> These complexes are crucial for the amplification and downstream signaling of external mechanical stimuli.<sup>[13]</sup> They have a direct impact on the remodeling of the actin cytoskeleton, which affects the mechanical properties and behaviors of the myofibers themselves. In recent years, scientists have mapped out the mechanotransduction pathways with a certain degree of success.<sup>[13,14]</sup> These pathways, and similar pathways derived

from other forms of stimulation such as electrical or chemical, result in the increased expression and activation of several proteins that have been noted for their specific importance in the regulation of the formation of functional muscle tissue, as well as for their role in the conversion of MHC from one isoform to another.<sup>[14a]</sup> In this review the effect of the other stimulations will be discussed in detail.

## 2.2. Development of Muscular Phenotypes

Skeletal muscles are similar in structure but can vary widely in both size and strength. Their sizes and strengths are important phenotypic characteristics, but what anatomical explanation is there for their variety in a single individual? The answer is found among the proteins of the sarcomere, which dictate its functional characteristics. One of the most important proteins for defining the structural and functional phenotype of the myofiber is myosin. Structurally, myosin has two globular head units with tails that curl around each other in an  $\alpha$ -helical structure.<sup>[15]</sup> A single head unit with its single tail is known as myosin heavy chain (MHC). There are a variety of isoforms or versions of MHC that correspond to several different myofibril phenotypes, which appear at different stages of muscle growth and development.<sup>[15]</sup> For example, MHC-emb and MHC-neo appear during the embryonic and neonatal stages of life, respectively, while m-MHC is found only in the mandibular regions of the body and cardiac- $\alpha$  MHC is found primarily in cardiac muscle cells.<sup>[16]</sup> In skeletal muscle cells, the MHC isoforms can be characterized by their unique ATPase activity, which in turn affects other downstream phenotypic attributes such as contraction velocity and resistance to fatigue.<sup>[14a]</sup> Each isoform is vital in determining the metabolic activity of the myofibril, which likewise affects the contractile behavior of the muscle cell itself.<sup>[15–17]</sup>

In the process of muscle formation, the existence of MHC isoforms is very important. Certain isoforms appear only in specific phases of one's life. MHC-emb is the MHC protein primarily found only during the embryonic phase of muscle formation.<sup>[18]</sup> This is the phase in which the embryonic myoblasts differentiate to form primary myofibers by fusing together. These myofibers are smaller in size than adult myofibers, as they are made up of a lower number of myoblasts in the early stages of muscle formation. It has been suggested that the reason that primary myofibers exist is to form the muscle pattern for the body to build upon.<sup>[8]</sup> After the muscle pattern has been laid down, fetal/neonatal myogenesis occurs. Neonatal myoblasts undergo differentiation by fusing to the primary myofibers directly, creating secondary myofibers.<sup>[8,16]</sup> Secondary myofibers follow the same shape and muscle pattern as the primary myofibers, but with noticeably larger fiber diameters and higher contractile force capabilities derived from the higher number of nuclei. In the first month of development, these myofibers express primarily MHC-neo, with a relatively smaller population of MHC-emb.<sup>[16]</sup> However, the myofibers quickly grow in mass and in functional strength, and the MHC isoforms likewise change to those associated with the adult myofibers.<sup>[8,14a,16]</sup>

Adult myofibers contain sarcomeres with varying proportions of the different MHC isoforms, dependent on the location

of the muscle and the various external stimuli it is subjected to. The most common MHC isoforms in adult skeletal muscle are slow type I, fast type IIa, fast type IIb, and fast type IIx.<sup>[16]</sup> Each MHC isoform functions slightly differently; muscles with predominantly slow type I isoforms are classified as “slow-twitch” fibers and are typically resistant to fatigue.<sup>[15]</sup> Muscles that primarily contain type IIx and type IIb isoforms are classified as “fast-twitch” fibers, due to their fast contraction speeds and their glycolytic metabolic pathways.<sup>[15]</sup> These phenotypic differences at the protein level create functionally and structurally different adult myofibers, thereby affecting the phenotype of the tissue itself. Researchers have thus begun measuring the MHC composition of the sarcomeres as a method of determining the phenotype of the myofiber, which can be applicable both for tissue explanted from a patient and tissue grown in vitro.<sup>[8]</sup>

## 2.3. Markers of Myogenic Differentiation

There are a few myogenic regulatory factors (MRFs) that are crucial for the appropriate proliferation and differentiation of myoblasts into myofibers. The four key MRFs are known as Myf5, MyoD, Mrf4, and Myogenin.<sup>[8]</sup> They are proteins primarily involved in transcriptional regulation of myogenesis.<sup>[17]</sup> By analyzing the presence of these proteins in groups of myoblasts or myofibers in vivo or in vitro, researchers are able to determine whether the cells are expressing the MRFs associated with mature, functional myofibers.<sup>[8]</sup> For example, Myf5 and MyoD are expressed by un-differentiated myoblasts prior to fusion, whereas Myogenin is significantly up-regulated in functional myofibers.<sup>[8]</sup> MyoD and Myf5 are not expressed after differentiation, as they are partially required for cell cycle regulation, which is unnecessary for the post-mitotic myofibers. Myogenin and Mrf4 are indicative of the successful fusion of myoblasts into myotubes and the formation of myofibrils respectively, with further myofiber maturation confirmed via the presence of MHC.<sup>[19]</sup>

The complexity of the natural regulatory pathways for skeletal muscle tissue cannot be overstated; there is a wide range of environmental cues that up-regulate and down-regulate specific genes in order to create an organic muscular “tapestry”, which is woven together with fibers comprised of various proportions of MHC proteins. The summation of all of the various isoforms results in a final, hybrid fiber with a net phenotype that is dependent on the relative proportions of those isoforms.<sup>[11]</sup> This structure is constantly changing as the body adapts to new loading regimes and electrical/hormonal changes, and as it tries to repair any fibers lost to damage or disease.

## 2.4. Diseased and Injured States

There are many different types of damage that muscle tissue can undergo during its lifetime, from temporary strains that decrease function over a short period of time to more intense tears that can permanently disable a muscle's ability to contract.<sup>[20]</sup> Due to the prevalence of sports and physical activities, as well as potential traumatic events in the average person's

lifetime, muscle injuries can be quite widespread.<sup>[21]</sup> For the majority of cases, a simple treatment consisting of rest and light rehabilitation can give the muscle tissue the environment it requires to naturally repair itself.<sup>[20b,21b]</sup> As with most types of tissue damage, complications can and do arise that require a more coordinated and direct method of intervention and treatment.<sup>[20b]</sup> Ramos et al.<sup>[20b]</sup> described three categories of specific damage to muscle tissues that would typically require surgery; i) severe muscle hematoma, ii) myositis ossificans, and iii) compartment syndrome. The first two categories can still be treated non-operatively in their mild phases, with surgery used only in the most severe of cases. The last category, compartment syndrome, will require surgery immediately upon diagnosis to save the tissues. Skeletal muscle tissue can self-renew up to a point, after which the damaged tissue is instead replaced by non-functional scar tissue.<sup>[20b]</sup> The loss of functional muscle fibers and their replacement with fibrotic scar tissue is a key characteristic of volumetric muscle loss (VML).<sup>[22]</sup> If a muscle suffers from more than a 20% loss in muscle volume, then it is seen as irreparable by traditional surgical methods.<sup>[20b]</sup> Current therapies, aimed at breaking the 20% VML replacement barrier, include complex autografts of existing muscle flaps and similar transplants, which are not optimal considering their induced donor site morbidity as well as their functional limitations.<sup>[22]</sup>

The ageing process also has a tremendous effect on the development and maintenance of SMT. Natural muscle atrophy, also known as sarcopenia, occurs past 50 years of age in most humans and is associated with a decrease in the total number of muscle fibers as well as a decrease in the fiber diameters. These morphological changes contribute to a lower total strength of the muscle.<sup>[23]</sup> With a growing elderly population in many developed countries, and the crucial role of muscle strength in mobility and quality of life, muscle repair becomes an increasingly pressing issue to tackle.

Unfortunately, sarcopenia can be exacerbated by various diseases. Cancer patients, for example, can experience an advanced form of muscle atrophy known as cachexia. The total volume loss of the affected muscles ranges from 20% to 70% on average, depending on the type and stage of the cancer.<sup>[24]</sup> Some of the many side-effects of the treatment of cancer, such as the decrease of food intake and physical activity as well as the increasing resting energy expenditure (REE) of skeletal muscle, lead to this environment of rapid muscle degeneration.

Altogether, cachexia accounts for 20–30% of all cancer-related deaths and is currently treated through physical therapy, while better treatments and interventions are being pursued via limited drug trials.<sup>[23a,24–25]</sup> Duchenne's Muscular Dystrophy (DMD) is a similarly debilitating disease in which the skeletal muscle cells lack the key dystrophin gene, leading to a constant cycle of muscular degeneration and regeneration that causes acute muscular atrophy.<sup>[26]</sup> For all the advancements in cell therapies, the resources available to clinicians are still insufficient to reverse many of the symptoms presented in cancer cachexia and DMD.<sup>[9]</sup> The tissue engineering of skeletal muscle is attractive due to its potential for the production of biologically relevant myofibers *in vitro*. However, the tissue engineering of skeletal muscle and the development of more mature and functional tissues *in vitro* remains a distinct challenge for researchers today. Tissue engineers are working to learn more

about the natural and diseased regulatory pathways in order to better design intervention strategies for the promotion of healthy, functional SMT. In the next section, we review the current state of SMT engineering from a new perspective and based on the various culture strategies used in bottom-up and top-down tissue engineering approaches (Figure 2).

### 3. Tissue Engineering Skeletal Muscle Tissue

Various tissue-engineering strategies have been introduced to engineer skeletal muscles with similar structure and functionality as a native tissue. In tissue engineering, mimicking the ECM is one of the major challenges currently addressed by various approaches. In the traditional, “top-down” approach introduced in 1959 by Feynman,<sup>[28]</sup> tools are used which can sculpt an object in different scales, such as photolithography. Later, Drexler<sup>[29]</sup> introduced the nano-manufacturing approach called the “bottom-up” approach, which focuses on fabrication of tissue structures from building blocks in microscale.<sup>[30]</sup> Most of the examples seen in regenerative medicine that deal with the production of a scaffold in a mold are examples of a top-down strategy; here, scaffolds are used to promote the pre-alignment of the muscle cells, while also promoting the anisotropic orientation of the differentiated myofibers after the fusion of the muscle cells.<sup>[31]</sup> While it is possible to inject muscle cells at the site of the injury or to transplant a blank scaffold, transplanting a cell-laden scaffold is a more promising strategy.<sup>[2,31a]</sup> The treatment of skeletal muscle tissues using intramuscular injection of cells results in poor therapeutic outcomes. The main limitations can be attributed to immune reactions, low cell integration into the host tissue, as well as patient discomfort and risk of infection. To avoid these issues, soft carriers can be used to locally deliver cells, or cell-encapsulated scaffolds can be used as an alternative to increase the efficiency of cell delivery at the injury site.<sup>[32]</sup> Preferably, scaffolds will mimic the native ECM with appropriate biophysical and biochemical cues<sup>[33]</sup>. In the bottom-up approach, the formation of the construct relies on the self-assembly or directed-assembly of a scaffold from small modules and components, with microscale precision; this allows the construct to be designed to carry out distinct tasks. In this case, it is possible to fabricate complex structures mimicking the target tissue structure. Various techniques have been employed to produce these microscale building units without biomaterials or cells, such as the development of cell sheets,<sup>[34]</sup> self-assembly of cells and cell aggregates,<sup>[35]</sup> microgels,<sup>[36]</sup> microfabrication of cell encapsulated hydrogels<sup>[30b]</sup> and 3D bioprinting.<sup>[30c,37]</sup> As with any other engineering process, it is easiest to describe the ideas behind 3D scaffolds by first comparing and contrasting how each dimension plays a part in the structure of native skeletal muscle.

#### 3.1. 1D and 2D Engineered Muscle Tissue

The unidirectional organization of the muscle fibers, an essential characteristic of the muscle tissue structure, has always been the first focus in imitating the functionality of that structure. Therefore, treating individual short and long fibers as

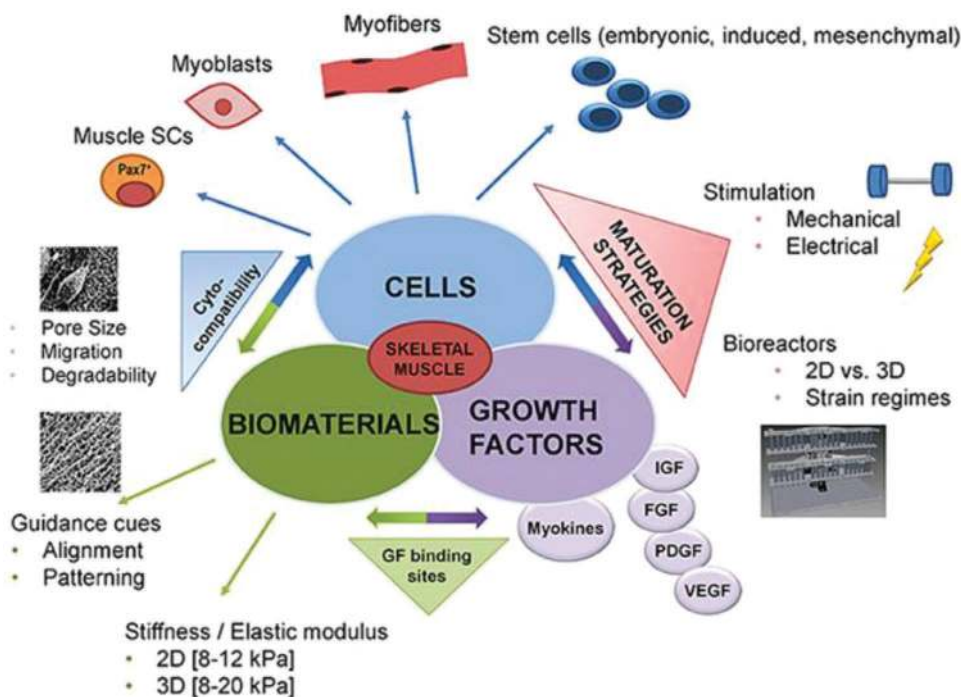


**Figure 2.** Advances in SMT engineering—from traditional to functional approaches. Traditional tissue engineering approach is the combination of the components such as biomaterials, cells, and growth factors. However, these three main components need to be combined with regulators or external stimuli allowing for more biomimetic characteristic in engineered SMT. Adapted with permission.<sup>[27]</sup> Copyright 2018, Frontiers.

1D systems was effective in initiating the necessary alignment, due to the effect of the topography induced onto the cells by the axis of the fibers. Using short fragments in the form of injectable ribbons we showed that cell-laden, 1D ribbons can effectively support the attachment of mouse muscle cells and their subsequent differentiation, guiding the formation of long myotubes with length about 400  $\mu\text{m}$ . They were fabricated using poly(lactic-co-glycolic acid) (PLGA) as short length ribbons with ultrathin thickness.<sup>[38]</sup> In contrast with the direct injection of cells, ultrathin ribbons could mechanically support the C2C12 cells precultured on their surface. To evaluate the effect of the nozzle size on the injectability of ribbons and the viability of the pre-loaded cells, various needle gauges were used. The cell viability was evaluated by aspirating and injecting the cells through the various needles. We showed that the viability and functionality of the cells adhered on the ribbons after injection was preserved (Figure 3).<sup>[38]</sup>

Using microfluidic techniques, we also microfabricated fibers with a microgrooved surface to generate an aligned muscle micro-tissue on 1D fibers.<sup>[39]</sup> The microfluidic spinning approach was used to fabricate gelatin methacryloyl (GelMA)-based fibers with well-defined micropatterns which could be combined in a study of topographical cues and biochemical stimulation using recombinant agrin. Microstructured fibers, in comparison with flat and smooth fibers, showed enhanced alignment of C2C12 cells and myotube formation after differentiation. The myogenic behavior of the cells on these fibers was assessed based on myotube length, aspect ratio, and mRNA expression of myogenic genes, where micropatterned fibers showed enhanced formation of differentiated myotubes. Furthermore, we studied the effect of agrin treatment during

the differentiation process and found it significantly enhanced the expression of acetylcholine receptor (AChR) and dystrophin. More AChR clusters and myotubes were formed, which indicated that the synergistic effect of topographical cues and agrin treatment could enhance the functionality of the created muscle tissue. Moreover, the differentiated myotubes showed synchronized contractility under electrical stimulation in high numbers (Figure 4).<sup>[39]</sup>

Mirani et al.<sup>[40]</sup> used a similar approach to demonstrate the fabrication and application of hydrogel-based fibers with micro-scale morphological features (grooved, solid, and hollow) for smart drug delivery, wearable or implantable medical devices, and soft robotics applications. The C2C12 myoblasts cultured on the grooved fibers showed improved alignment as well as enhanced and controlled myogenic differentiation. The morphology of the cells varied depending on the groove size of fibers (Figure 5A), as well as the specific material composition (Figure 5B); cells on smooth fibers showed random orientation, while on the grooved fibers they demonstrated an increase in directional alignment toward the direction of the grooves, possibly due to decreased groove sizes (Figure 5A).<sup>[40]</sup>

Fallahi et al.<sup>[41]</sup> also fabricated multi-component composite fibers, made of a polymer core and coated with a GelMA/alginate hydrogel. Fibers were later assembled through textile processes in various 2D and 3D structures to tailor tissue-level properties and guide the direction of cellular growth within the 3D microenvironment. The core fibers were made of polydisoxanone (PDMS), polyglycolic acid, collagen, and cotton, and were coated by a cell-encapsulated layer of GelMA/alginate hydrogel blend. Furthermore, as conductive materials such as graphene or carbon nanotubes can affect the function and maturation

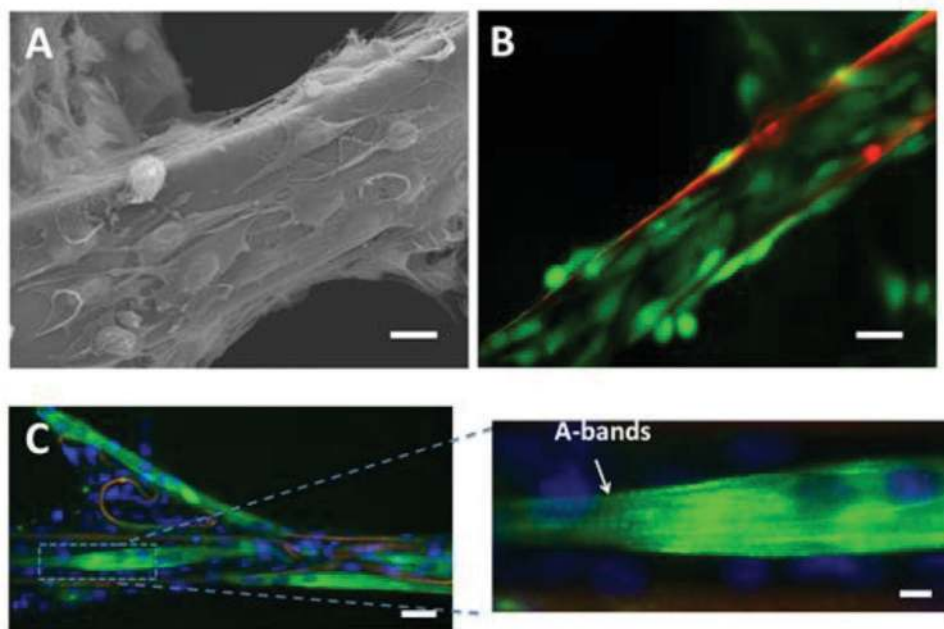


**Figure 3.** A) Field emission-scanning electron microscopy image of C2C12 cells adhered on a ribbon after 2 days of culture (scale bar: 10  $\mu\text{m}$ ). B) Cell viability of skeletal muscle cells cultured on PLGA ribbons after 2 days of culture using live/dead staining (scale bar: 20  $\mu\text{m}$ ). C) Myotube formation on freestanding ribbons (scale bar: 50  $\mu\text{m}$ ) and exhibiting sharp A-bands (enlargement (scale bar: 5  $\mu\text{m}$ )). Adapted with permission.<sup>[38]</sup> Copyright 2017, American Chemical Society.

of electro-physiologically responsive tissues such as cardiac, skeletal muscles and neural tissues, they fabricated electrically conductive fibers using reduced graphene oxide (rGO). C2C12 mouse myoblasts cells encapsulated in both coated and non-coated fibers showed enhanced adhesion, proliferation, and maturation in the direction of the fibers. However, C2C12 cells encapsulated in rGO-coated fibers seemed to be more elongated and confluent than their non-coated counterparts.<sup>[41]</sup>

1D models, such as the previously-discussed single fibers, can only carry the cells on their surface. To imitate the 3D environment of the muscle tissue, and to grow an effective and mature tissue model, the 1D building blocks/1D models must be assembled using a bottom-up approach through a variety of processing techniques. For example, Yang et al.<sup>[56]</sup> reported on the fabrication of a poly( $\epsilon$ -caprolactone) (PCL)-based scaffold using 3D printing. In this case, uniaxially aligned surface topography provided a 2D culture surface platform, created by the stretching of a 3D-printed scaffold. The aligned myotubes produced on the stretched 3D printed PCL fibers were compared to those formed on unstretched PCL struts. Not surprisingly, the stretched PCL fibers showed greater myoblast alignment and more elongated morphology. After 7 and 14 days of culture, the myotube formation on all samples was determined using myosin staining. The level of mRNA expression of various muscle-specific genes was analyzed and demonstrated that Myf5, MyoD, Myogenin, and MHC were significantly increased in stretched-PCL compared to those in unstretched-PCL struts. The expression of Myf5 and MyoD before myogenic differentiation are relatively higher, as Myf5 is associated with myoblast positioning, and MyoD is responsible for muscle cell regeneration.<sup>[57,58]</sup> In contrast, Myogenin and MyHC are involved

in the differentiation of myoblasts into myotubes; therefore, their expression was significantly greater in cells grown on the stretched PCL.<sup>[56]</sup>

Liu et al.<sup>[44]</sup> demonstrated the application of collagen fibers for the culture of myoblasts as 2D collagen fiber networks. These cell-laden fibers were embedded into non-cell-adherent agarose hydrogels, which then displayed greater alignment and increased differentiation of the myoblasts.<sup>[44]</sup> The 2D collagenous network was made by layering the fibers on a collector, thereby forming organized meshes with controlled alignment. By varying the number of assembled layers, or by embedding the fibers in a hydrogel, the system could be upgraded to a 3D network to grow the skeletal muscle cells (**Figure 6A**). Over 3 days of culture, C2C12 cells adhered and grew along the fibers, forming fascicle-like structures (**Figure 6B**). Myotube-like structures were formed on fibers which were embedded in hydrogels containing collagen rather than pure agarose hydrogels (**Figure 6C**). Immunostaining confirmed the expression of key markers for differentiation such as myosin heavy chain, parvalbumin ( $\text{Ca}^{2+}$ -binding protein in fast-contracting skeletal muscle fibers), and the nitric oxide synthase isoform (NOS-1) in most of the aligned skeletal muscle cells growing on collagen fibers (**Figure 6C–F**).

Topographical cues can also be introduced into SMT engineering systems via surface patterning and applied coatings. Micropatterning has been used for the generation of simple or complicated motifs (e.g., grooves and ridges, pillars, and wells) and microstructures on various substrates with flat or curved features and can be applied by photolithography. It enables us to direct specific cell behaviors, such as the spatial arrangement and differentiation of muscle myoblasts.<sup>[31a,45]</sup> Denes et al.<sup>[46]</sup> applied this method to fabricate micropatterned

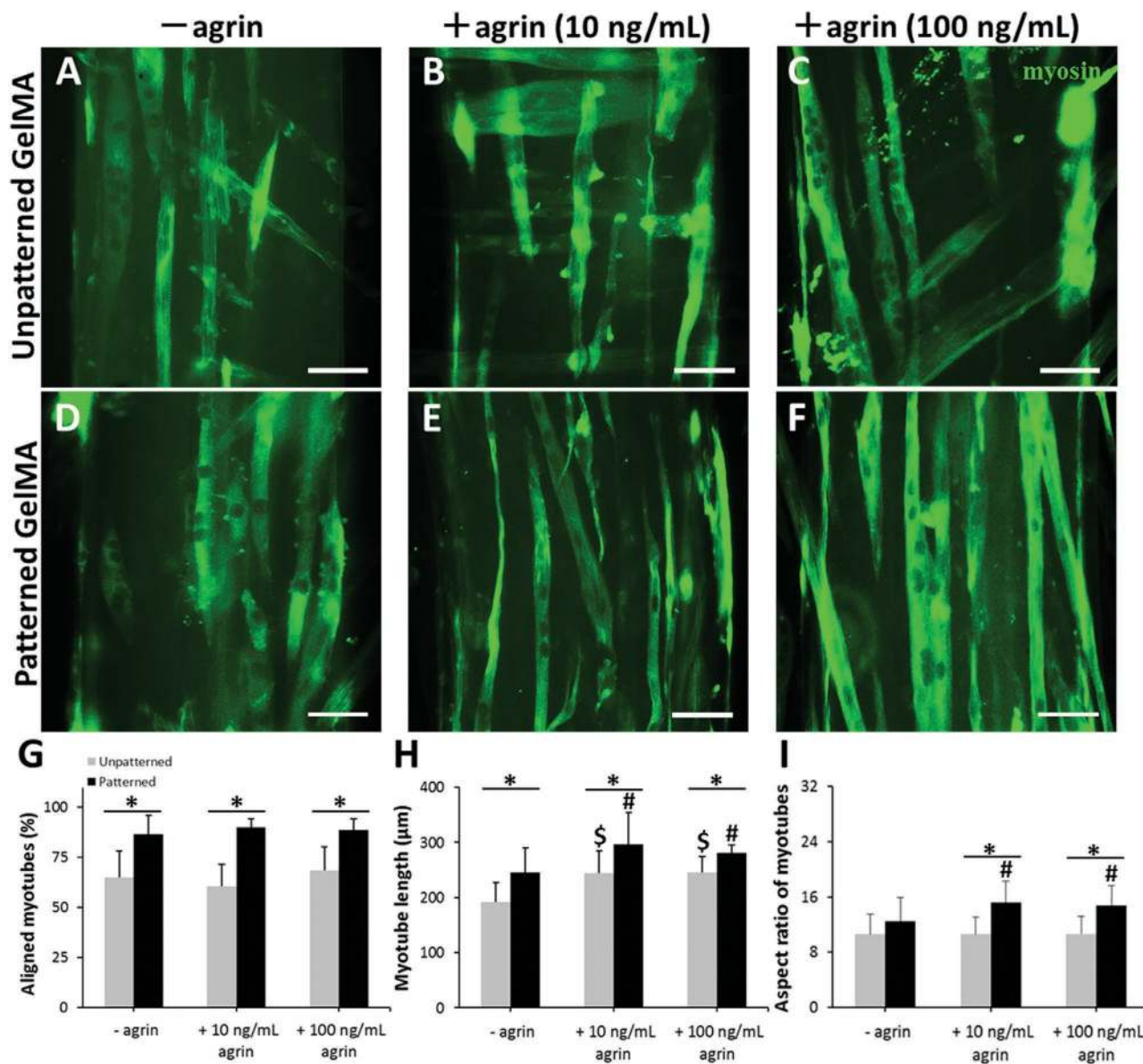


**Figure 4.** A–F) myotubes formed on micropatterned and smooth GelMA fibers treated with and without agrin showed various length and aspect ratios. Immunostaining was performed using mouse antimyosin (MY-32) antibody (scale bars: 50 μm). Quantification analysis of G) alignment, H) length, and the I) aspect ratio of myotubes after 7 days of differentiation. Reproduced with permission.<sup>[39]</sup> Copyright 2018, John Wiley and Sons.

and unpatterned gelatin hydrogels in order to study the alignment and differentiation of C2C12 myoblasts.<sup>[46]</sup> The formation of aligned sarcomeres and myofilament protein concentration on C2C12 myotubes, grown in 10 μm-wide microgrooves imprinted in a gelatin hydrogel, was characterized. Moreover, the sarcomeric structures formed by the aligned cells, in comparison to the cells grown on the unpatterned surface, showed an increase in contractile protein content. A higher expression of genes related to the development of contractile proteins and in vivo muscle maturation has been detected in those cells grown on patterned structures (Figure 7).<sup>[46]</sup>

Similar to the 1D case, the micropatterned films or cell sheets, as a 2D culture model, cannot represent the true 3D

structure of native muscle tissue; therefore, to create more flexibility and higher freedom for cells to grow in a 3D environment, the cell sheets can be stacked and assembled as a multilayered constructs. This approach was investigated by Fujie et al.<sup>[47]</sup> by creating nanoribbon-sheets using microfabrication and spin coating from PLGA and stacking them together, with gaps between the single strips. They showed two or more of these cell-laden structures could be placed on top of each other with anisotropic (orthogonal) and isotropic (parallel) orientations, better resembling the hierarchical structure of skeletal muscle tissue. They found that this method significantly facilitated the alignment of C2C12 cells into bilayer cell sheets, and improved the expression of muscle related genes such as

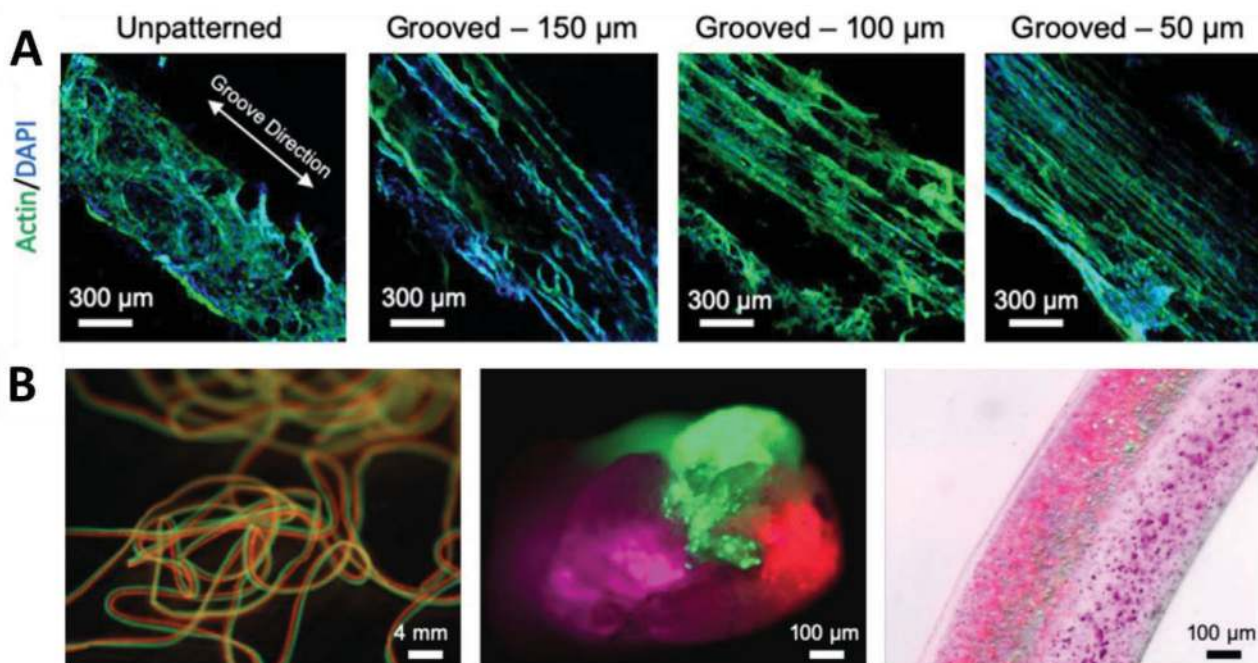


**Figure 5.** A) Alignment of the C2C12 myoblasts on smooth and microgrooved fibers with different groove sizes (50 to 150  $\mu\text{m}$ ). B) Multicomponent fibers fabricated from GelMA and Alginate are shown in length and cross section. As a core shell fibers, GelMA 10% was used as a core and Alginate 2% was used as a shell which could be removed after the crosslinking of GelMA. Adapted with permission.<sup>[40]</sup> Copyright 2020, American Chemical Society.

Myogenin, Mrf4, MHC IIa, MHC II d (x); this method also led to spontaneous contractions without stimulation.<sup>[47]</sup>

### 3.2. 3D Engineered Muscle Tissue

Most studies on skeletal muscle have used 2D surface structures, as mentioned above, patterned in the micro-/nanoscales with various sizes and shapes inducing the alignment of myoblasts, towards the formation of myotubes. However, due to the lack of 3D structure they cannot be successfully transferred to the clinic. Therefore, various 3D culture systems with greater similarity to the 3D environment of native skeletal muscles are introduced and evaluated, further increasing the complexity of the culture system. Herein, we will shortly review important recent work in order to introduce the potential of this substrate to develop mature, functional muscle micro-tissues. For instance, aligned fibrous scaffolds were extensively used in recent years to take the field into 3D space.<sup>[48]</sup> Aligned fibrous scaffolds, due to their anisotropic structure, are one of the potential substrates that are highly successful, due to their resemblance of the anisotropic ECM of skeletal muscle. They can also be fabricated using various efficient processing techniques, such as electrospinning.<sup>[49]</sup> Several studies have shown that aligned fibers significantly improved the orientation of muscle cells and their myogenic response, while also promoting the up-regulation of the genes typical for muscle tissue development.<sup>[48b,50]</sup>

Narayanan et al. showed the diameter of parallel electrospun PLGA fibers are also effective for the elongation of muscle cells. Aligned fibers, with fiber diameters ranging from  $335 \pm 154$  nm

to  $3013 \pm 531$  nm, were characterized for their interactions with myoblasts. During in vitro culture, larger fiber diameters showed enhanced alignment and further facilitated the differentiation of the cells, via the phosphorylation of the p38 MAPK chemical pathway. Furthermore, the expression of important MRFs, such as Myogenin and myosin heavy chain, were upregulated. In vivo studies also revealed that in dystrophin-deficient mdx mouse model, optimized fibrous scaffolds could support the formation of dystrophin-positive myofibers network in tibialis anterior muscles.<sup>[50]</sup>

After ensuring the positive effects of aligned electrospun fibers, consisting of PCL and decellularized-ECM (D-ECM), on the development of primary satellite cells in vitro, Patel et al. investigated the treatment of VML in murine models by implanting these fibers.<sup>[51]</sup> Their previous in vivo study using D-ECM fibers showed poor mechanical stability and quick degradation; therefore, in this study they produced the PCL/D-ECM blend, which effectively improved the anti-inflammatory activities and the myofiber formation in vivo. The myogenic protein expression of MyoD and myogenin, as well as the production of myokines, were all improved using the aligned blend of PCL/D-ECM fibers. However, there were no effects on the mass of myofibers grown in the VML injury model and force production apparent.<sup>[51–52]</sup>

Application of conductive fibrous scaffolds have also been used to improve the myogenic capabilities of muscle cells. We demonstrated that composite electrospun gelatin-polyaniline (PANI) nanofibers doped with camphorsulfonic acid (CSA) could effectively support the culture of C2C12 myoblasts.<sup>[53]</sup> We observed that myotube formation on composite gelatin-PANI nanofibers was improved when compared to non-conductive



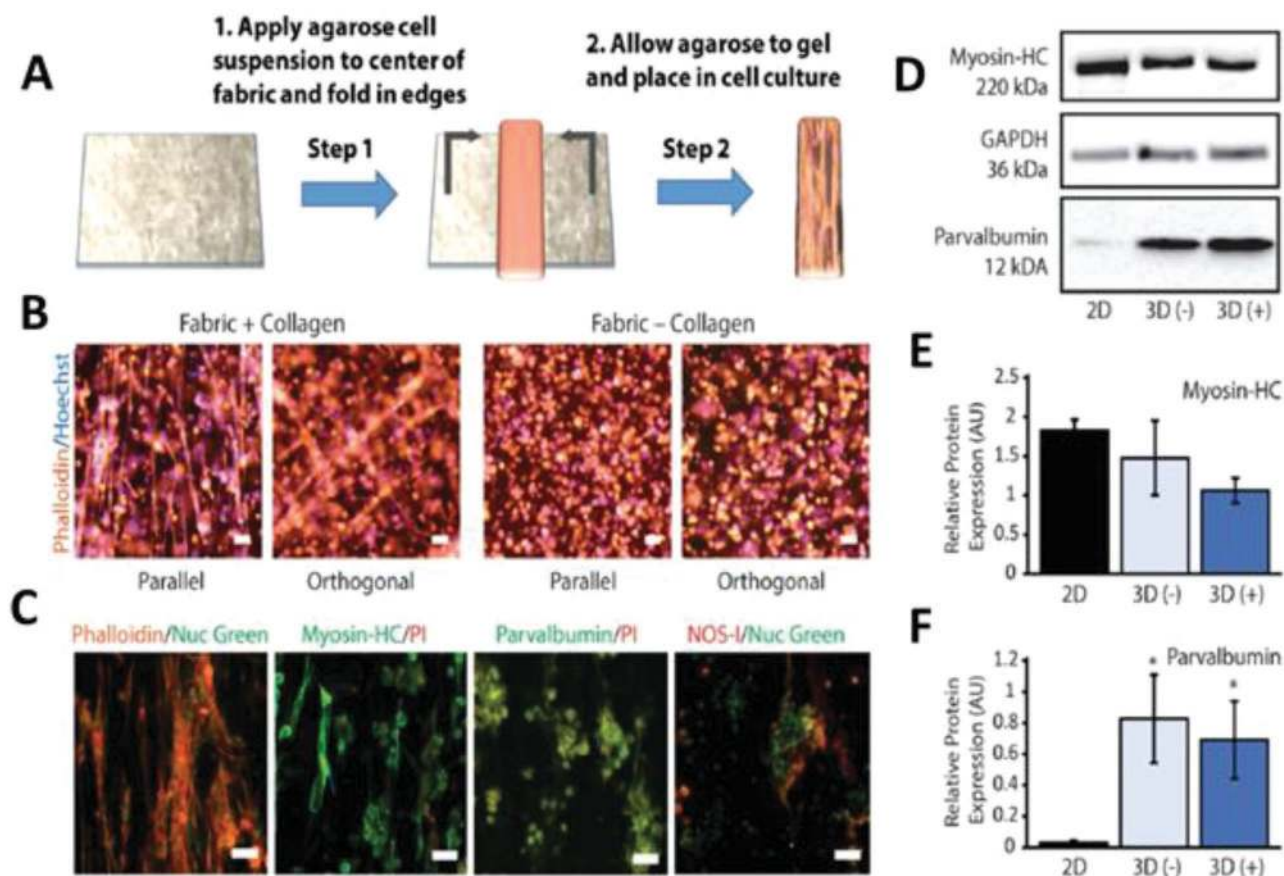


**Figure 6.** Incorporation of collagenous networks in 3D hydrogel scaffolds to support the cell alignment and myogenesis. A) Incorporation of dry fabrics in agarose. B) Epifluorescence images showing the distribution of actin filaments in constructs with and without fabrics to promote the alignment of encapsulated C2C12 cells. C) Confocal microscopy images showing details of aligned fascicle-like structures. C2C12 cells adhered to collagen networks within the hydrogels display differentiation markers such as myosin heavy chain, parvalbumin and NOS-I. All scale bars, 50  $\mu\text{m}$ . D) Western blots confirmed the expression of myosin heavy chain, parvalbumin for cells grown in 2D in comparison with cells grown in 3D with (3D (+)) and without (3D (-)) fabrics. Expression of myosin heavy chain E) and parvalbumin F) relative to GAPDH measured by quantitative polymerase chain reaction (qPCR). Adapted with permission.<sup>[44]</sup> Copyright 2017, Springer Nature.

gelatin nanofibers; these benefits were in addition to their ability to concomitantly promote myotube maturation. The maturation of myotubes was further studied by analyzing the intracellular organization and formation of sarcomeric actin units, as well as through characterization of the co-localization of the dihydropyridine receptor (DHPR) and ryanodine receptor (RyR), calcium transients, myotube contractibility and the expression of genes correlated to the excitation-contraction (E-C) coupling apparatus, which were all significantly enhanced. A fibrous system comprised of electrically conductive fibers with diameters in the range of 300 nm showed effective combination of topography and electrical conductivity promoting the maturation of muscle tissue (Figure 8).<sup>[53]</sup>

Graphene-containing fibers also showed similar improvements of myoblast differentiation, demonstrating the synergistic effect of the substrate's micro-/nanostructure and its electro-responsive properties. Interestingly, Patel et al.<sup>[54]</sup> induced the differentiation of muscle cells on graphene composite PCL fibers in the complete absence of differentiation media. The resulting graphene-PCL scaffolds presented improved mechanical and physical properties, which could be

tuned by varying the graphene concentrations. It supported the adhesion and proliferation of C2C12 mouse myoblasts as well as the differentiation of those cells in normal growth media, suggesting the cell-instructive potential of the scaffolds. Patel et al.<sup>[55]</sup> further showed the effect of growing carbon nanotube (CNT) carpets on carbon-based scaffolds, composed of interconnected microporous carbon foams and aligned carbon fiber mats, to study the multiscale hierarchy architecture with controlled physico-chemical properties. Controlled nano-roughness and wettability facilitated the myoblasts' ability to adhere, grow and differentiate on the surface of the CNT carpet. Microporous foam architecture, in this case, failed to promote their fusion into multinucleated myotubes, which can be due to the absence of the anisotropic orientation within the foam structure. Nevertheless, the aligned fibrous architecture was still able to stimulate the successful formation of multinucleated myotubes.<sup>[55]</sup>

It must be noted that while carbon-based nanomaterials, such as graphene, graphene oxide, reduced graphene oxide and carbon nanotubes, may enhance desired muscle cell functions in vitro, their safety requires careful assessment. A significant number of studies have been performed to study the short- and

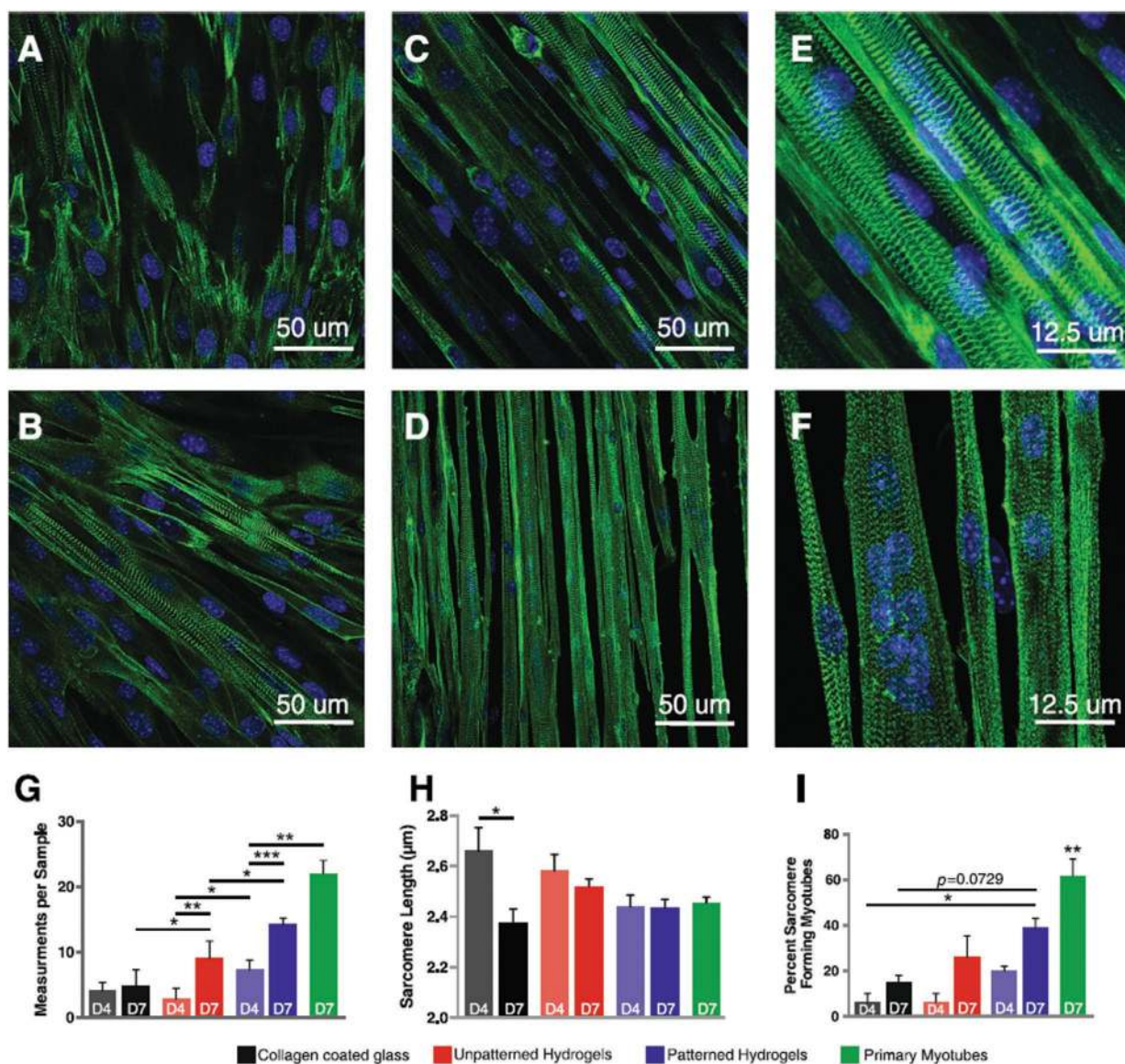


**Figure 7.** Immunofluorescence images showing sarcomere formation after post differentiation of the C2C12 cells cultured on A) Collagen coated glass B) Unpatterned gelatin hydrogels C–F) Patterned gelatin hydrogels. G) Greater formation of sarcomeres on patterned surface in comparison with others: H) Sarcomere length I) Percentage of sarcomere forming myotubes. Adapted with permission.<sup>[46]</sup> Copyright 2019, Springer Nature.

long-term in vivo cyto- and bio-compatibility, as well as carcinogenic potential of graphene-based nanomaterials synthesized with a variety of methods and starting materials.<sup>[56]</sup> Fadeel et al.<sup>[57]</sup> in an extensive recent review article summarized the safety assessment of these materials with respect to their potential effects on human health and the environment.

Hydrogels have had great success in similar tissue engineering applications due to their inherent tunable physical and chemical properties, as well as their hydrophilicity, high water content and structural allowance for the diffusion of oxygen, nutrients, and bioactive molecules. Their mechanical properties, such as elastic modulus, can be tuned using various physical and chemical crosslinking techniques to be more similar to those of native skeletal muscle, to support the mature skeletal muscle development.<sup>[58]</sup>

Hydrogels can be derived from a wide variety of natural, synthetic, or hybrid materials.<sup>[58–59]</sup> Pollot et al.<sup>[60]</sup> has screened

different types of hydrogels for to determine their suitability in SMT engineering. They investigated the tensile mechanical properties of collagen I, agarose, alginate, fibrin, and collagen-chitosan, and investigated their ability to grow skeletal muscle in vitro during 14 days of myoblast culture. In the listed materials, collagen, fibrin, and collagen-chitosan hydrogels, with average elastic moduli ranging from 2.7 to 3.7 MPa, all demonstrated better myogenic results. However, neither the very stiff agarose hydrogel (elastic modulus of  $87.3 \pm 32.6$  MPa) nor the very brittle alginate hydrogel, which was very poor in handling, promoted myogenesis. The researchers successfully tested the collagen, fibrin, and collagen-chitosan hydrogels in vitro, and found that the primary rat satellite cells cultured on them after stretching could get activated and elongated without failing. The behavior of satellite cells, characterized by their genetic RNA expression of MHC, MyoD, and Myogenin, indicated the differentiation and maturation of satellite into contractile units.

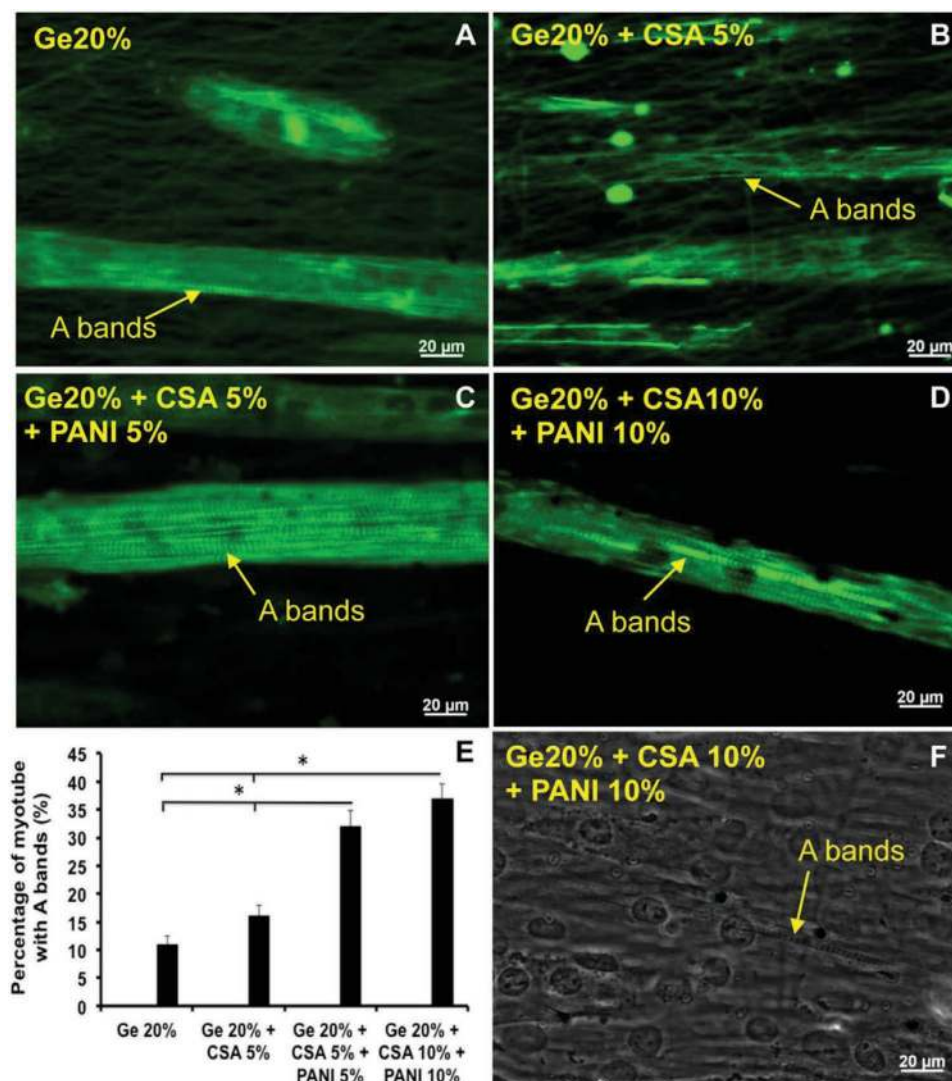


**Figure 8.** Myotube formation after 6 days of differentiation shown by fluorescence microscopy on A–D) Aligned electrospun gelatin nanofibers with and without CSA and PANI. E) Percentage of myotubes which showed A bands in their structure and F) Phase-contrast image showing the A bands in myotubes at day 4 of differentiation. Adapted with permission.<sup>[53]</sup> Copyright 2017, American Chemical Society.

MyoD expression had decreased during the 14 days of culture, while the expression of Myogenin had peaked on day 7 before decreasing for all five hydrogel types. In the end, only fibrin had significantly greater MHC expression on days 7 and 14 of culture.<sup>[60]</sup>

Gholobova et al.<sup>[61]</sup> showed fabrication of bio-artificial tissue constructs into organoids of skeletal muscle. They were made of a muscle bundle consisting of aligned myofibers, able to contract upon electrical and/or mechanical stimulation. Various types of muscle cells (C2C12 mouse myoblasts, human myoblasts or human mixed muscle cells isolated from muscle biopsies) were mixed with a natural, human fibrin hydrogel in a silicone mold, which contained two anchor points. Within a week of culture, the cell-gel mix contracted to form multinucleated myotubes aligned between the anchors. The aim was to use this system as a model for intramuscular drug injection, in order to decrease the need of in vivo animal studies.<sup>[61]</sup>

Unfortunately, the hydrogel itself is not able to provide any topographical cues to the encapsulated cells to promote the formation of mature and functional skeletal muscle tissue. To form aligned myofibers within the hydrogels, either external stretching is required or a variety of processing techniques are necessary; additionally, a second component to the structure can be used as a topographical cue to modify the structure and properties of the hydrogels.<sup>[59,62]</sup> For example, Kim et al.<sup>[63]</sup> published a report on an innovative hydrogel which consisted of uniaxially surface-patterned cylindrical struts. Collagen matrix, a main component of the muscle ECM in the form of micropatterned struts, and PCL were used to generate this 3D hydrogel and induce anisotropic cell alignment. The fibrillated poly(vinyl alcohol) (PVA), here used as a sacrificial material, was either mixed with PCL (PVA/PCL solution (PVA:PCL = 3:7)) or collagen (20 wt% PVA and 4 wt% collagen) to create filaments for the 3D printing of micropatterned PCL and collagen struts

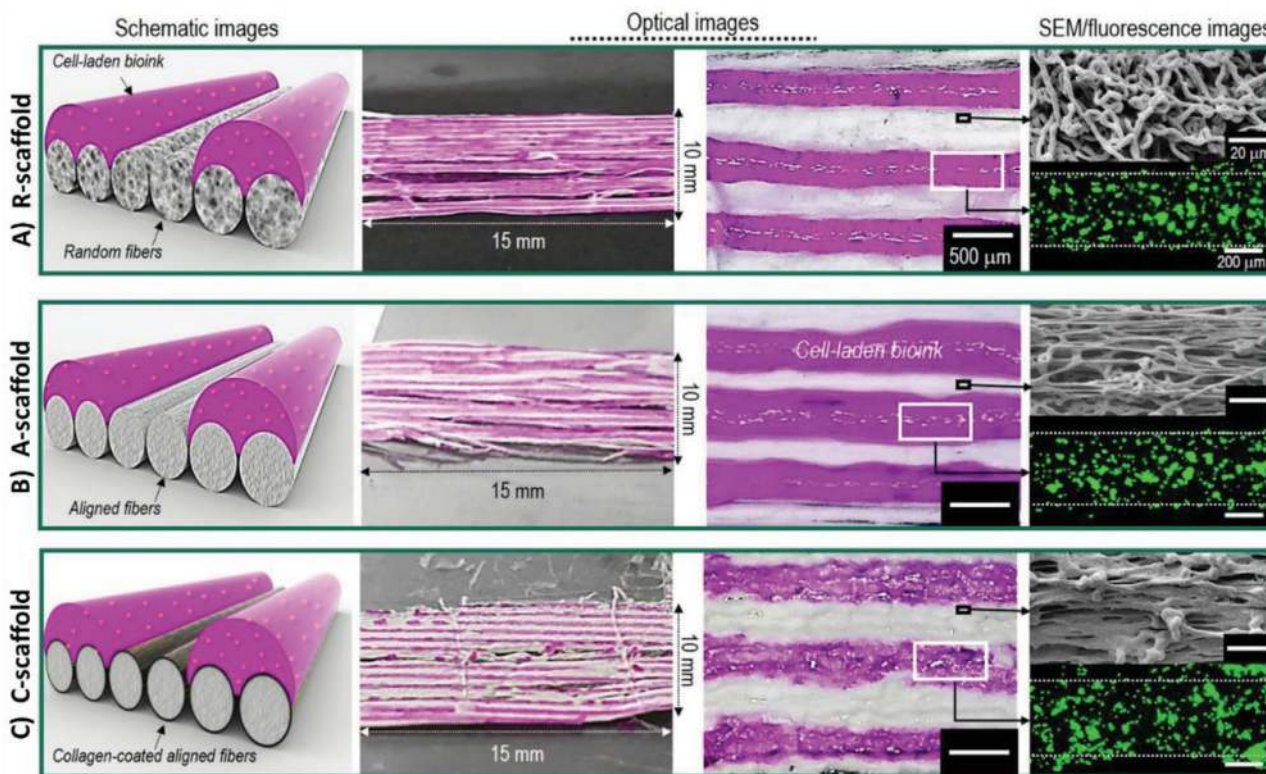


**Figure 9.** Schematic and microscopy images of cell laden construct. R-scaffold refer to random, A-Scaffold to aligned A), and C-Scaffold refer to collagen-coated C) scaffolds. Adapted with permission.<sup>[65]</sup> Copyright 2018, American Chemical Society.

with an aligned/anisotropic surface. After the printing, PVA was leached out and eventually the PCL or collagen struts with specifically aligned/anisotropic surface patterns were obtained. Furthermore, struts were coated with 0.5 wt% collagen and immersed in 1-ethyl-3-(3-dimethylamino propyl) carbodiimide (EDC) for crosslinking. On the micropatterned collagen surfaces, myoblasts showed full alignment as well as a significantly higher level of myotube formation, in comparison to the collagen structures that were not treated with the micropatterning process.<sup>[63–64]</sup> This group also used collagen, combined with a 3D fibrous bundle structure fabricated by an electrohydrodynamic (EHD) process. The fabricated scaffold is composed of 3D microfibrillar bundles laden with myoblasts encapsulated in a collagen bioink. The fibers after stretching became uniaxially aligned to obtain a fully aligned 3D structure. Encapsulated muscle cells were later released from the collagen bioink, aligned on struts and differentiated to myotubes. They showed generation of a well-organized muscle tissue, by applying the synergistic combination of the aligned topological cues and high biocompatibility of collagen to enhance the relative expression of myogenic genes (Myf5, Myh2, MyoD, and Myogenin) (Figure 9).<sup>[65]</sup>

Other than hydrogels reinforced with fibers, or fibers which are modified by a hydrogel coating, various types of cell-laden fiber structures are also introduced as a 3D model to develop engineered SMT. The morphology and fabrication techniques that apply shear forces during the fiber formation can align the cells and provide a 3D environment for the cells to thrive. In a recent study, Urciuolo et al.<sup>[66]</sup> demonstrated the formation of

a 3D structure from primary myoblasts, or myoblasts derived from embryonic stem cells, as an in vitro model of human skeletal muscle with a fascicle-like morphology. This construct has the structure of a single fiber, and is formed within laminin-coated micrometric channels constructed inside a 3D hydrogel. The stiffness of the hydrogel was adjusted to that of native skeletal muscle, in order to successfully promote myogenesis. Primary myoblasts cultured in this 3D culture model were able to undergo differentiation and maturation to form myotubes, characterized by the expression and localization of key components of the sarcomere and sarcolemma. This approach supported the formation of human myobundles of  $\approx 10$  mm in length and  $\approx 120$   $\mu\text{m}$  in diameter. Critically, it showed spontaneous contraction after 7 days of culture. In comparison to the 2D culture of primary cells, transcriptome analyses showed higher similarity of the developed system in this work and natural muscle tissue. In addition, this culture model promoted the differentiation of myoblasts derived from embryonic stem cells. (Figure 10).<sup>[66]</sup>

Similarly, Chen et al.<sup>[67]</sup> showed fabrication of cell-laden fibers similar to skeletal myofibers made of photocrosslinkable hydrogels tens of centimeters long. The mechanical properties of the fabricated fibers could be tuned by modulating the exposure time and the concentration of hydrogel. Additionally, external stretching provided an axis of alignment for the development of a more mature and functional tissue. Afterwards, C2C12 cells were well spread, elongated, and aligned themselves in the direction of uniaxial stretching (Figure 11).<sup>[67]</sup>

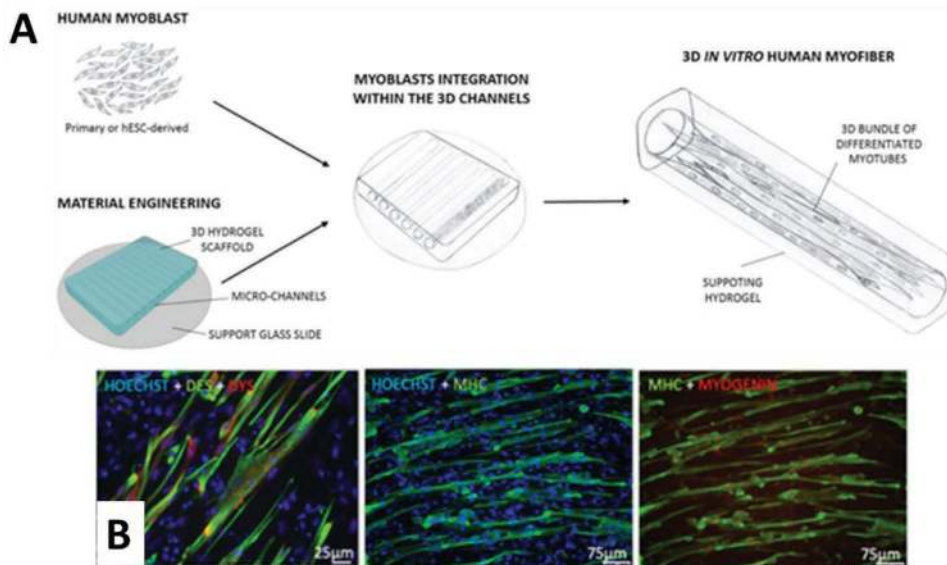


**Figure 10.** A) Schematic showing formation of cell-laden microfibers to form human myobundles. Human primary or embryonic stem cells (ES)-derived myoblasts were encapsulated into the micro-channels within the 2D hydrogel scaffold which were differentiated in myotubes forming 3D myobundle supported by the surrounding hydrogel. B) Immunofluorescence analysis for desmin (green) and dystrophin (red), for MHC (green) and for MHC and myogenin (red). Nuclei were stained with HOECHST (blue) in hESC cultured inside the 3D micrometric channels. Adapted with permission.<sup>[66]</sup> Copyright 2020, PLOS.

Additive manufacturing and 3D bioprinting techniques have also improved the precise fabrication of muscle tissue using a bottom-up tissue engineering approach. Biofabrication

of a 3D construct more representative of the native structure was achieved via the fabrication of multi-layer structures. Yeo et al.,<sup>[68]</sup> for example, investigated the effect of electrospon

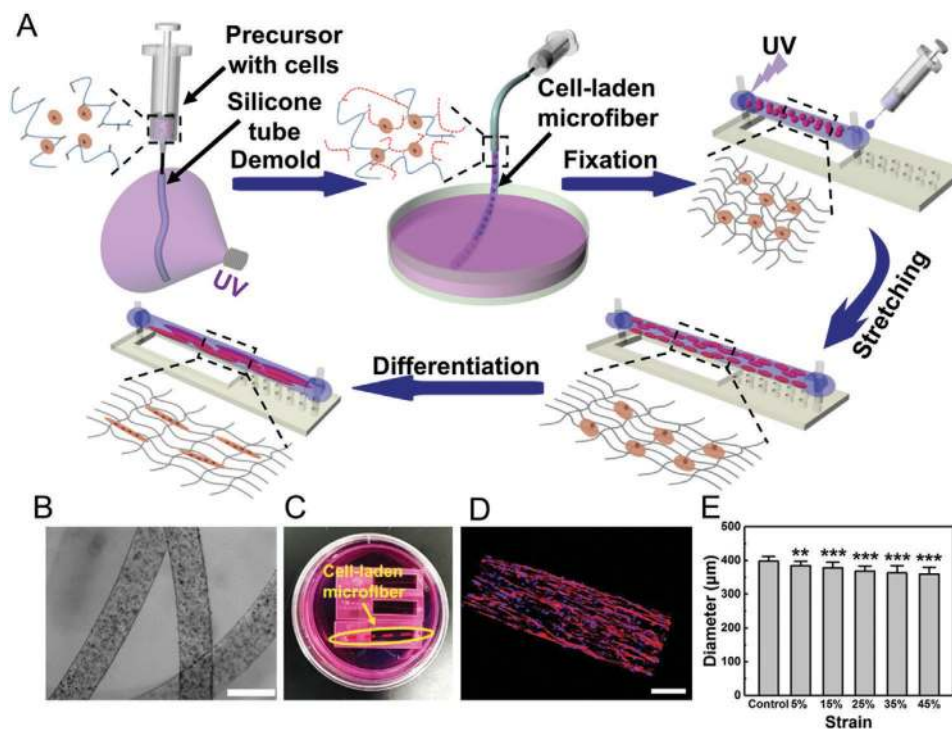


**Figure 11.** A) Schematic showing the fabrication of cell encapsulated microfibers, the fixation and mechanical stretching of the cell laden fibers. Applied uniaxial stretching, promoted the alignment, elongation and differentiation of the C2C12 cells. B) Bright field image of the cell-laden fibers (scale bar 500 µm). C) Image of fixed and stretched microfiber under various strain ratios, D) myotubes formed within the microfibers in GelMA hydrogel, E) the diameter variation of the microfiber after stretching under various strain ratio. Adapted with permission.<sup>[67]</sup> Copyright 2020, American Chemical Society.

PCL micro/nanofibers on the development of skeletal muscle cells. These cells were printed in an alginate/PEO hydrogel reinforced by PCL struts, in order to obtain a higher 3D structure. The researchers found that the cells aligned according to the direction of the aligned electrospun fibers. Compared to a random fiber mat as well as an example without any microfibers at all, the cells grown on the aligned fiber scaffolds showed a higher expression of factors relevant for muscle development.<sup>[68]</sup> Other materials explored for mechanically supporting the biofabricates are PLGA<sup>[69]</sup> or poly (ethylene glycol) diacrylate (PEGDA).<sup>[70]</sup> These materials supported the shape fidelity of the printed constructs during cell culture.

Zhang et al.<sup>[71]</sup> also showed application of melt electrowriting (MEW) technique in fabrication of a hierarchically organized, anisotropic and conductive scaffold with microscale grooves aligned on the top of unidirectionally-oriented nanofibrous mesh. These microfeatures supported the contact guidance and orientation of muscle progenitors, promoting the formation of anisotropic and mature tissue. After 7 days of culture, the H9c2 myoblasts produced an increased myogenic response due to the combination of nanoscale and microscale anisotropic surface topography in the fabricated scaffold. The differentiated myotubes formed on parallel patterned scaffold were longer than 600  $\mu\text{m}$ , with higher expression of MHC and maturation index (2.4-fold MHC surface coverage, 1.6-fold maturation index).

The issue of recreating the 3D environment for muscle cells which is key to the growth and development of functional muscle tissue can also be tackled from a different angle. Naik et al.<sup>[72]</sup> reported application of decellularized muscle tissue instead of processed polymers to mimic the hierarchical structures found in the native muscle tissue. The native skeletal muscle tissue derived from human tissue was decellularized and the remaining 3D structures containing collagen, laminin and fibronectin were examined for their biocompatibility after the chemical processing of the tissue. An in vitro study over 7 days with fibroblast cells confirmed the biocompatibility of the scaffolds. To examine the effects of the chemical removal of the cells on the mechanical properties of the native extracellular matrix Renya et al.<sup>[73]</sup> conducted tensile tests with decellularized scaffolds obtained from pigs. They reported no significant differences between the native and the processed tissue. An investigation of the intrinsic structure of decellularized scaffolds acquired from pigs was conducted by Wassenaar et al.<sup>[74]</sup> Analyzing the scaffolds with SEM revealed the natural honeycomb structure from the remaining connective tissue.<sup>[74]</sup> The implantation of such scaffolds has proven to be beneficial for tissue regeneration.<sup>[75]</sup>

To further improve the scaffolds-cell-interaction Lee et al.<sup>[76]</sup> coated a D-ECM with an insulin growth factor (IGF) after the decellularization process. The additional growth factor supported the cell viability and the expression of a higher amount of myosin heavy chains compared to a D-ECM in comparison with collagen as control and without any additional factors after 7 days of culture. These findings could be confirmed in an in vivo study over 1 and 2 months in rabbits with a tibialis anterior muscle defect. The implanted grafts resulted in a higher amount of myofibers when coated with IGF.<sup>[76]</sup>

In conclusion, the decellularized tissue provides the necessary structures with the corresponding mechanical properties as well as the natural composition of the components on which the cells adhere. The positive properties of the natural scaffolds might give the impression that further research of synthetic scaffolds made from materials other than natural derived polymers is unnecessary. But there are several limiting factors that make other methods necessary. Due to the batch to batch variation of natural tissues a standardization of scaffolds derived from such tissue is difficult. The morphology of the obtained scaffolds cannot be adjusted to the patient's needs and a rejection of the transplanted scaffolds due to immunogenicity cannot be excluded. Therefore, the investigation of the other methods described in this review is of great importance.

### 3.3. 4D Engineered Muscle Tissue

Taking SMT engineering one-step further, time is added as a parameter for changing the morphology of the material on which the muscle cells are grown. Therefore, the concept of time is integrated within the 3D structure as the fourth dimension to introduce the next-generation of scaffolding to SMT engineering. 4D biofabrication techniques are used to fabricate dynamic and complex 3D architectures with specific geometry out of stimuli-responsive materials that can undergo shape transformation after exposure to various stimuli.<sup>[58b,77]</sup> We recently showed that 4D biofabrication can be used to increase the complexity of tissue-like constructs and precisely fabricate a complicated structure, such as skeletal muscle with tubular shape in a hierarchical manner.<sup>[78]</sup> Self-rolling bilayer PCL/ methacrylated alginate fibrous mats were used as substrate to culture muscle cells. By triggering the swelling ratio of the bilayer, it could undergo a shape transformation and encapsulate myoblasts C2C12 cells and form a tubular shape. The overall thickness of the bilayer, the thickness of each layer, and the geometry of the mat are the key parameters in controlling the direction of rolling and the diameter of the generated tubular shape. The myoblasts cells, after a total 14 days of culture and 7 days of differentiation, showed a highly aligned structure along the axis of the anisotropic PCL fibers and further differentiated into contractile myotubes upon electrical stimulation and formed a skeletal muscle microtissue.<sup>[78]</sup> Similarly, Vannozzi et al.<sup>[79]</sup> reported fabrication of a fascicle-like implantable muscle construct from two stacked layers with differential swelling degree, stiffness, and thickness. The bilayer made of two PEGDA hydrogel layers at different molecular weights could undergo a programmed self-folding and form a 3D tubular shape. In this construct, the inner side of the tubes could guide the muscle cell adhesion and their spatial alignment. This construct was tested further for both skeletal and cardiac muscle cells (human induced pluripotent stem cell-derived cardiomyocytes). High viability was measured for both types of cells and cardiac myocytes maintained their contractile function over a course of 7 days.<sup>[79]</sup>

Miao's group<sup>[80]</sup> created a 4D anisotropic skeletal muscle tissue using a staircase defect strategy. A staircase defect is an inevitable type of defect in fused deposition modeling (FDM) due to the nature of the layer-by-layer deposition of the material during the

3D printing and thus, as a result, the surface of the construct exhibits contour-like topography. Contour-like topography is composed of aligned lines, and this group studied the effect of such an oriented structure on the formation of an anisotropic skeletal muscle tissue. The myogenic differentiation of bone marrow human mesenchymal stem cells under the influence of these topographical patterns showed that 3D printed PCL could regulate the behavior of cells toward SMT.<sup>[80]</sup> Combination of the surface coating techniques and shape memory polymers such as PCL supported the fabrication of 4D structures. It was shown that this biomimetic strategy supported the formation of highly organized functional SMT where higher myogenic genes expression such as myoblast differentiation protein-1, desmin, and MHC-II after 14 days of culture was detected.<sup>[80]</sup>

The techniques that utilize time during the transformation and formation of mature and functional tissue from printed, cell-laden constructs are also frequently regarded as 4D bio-printing. These potential interventions, unfortunately, have not been extensively researched for their applications in skeletal muscle tissue engineering.

For more serious injuries, the implantation of fully developed muscle tissue is necessary to completely restore the function of the tissue. Merely growing muscle cells on a scaffold is not enough to induce myotube formation with a mature intracellular structure capable of generating significantly higher forces. Therefore, in addition to the previously-discussed biomaterials, various external stimuli can be deployed to improve the development of the myoblasts; several important studies involving these external stimuli are extensively reviewed in the following sections of this review paper. The incorporation of dynamic culture systems into existing classical SMT engineering approaches has great potential for the improvement of tissue maturation.

## 4. External Stimulators

A robust background in muscle physiology is key to understanding how skeletal muscle tissue responds to various external stimuli. The sensitivity of muscle maturity to these stimuli is often attributed to the myofibers' capacity for adaptation, where physical forces can encourage the regeneration of current muscle structures. The application of external cues can not only activate the gene and protein production, but also augment the accelerated growth, leading to a more rapid development of the tissue.<sup>[81]</sup>

Muscle cells proliferate more efficiently when biomaterials support their self-regenerative abilities and guide them through different biological pathways.<sup>[82]</sup> However, such static systems are not delivering the right amount of nutrients and growth factors in order to accelerate the regeneration process. Consequently, pre alignment of the cells prior to their differentiation is key, as it promotes appropriate differentiation into functional myofibers, as the various approaches to align the cells demonstrated in the previous section.<sup>[82]</sup> Skeletal muscle has an inherent highly adaptive capacity; however, when it is not properly trained, wasting and weakness can hinder potential recovery after treatment.<sup>[83]</sup> While this is a problem for muscles that have not been properly stimulated, the main advantage of

muscle is that the benefits of training, such as increased resistance, can be induced even after long periods of non-stimulation.<sup>[83]</sup> **Figure 12** summarizes different types of stimuli which have been used to restore the loss of normal functionality of muscle tissue. In this section, the effect and role of various external stimuli on skeletal muscle maturation and functionality will be reviewed.

### 4.1. Mechanical Stimulation

The importance of sustained loading for tissue development cannot be understated, especially in the beginning phases of skeletal muscle growth. During embryogenesis, besides determining myofilament organization, passive tensions play a role in the formation of myofilaments with specified weights, diameters and lengths.<sup>[88]</sup> Furthermore, such stretching is effective in the preservation of healthy muscle throughout a person's life; muscle stretching is particularly crucial for the developmental process of muscle, driven by the regulation of specific genes, the synthesis of new proteins, and the release of nitric oxide. The mechanical forces applied on muscle will be translated into chemical signals via mechanotransduction, which subsequently triggers the activation of satellite cells. This process increases the rate of protein synthesis, leading to increased hypertrophy and hyperplasia.<sup>[89]</sup> In short, the external mechanical signals will be measured by the cells through a variety of receptors, integrins, and focal adhesions.<sup>[90]</sup> Thus, the cytoskeleton will start rearranging, transforming the deformations caused by these mechanical signals into important factors that may boost the tissue maturation.<sup>[91]</sup> Skeletal muscle is composed of thousands of fiber arrays that are tightly packed in the tissue. This array contributes to a more resistant structure, capable of undergoing repeated cycles of stretching and contraction without easily rupturing. These fiber arrays are themselves composed of thousands of differentiated myoblasts. The focal adhesions on the surface of these myotubes receive external mechanical cues, thereby stimulating a variety of the cellular membrane receptors, including integrins and cadherins. Subsequently, the mechanical stimulation (MS) of these receptors activates particular signaling pathways throughout the cell body, boosting the rearrangement of the cytoskeleton according to the direction where stimuli was initially applied.<sup>[12–14b]</sup> The response of skeletal muscle cells also varies depending on in-vivo or in-vitro tissue models, both in 2D and 3D.

Most of the myofibers in the body can express the whole gamut of available skeletal MHC isoforms; the specific protein composition of each fiber is driven by the stimuli that myofibers receive from the environment. As an example, researchers have reduced the stretch-induced strain typically experienced by a muscle, and saw the activation of certain intracellular regulatory pathways, which resulted in the MHC proteins converting from predominantly slow-type isoforms to primarily fast-type.<sup>[16]</sup> Through methods such as these, tissue engineers can directly impact the phenotypes of lab-grown myofibers to their benefit. Although there is a lot of published information about which strain profiles cause which isoform conversions, there are still significant gaps in our knowledge about the actual mechanisms behind many of these conversions.<sup>[8,13,14b,16,92]</sup>

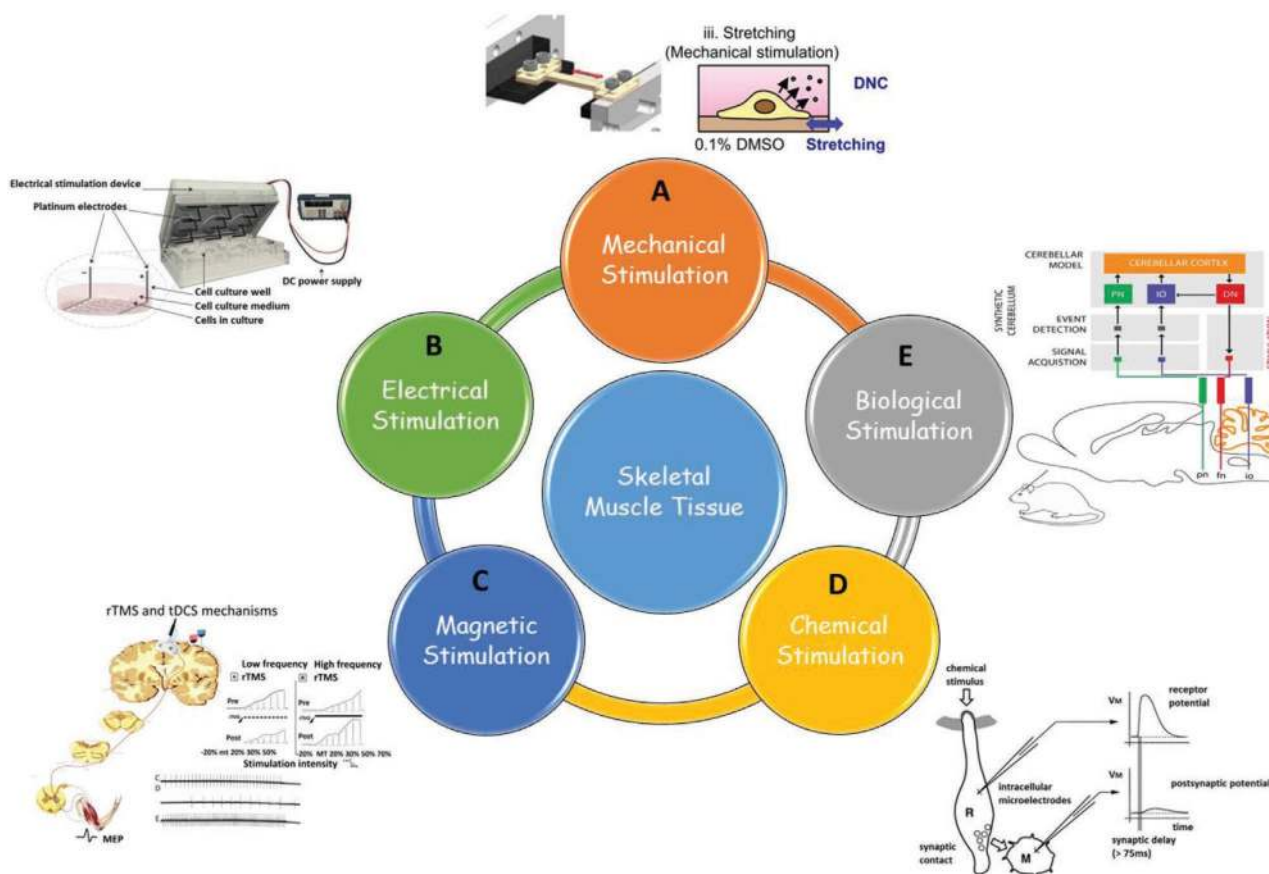


**Figure 12.** Types of external stimuli for skeletal muscle tissue engineering. A) Mechanical stimulation, B) electrical stimulation, C) magnetic stimulation, D) chemical stimulation, and E) biological stimulation. A) Adapted with permission.<sup>[82]</sup> Copyright 2019, Nature Research. B) Adapted with permission.<sup>[83]</sup> Copyright 2017, Spandidos Publications Ltd. C) Adapted with permission.<sup>[84]</sup> Copyright 2015, Elsevier. D) Adapted with permission.<sup>[86]</sup> Copyright 2002, Elsevier. E) Adapted with permission.<sup>[85]</sup> Copyright 2014, Frontiers.

However, there has been various reports on the effect of mechanical stimulation as an external treatment of muscular injuries, triggering the self-regenerative capacity of the tissue in the process. Some of the first investigations conducted about effects of mechanical stimulation on skeletal muscle was in 1991 by Goldspink et al.<sup>[91]</sup> who demonstrated the effect of 3 days of MS on soleus muscle hind limbs. These limbs had been surgically extracted from rabbits by using a self-made external stimulator. Stimulation at 10 Hz addressed the rapid activation of MHC and fast sarcoplasmic reticulum  $\text{Ca}^{2+}$  ATPase proteins, repressing normal fast myosin heavy and light chain genes, slowing the contraction and relaxation characteristics. This leads to a faster mRNA expression, one which will increase the production of slow, type I, and fast oxidative IIA fibers that are critical for enhancing oxidative muscle capacity. Consequently, in comparison with non-stimulated muscle limbs (control), collagen concentrations were reduced, leading to thickened connective tissue within the muscle, showing sarcomeric restoration, which exhibited higher fatigue resistance and better functionality.

Powell et al.<sup>[86]</sup> studied the effect of external mechanical stimulation on human bioartificial muscles (HBAMs) fabricated from a collagen/Matrigel mixture, where muscle cells were kept in cultivation for up to 8 days prior to differentiation. Initially,

HBAMs were placed on silicone rubber tissue molds supported by 2 mm stainless steel pins. A self-made mechanical cell stimulator version 4 (MCS4) was used to stretch HBAMs for 4 days in intervals of  $\approx 3.5 \mu\text{m}$  every 10 min. One of the pins was in direct contact with the simulator to allow the transference of a unidirectional stretch amplitude of 25% (before rupture) and velocity up to  $0.5 \text{ mm s}^{-1}$ . Sarcomeric analysis of static HBAMs showed formation of myofibers in only 2–10% of their cross-sectional area with fiber diameters  $< 10 \mu\text{m}$  after 16 days of stimulation. In contrast to the static systems, the mechanically stimulated HBAMs showed a two- to three-fold difference after 8 days of stimulation, where the fiber diameter increased by 12% ( $6.4\text{--}7.1 \mu\text{m}$ ) and myofiber area increased by 40%. In this study, they showed that periodic training is key for muscle fiber hypertrophy and growing more elastic muscle fibers in comparison with static controls. Moreover, mechanical conditioning allows rapid diffusion of nutrients towards the cells and faster remodeling of the tissue associated with repetitive mechanical loading.<sup>[86]</sup>

Recent advances of SMT engineering have enabled the development of functional in vitro models. One of the principal stimulators that is highly responsive to such effects is Interleukin 6 (IL-6). Hicks et al.<sup>[92]</sup> stated that IL-6 induces proliferation of human dermal fibroblasts (NHDF)/C2C12 coculture systems,



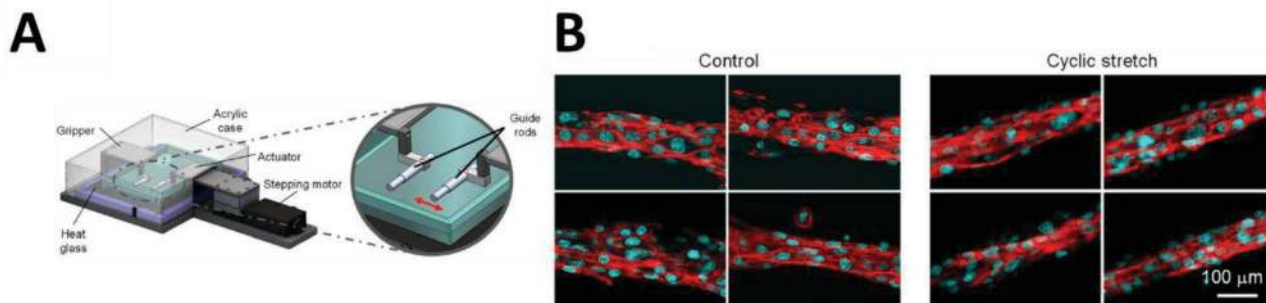


**Figure 13.** A) Self-made cell device used for imposing cyclic stretching on C2C12 cells encapsulated in core–shell collagen gels. B) Fluorescent images of culture C2C12 cells on hydrogel microfibers before and after being cyclically stretching for 6 days at 1 Hz, with a 3% tensile strain. Adapted with permission.<sup>[94]</sup> Copyright 2019, MDPI.

facilitating myoblast fusion and accelerating the overall tissue maturation. In their study, a Flexercell FX-4000 Tension Plus System was used to induce stretching on Bioflex culture plates throughout vacuum assisted regimes. Bioflex plates owned an elastomeric surface that allowed both cells (NHDF/C2C12) to adhere, creating cellular monolayers that were tested under different stretching conditions: Cyclic short-duration stretches (CSDS) (10% strain, unloading rate of 33%/s, frequency of 0.6 Hz, for 8 h), acyclic long-duration stretch (ALDS) (6% strain, loading rate of 3%/s, 60 s) and a combination of CSDS and ALDS (CSDS for 8 h, followed by 3 h resting and ALDS for 60 s). Non-stretched cells in differentiation medium were used as a control to characterize how myotube formation was impacted by the stretching device. To prepare the coculture system within the stretching device, fibroblasts were seeded in the Bioflex membranes, whilst myoblasts were seeded on non-deformable glass slips facing downward the fibroblasts monolayer with a 2 mm distance between them. In the coculture system the strain was applied on fibroblasts only, however the diffusion of differentiation mediators secreted by fibroblasts could affect the unstrained myoblasts on coverslips. In cocultures and after 96 h, ALDS following CSDS showed enhanced myogenesis and formation of higher number of myotubes by 78% versus CSDS alone. Cocultures systems subjected to a combination of both types of cyclic stretches (CSDS+ALDS) demonstrated an enhancement in the myotube formation in comparison to the monoculture system (myoblasts treated by 0–100 ng mL<sup>-1</sup> IL-6); similarly, fusion efficiency was significantly higher in contrast to cells which had undergone either ALDS or CSDS conditions.<sup>[92]</sup>

As it has been discussed in previous sections, biomaterials are an attractive tool to use in the production of successful 3D cell-constructs, due to their beneficial properties for the promotion of cell binding and their ability to serve as carrier for several growth factors.<sup>[93]</sup> It has been shown that hydrogels, despite their relatively weak mechanics, can be easily stretched under static and cyclic conditions. The viscoelasticity of hydrogels offers a possibility to fabricate scalable and supportive materials for tissue fabrication. For instance, Bansai et al.<sup>[94]</sup> studied the effect of cyclic stretching (3% tensile strain at 1 Hz) applied on murine C2C12 cells encapsulated in core–shell hydrogel microfibers. The C2C12 cells were encapsulated in the collagen gel as a core of alginate fibers, which were fabricated using a double-coaxial laminar-flow microfluidic device; this device therefore

resulted in a higher myotube length in comparison with typical static culture systems (C2C12 monolayer). They observed that applying a constant stimulation on microfibers using a custom-made cell culture device resulted in decreasing cell viability (Figure 13A). Contrary to this, cells in collagen hydrogels resulted in 70% of myoblasts successfully forming mature myotube structures. Cytoskeleton staining showed that encapsulated cells in the microfibers under cyclic stretching were significantly more aligned in comparison with the cultured monolayer as well as with the non-stretched cell-laden microfibers (Figure 13B).<sup>[94]</sup>

Such results were congruent with Heher et al.<sup>[93]</sup> where static mechanical strain (10%) was applied through a self-built device (MagneTissue) to stimulate myoblasts embedded in fibrin gels for ≈10 days. They tested different fibrin concentrations, starting from the softest (10 mg mL<sup>-1</sup>) to the stiffest (40 mg mL<sup>-1</sup>) with stiffnesses in the range of 11.57–17.21 kPa. A concentration of 20 mg mL<sup>-1</sup> of fibrin was chosen as an optimal concentration for further MS. They detected the formation of a higher number of mature myotubes, characterized by length and diameter values in the range of 12–15 and 200–400 μm, respectively. After 3 days of mechanical strain (6 h), the alignment of the cells embedded in the fibrin gels was attributed to the transmission of the strain applied by MagneTissue. Moreover, RT-qPCR depicted a higher myogenic expression of MyoD and Myogenin after static strain. They also showed that mechanical stretching of the monolayer of cells (2D) did not produce similar results. Only partial alignment in the 2D system was detected, in comparison to the enhanced mRNA expression, sarcomeric production, and cellular alignment results obtained in 3D cultured systems.

Chen et al.<sup>[67]</sup> also reported upon their work on 3D, fiber-shaped cellular constructs, primarily used as a platform to grow functional and organized muscle tissue derived from the application of mechanical stimulation. A silicone tube-based coagulant bath was used to fabricate centimeters long cell-laden microfibers, which then could be combined with photocrosslinkable hydrogels such as GelMA to form the microfibers with tissue-like microstructures. By varying the exposure time, the researchers were able to tune the mechanical properties of the hydrogel. The cell-laden fibers were later stretched using a pillar well array-based stretching device embedded in a culture system, to apply uniaxial stretching with various strain ratios in situ. C2C12 myoblasts showed improved spreading, elongation, and alignment under uniaxial stretching, and the

differentiation of the cells under uniaxial stretching was also improved. By increasing the strain ratio up to  $\approx 35\%$ , the contractility of myofibers became more pronounced and reached a saturation level (Figures 11 and 14).<sup>[67]</sup>

It has been stated that stiffness of the scaffold material (hydrogels, electrospun meshes, etc.) is critical for mechanical stimulation. It is important that the materials used for encapsulation of cells withstand several mechanical loadings in order to induce morphological changes in the cells. Therefore, it has been important to investigate the role of chemical and mechanical properties of scaffolds fabricated by different techniques in transmission of the mechanical stimuli to cells and their response.<sup>[95]</sup>

For instance, the use of electrospun scaffolds of a DegraPol block co-polymer were also used by Candiani et al.<sup>[96]</sup> as an

alternative to hydrogels. They investigated the application of a self-made bioreactor, to study the role of static and cyclic stimulation on microfibrinous scaffolds (DegraPol strips with sizes of  $50 \times 5$  mm) for 13 days. After 4 days of culture, prior to starting dynamic cultivation, an additional batch of cells was added to samples aiming to improve efficiency of differentiating myoblasts. Samples inside the bioreactor were stimulated under cyclic stretching (frequency 0.5 Hz, amplitude 1 mm, comprising 30 sec rest and followed by 28 min rest). During initial stretching, no differences in terms of expression of MHC was seen between static and cyclic conditions; however, from day 7 in the static system, there was a reduction of 36% in expression of MHC in comparison to the dynamic stretching which showed an increase of 67%. Besides that, densitometric

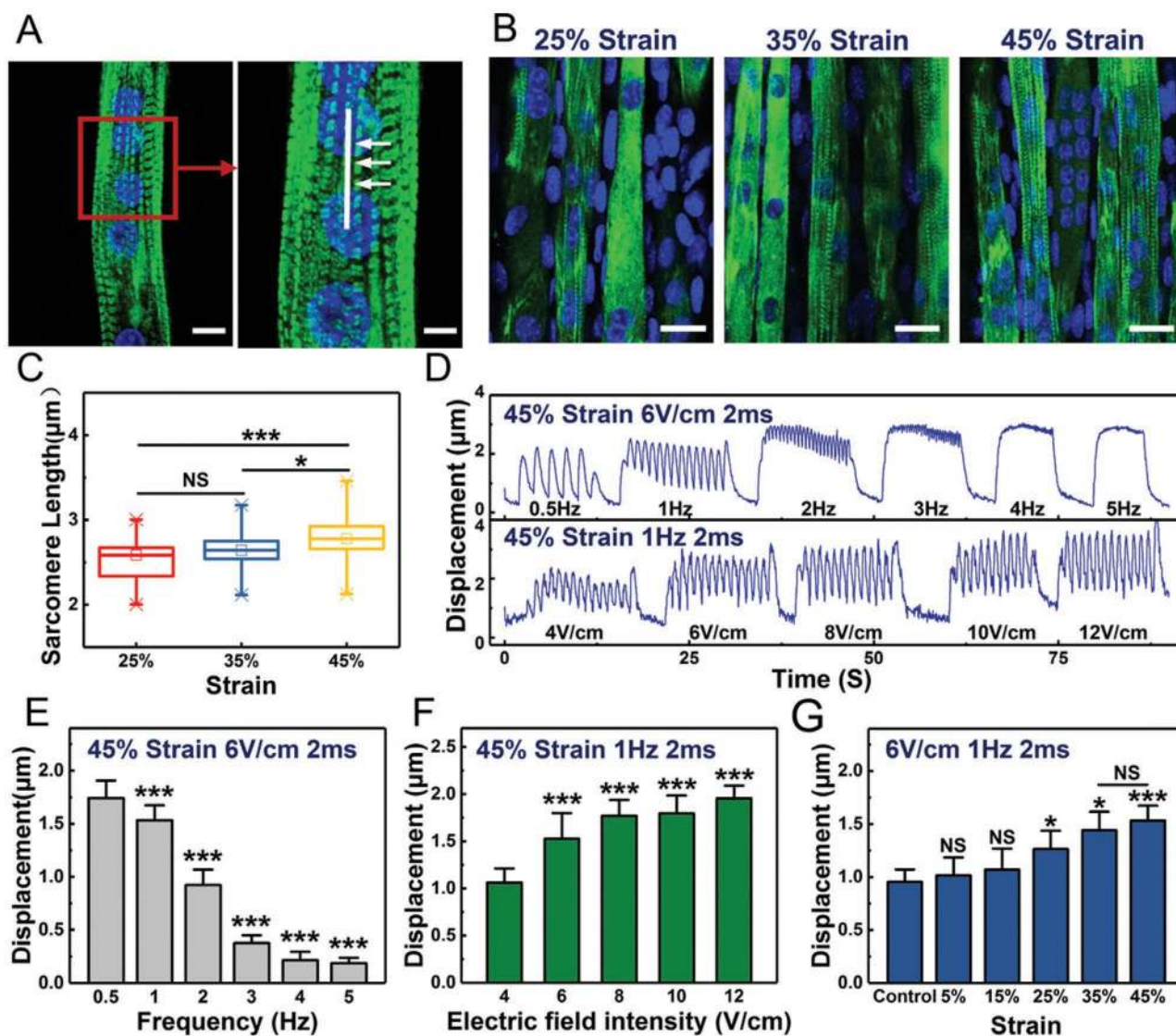


**Figure 14.** A) Fluorescent microscopy images showing the uniform distribution of the sarcomeres and Z-line striation in mature myotubes. The length of the sarcomere is measured by manually drawn white line in the right figure. White scale bar equals to 10  $\mu\text{m}$  (left) and 5  $\mu\text{m}$  (right). B) Confocal images of the myotubes under 25%, 35%, 45% strain showing a partial striated pattern. White scale bars equal to 25  $\mu\text{m}$ . C) Correlation of the strain ratios (25%, 35%, 45%) and the sarcomere length of myotubes grown within microfibers. D) Contraction displacement of myotubes is shown as a waveform graph after electrical stimulation: 6  $\text{V cm}^{-1}$ , 2 ms, different frequency (the top); 1 Hz, 2 ms, different field electric field intensity (the bottom). Quantification of myotube contraction displacements under various parameters related to ES such as E) Frequency F) Electric field intensity and G) Strains. Adapted with permission.<sup>[67]</sup> Copyright 2020, American Chemical Society.

analysis demonstrated that at day 10 there was a significant 8-fold increase in the expression of MHC protein due to the mechanical effect produced by the cyclic stretching imposed within the bioreactor. Such a mechanical effect was also confirmed with MHC immunostaining, where stretched strips were assessed with an epifluorescence microscope, exhibiting denser fiber arrays within more defined myotube packs. In conclusion, in vitro mechanical stimulation of 3D culture models could effectively accelerate the maturation of engineered muscle constructs in comparison with 2D systems.<sup>[96]</sup>

#### 4.2. Electrical Stimulation

Motor neurons (MNs) within skeletal muscle regulate cell membranes' depolarization during fiber stimulation, leading to proper contraction response (force) that is dependent on the size and the healthy state of the muscle fibers. Unfortunately, loss of force is one of the common issues coming from the fatigue of skeletal musculature, where the MNs' frequency starts decreasing (20 to 10 Hz) and as a response skeletal muscle shows a reduction in the tetanic ability (contraction).<sup>[97]</sup> External ES is one of the most often used techniques for nerve stimulation, in order to circumvent muscular fatigue. Since electrical stimulation (ES) is also crucial for the function of skeletal muscles, it is logical to study the effects of electrical stimulation, and the presence of the neural structures that provide that stimulation in vivo, which activate similar regulatory feedback systems in the myofibers. For example, during the first month of neonatal muscular development, scientists have discovered that the presence of an intact nerve is necessary for the proper growth and maturation of new fibers.<sup>[16]</sup> The mature musculature is innervated by neural structures in vivo which provide further stimuli for the differentiation of satellite cells and the conversion of MHC isoforms. Neuromuscular junctions (NMJs), where neurons attach to skeletal muscle fibers, provide the appropriate environment to send and receive important neurotransmitters, such as acetylcholine.<sup>[98]</sup> Once an action potential is propagated into the skeletal muscle environment via the NMJ, a series of ions such as  $\text{Ca}^{2+}$  flood from their respective stores to the intracellular environment, eventually leading to a contraction of the sarcomere.<sup>[99]</sup> They observed that applying electrical functional fields on C2C12 muscle monolayers, can affect the fiber response to electrical stimulus by repeatedly stimulating the actin and myosin proteins inside of the myofibrils.<sup>[100]</sup> While this mechanism is dissimilar from the mechanotransduction pathways, the results indicate that both methods have some degree of authority over the MHC composition of the myofibers.<sup>[101]</sup> Moreover, declination of muscular efficiency is one of the principal issues produced by aging. Reduction of the myofiber size, denervation or even contractibility problems are common factors produced by the muscle weakness. ES has been commonly used as a rehabilitation technique in order to circumvent aging diseases. For instance, Mosole et al.<sup>[102]</sup> studied the neuromuscular responses triggered by ES for 7 days using a self-made battery-powered stimulator (I:  $128 \pm 16$  mA and V:  $39 \pm 14$  V) on a few patients after placing rubber electrodes on the skin. Muscle biopsies from stimulated patients showed a faster muscle restoration response.

ES can reactivate the regulation of important markers such as Serca2, pCamKII that would increase the numbers of suitable myofibers in order to tackle muscle weakness and fatigue conditions associated with aging-related pathologies.

Kaji et al.<sup>[103]</sup> showed that a monolayer of cells which were electrically stimulated exhibited formation of internal structure and sarcomeric units. The excitation-contraction coupling in the stimulated cells showed higher reflux of  $\text{Ca}^{2+}$  in comparison with non-stimulated cells indicative of higher maturation. They cultured the C2C12 cells as a confluent and differentiated layer on an alumina porous membrane coated with a thin PDMS layer (0.1 mm) from the underside and an atelocollagen membrane (20  $\mu\text{m}$ ) on the upper side. In a self-made electrical stimulator, they placed two platinum (Pt) electrodes above and under the alumina membrane to focus the electrical pulses on the cells using amplitude: 4 mA, duration: 20 ms, frequency: 1 Hz. Differentiated myotubes were grown on the atelocollagen membrane with muscle tissue-like stiffness. The contractile myotubes also showed higher glucose uptake after measuring the uptake of fluorescence-labeled glucose (2-NBDG) and detecting significantly higher GLUT-4 translocation.<sup>[103]</sup>

Furthermore, the effect of electrical stimulation on muscle cell maturation, cultured in vitro in 2D and 3D culture systems, was studied by Langelaan et al.<sup>[104]</sup> They observed applied electrical fields on C2C12 muscle monolayers (2D culture system) leads to rapid consumption and reduction of nutrients within the medium. Expression of  $\alpha$ -actinin and sarcomeric myosin showed no cross striation formation on 2D controls. Later, they have translated the results found in cell lines (C2C12) to a primary cell source, muscle progenitor cells (MPCs), which were encapsulated in collagen type I/Matrigel hydrogel generating a 3D culture system. In contrast, in 3D system and using MPCs, fabricated bioartificial muscle models (mBAMs) after 3 days of ES (4 V  $\text{cm}^{-1}$ , 6 ms pulses at a frequency of 2 Hz) showed cross-striations and higher expression of mature MHC isoforms. Significantly higher numbers of aligned myotubes were formed and the expression of important muscle markers such as  $\alpha$ -actinin, MLP, MYH8 and sarcomeric myosin was upregulated confirming the formation of sarcomeric units after 48 h of stimulation. This study could clearly confirm the synergy of external stimulation, 3D culture systems, and suitable cell sources such as MPCs in supporting muscle maturation, myogenesis and accelerating the sarcomere assembly towards higher contractility.<sup>[104]</sup>

Furthermore, 3D cell culture systems have been used in various studies for evaluation of electrical stimulation. For example, Davis et al.<sup>[105]</sup> studied how direct electrical stimulation led to fast oxygen consumption by human muscle cells. They seeded human myoblasts on a Matrigel/fibrin gel within a PDMS mold and studied mitochondrial respiratory function, before and after stimulation, using an Oxygraph-O2 respirometer. After differentiation, the myobundles were moved to a self-made microphysiological flow chamber and electrically stimulated using carbon flat electrodes (40 V  $\text{cm}^{-1}$ , twitch: 1 Hz duration:10 ms and tetanic: 20 Hz, 1 s). Under this stimulation, the myobundles' respiration tends to increase; however, the Matrigel significantly affected the oxygen consumption in the contractile myobundles. Furthermore, they studied the oxygen transport in human skeletal muscle cells encapsulated in the gel with ES for 30 min., which showed a 20-fold increase

in the respiration of skeletal muscle cells when no matrix was provided.<sup>[105]</sup> Continuing studying the role of biomaterials in reducing the side-effects produced by applied electrical fields on human myoblasts, Khodabakus et al.<sup>[106]</sup> studied the formation of myobundles (iSKM) in Matrigel and the effect of intermittent ES (1–10 Hz, 70 mA amplitude and 2 ms duration) on the rate of maturation of the myotubes. After differentiation, ES was continuously performed on a self-made PDMS chamber between week 1 and 2 of differentiation using the program LabVIEW. Immunostaining showed that the number of nuclei in simulated 3D myobundles was augmented 1.5 fold in comparison with non-stimulated control and non-stimulated 3D myobundles. Furthermore, there was a 1.8-fold increase in the myobundles' cross sections. Additionally, Dystrophin/nuclei staining exhibited a higher sarcomeric organization due to the increase in the myotube length under the constant effect of electrical stimulation. Western blots confirmed the results by displaying higher expression of sarcomeric proteins such as dystrophin and MHC in comparison with 2D controls and non-stimulated myobundles. After applying the constant tetanic contractions triggered by ES, fatigability of cells was studied by measuring the glycolytic metabolism. Higher expression of glucose transport proteins confirmed the reduced fatigue resistance in comparison with non-stimulated myobundles.<sup>[106]</sup>

Another evaluation on mature muscle tissue involved measuring the release rate of myokines from skeletal muscle cells stimulated electrically using an external electrode system (Figure 15A). It was shown by Nagamine et al.<sup>[107]</sup> that myokines, as specialized cytokines in charge of regulating levels of glucose within the body and remodeling responses in an injured muscle, increased under ES.<sup>[108]</sup> Encapsulated C2C12 muscle cells in collagen and Matrigel were cultured around poly(3,4-ethylenedioxythiophene (PEDOT)/polyurethane (PU) wire films (3  $\mu\text{m}$  thickness) and stimulated with non-faradaic ES using charge and discharge currents (5 mA amplitude, 10 ms duration, 50  $\mu\text{C}$  charge). SEM images of cells around the wire showed an early alignment and no toxicity was detected after 3 days of culture (Figure 15B). After 7 days of differentiation, myotubes displayed contractile behavior with twitch forces at low frequencies of 1 and 5 Hz and tetanic contraction at high frequencies of 10 and 20 Hz (Figure 15C). The lack of

cell detachment not only proved that the faradaic contraction did not cause significant damage to the cells, but also enhanced their sarcomere maturation in comparison with conventional systems using external electrodes.

In conclusion, ES can trigger partial restoration of the normal contractility functions of muscle cells, but still lacks proper control over complete reformation and functionalization of muscle tissue. Contractility of the myotubes is highly affected by the stiffness and mechanical properties of the scaffold used. However, ES still faces problems in the way stimuli are transmitted along the scaffolds and reach the cells, causing suppression of MHC expression, and reduction of myoblast differentiation.

### 4.3. Magnetic Stimulation

As an alternative to electrical stimulation on the actual muscle, which is traditionally done by stimulating the nerve trunk through the skin, magnetic fields have been proposed as they can be effective while being a less invasive approach.<sup>[109]</sup> It still can penetrate deep into the muscle and stimulate it by generating a depolarization of the muscle cell membranes, which is an important feature as this depolarization is critical to effectively regulate the intensity of the contractile forces applied by the cells.<sup>[110]</sup> Originally, magnetic stimulation was proposed for the stimulation of the nervous system or for the treatment of urinary incontinence. However, few studies have confirmed its potential application for skeletal muscle regeneration due to the reduction in the twitch force generated by constant magnetic pulses.<sup>[111]</sup> Despite its great potential, the mechanism of how magnetic fields stimulate these cells, thereby triggering muscle restoration, has not been deeply studied in *in vitro* models, as the majority of the studies are focused on boosting rehabilitation in mice and humans models. For instance, Stölting et al.<sup>[112]</sup> tested the effects of direct magnetic fields on a transverse injury generated in the quadriceps from C57 mice, using a Biocon 2000 W. The thighs from the animals were placed in the coils of the magnetic stimulator and subjected to a 20 min session conducted for 10 min at 10 Hz and 10 min at 50 Hz. Non-stimulated animals were considered as controls in order to characterize the extent of the muscle restoration. Tissue removed

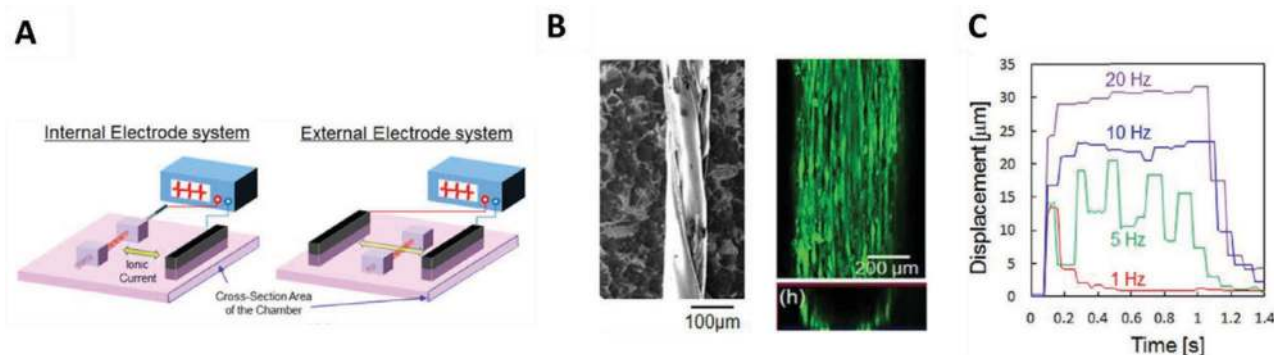


**Figure 15.** ES stimulation approaching 3D muscle-like systems. A) internal and external electrode systems used for excitation of skeletal muscle bundles composed of a myobundle layer wrapped around a PEDOT/PU conductive wire film, B) SEM image of conductive wire and C) Displacement triggered by contraction response of myotubes around the wire against the duration of the applied electrical pulse. Adapted with permission.<sup>[107]</sup> Copyright 2018, Springer Nature

from the quadriceps after 5 days of stimulation depicted a faster restoration of the injury, characterized by cross-sections of the regrown tissue in comparison with those of non-stimulated specimens. In this experiment, non-stimulated controls exhibited atrophic muscles due to the lack of hypertrophy promoted by magnetic stimulation. Immunostaining of muscles depicted higher expression of MHC in comparison with controls, and western blots confirmed previous results showing a 3-fold increase in MyH1 in contrast with non-stimulated tissues. Moreover, magnetic fields showed the ability to improve the contraction of muscles, due to re-innervation effects produced by the stimulation. Under magnetic stimulation, 3-fold higher formations of NMJ were confirmed in the stimulated tissues in comparison with controls. This observation confirmed the effects of magnetic stimulation as a potential treatment for muscle injuries as well as on nerve regeneration during muscle failure.

Magnetic stimulation has also been implemented in SMT engineering to study its effects in *in vitro* models in 2D or 3D cultured systems; however, one of the major drawbacks of applying direct magnetic fields on different types of cells is the possibility to generate abnormality in terms of cell growth (cancer) due to the rising magnitude of the magnetic field (1–10 T).<sup>[113]</sup> For instance, 2D culture of skeletal muscle (L6) cells was studied by Coletti et al.<sup>[114]</sup> using static magnetic fields (SMF). Initially, cells were cultivated for 1 day and differentiated for 4 days. SMF exposure started immediately after cell seeding and continued throughout the duration of the experiments. Magnetic stimulation (80 mT) was applied on the cell monolayer using a custom-made device, while a control system was cultured without stimulation for 5 days. Aligned and organized actin filaments were detected after Actin/nuclei staining in contrasts with non-stimulated controls, and a significant number of cells showed successful fusion and formation of myotubes (65% ± 3.6%). Mueller et al.<sup>[115]</sup> also studied the application and effect of a SMF  $\approx 80 \pm 5$  mT on a coculture system of myoblasts/mesenchymal stem cells. In this study, no difference in terms of the levels of Myf5 marker was detected.<sup>[115]</sup>

Strong SMFs are often discussed, as they have the potential to help guide myofilament orientation. Sakurai et al.<sup>[116]</sup> used a magnetic gradient of  $0\text{--}41.7$  T m<sup>-1</sup> with a flux density of  $0\text{--}10$  T on differentiated C2C12 myoblasts, in order to assess the minimum field necessary for guiding myotubes orientation during differentiation. As a result, after 6 days of differentiation and magnetic stimulation, C2C12 cells showed a positive time-dependent proliferative response, with the myoblasts successfully forming a closely packed and aligned structure. When a magnetic field is applied on biological materials, there is the production of a torque force (diamagnetic anisotropy), that is key for aligning the actin within differentiated myotubes, subsequently increasing their length. These results suggested that the highest magnetic gradient (41.7 T m<sup>-1</sup>) and density (10 T) depicted significantly better myotube orientation in contrast with lowest tested densities (3 T), which provided only a moderate flux and no production of diamagnetic anisotropy. Finally, differentiation and proliferation characteristics of both stimulated and non-stimulated cells were studied by immunostaining of MHC. Results showed that even where there was a slight increase in the MHC content of stimulated cells in comparison

with control, the differences were not significant. Furthermore, no differences in cell viability were detected, indicating that the magnetic fields did not lead to any observable apoptotic effect on studied 2D models.<sup>[116]</sup>

Limited studies on the application of magnetic fields on 3D models have also been reported. For instance, Li et al.<sup>[117]</sup> reported on the application of a non-mechanical actuation by imposing an external magnetic field on self-fabricated cell-laden hydrogels ( $\mu$ MACs) in GelMA.  $\mu$ MACs were fabricated by developing a mold system composed of poly(methyl methacrylate). Subsequently, a layer of poly(ethylene) terephthalate (PET) was used to cover the base of the mold, whilst the top part was covered with a photomask. To induce magnetic actuation on the constructs, the authors applied different strains (10, 20, 40 and 60%) on a mold coated with a mixture of poly(ethylene glycol) dimethacrylate (PEGDMA)/Fe<sub>3</sub>O<sub>4</sub> particles. Finally, different GelMA solutions (10%, 15 and 20% w/v) containing C2C12 cells were pipetted on top of the magnetic layer. As a control system, a PEGDMA (10% w/v) sphere encapsulating just Fe<sub>3</sub>O<sub>4</sub> nanoparticles (5% w/v) underwent the same magnetic fields (Figure 16A). Subsequently, after 6 h of encapsulation, both the muscle-like constructs and the control were magnetically stimulated for 10 h per day (10 days) using a NdFeB permanent magnet (Figure 16B). After 10 days of differentiation in the 10% GelMA/PEDGMA magnetic hydrogel, the results showed successful myotube maturation and alignment within cell-laden constructs strained at 40%. In contrast, there were few differentiated myotubes with constructs strained at 60%, and no myotube development at all with constructs strained at 20% (Figure 16C). Moreover, higher mRNA levels of transcriptional regulators such as MHC ( $\approx 0.1$ ) for 3D constructs strained at 40%, in comparison with  $\mu$ MACs strained at 20% ( $\approx 0.01$ ) and 60% ( $\approx 0.025$ ). It was concluded that higher magnetic strains (40 and 60%) can enhance the maturation of differentiated myotubes. Nonetheless, in order to appropriately construct a closely packed array of healthy myotubes, 40% strain was determined to be the best condition to provide appropriate external cues. These cues were determined to be able to trigger the required mechanobiological properties of encapsulated cells.<sup>[117]</sup>

Another report on the benefits of magnetic fields on SMT engineered constructs were published by Yamamoto et al.<sup>[118]</sup> They cultured C2C12 cells in medium containing magnetite cationic liposomes (MCLs) for 8 h in order to induce the cellular uptake of the MCLs (100 pg/cell). Subsequently, MCL-labeled cells were seeded in an annular gap between the wall of a 24 well-plate and a fixed polycarbonate cylinder (12 mm diameter) within the well, with a cylindrical neodymium magnet (30 mm × 15 mm) providing the external magnetic field. Formation of a ring-cell shape structure was achieved after 2 days of cultivation, after which 0.1 mL of ECM solution (collagen type I/Matrigel) was poured on top of the cells. After a further 4 h of culture, the cell-ring structure was placed on two stainless-steel pins in a 35mm culture dish to promote alignment via static strain, and myogenesis was induced by adding differentiation medium. Moreover, two carbon electrodes were placed on both sides of the petri dish and magnetic induction of 0.4 T was imposed using electrical pulses (15 V, 10 ms) for  $\approx 20$  days. Histological analysis showed

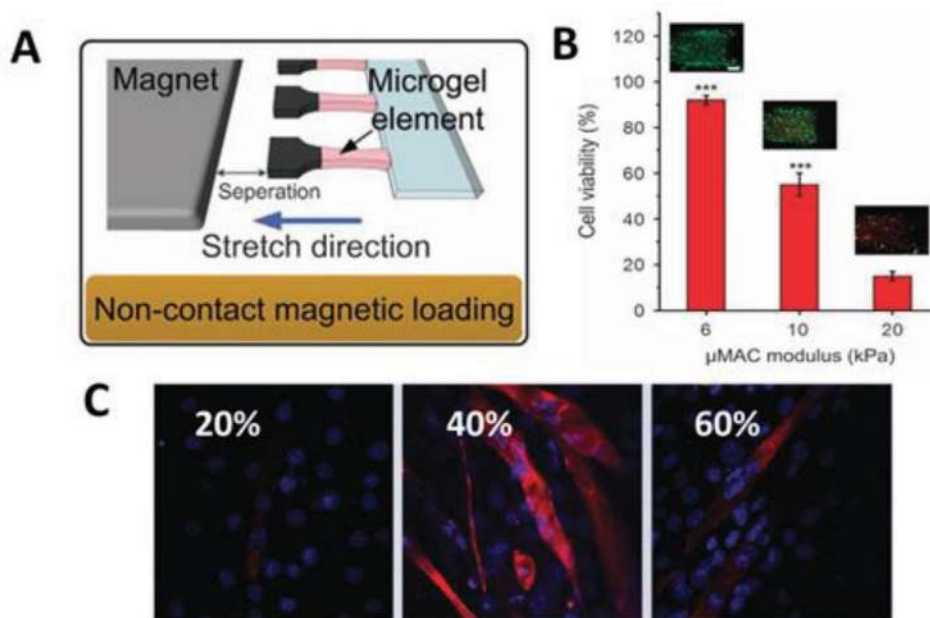


**Figure 16.** Magnetic stimulation approaching 3D muscle-like systems. A) Schematic representation of cell-laden hydrogels stimulated magnetically using a non-contact magnet, B) Viability percentage and Live/dead fluorescent images of C2C12 cells stretched on  $\mu$ MACs with different GelMA concentrations (10, 15 and 20 w/v%) displaying correspondent elastic moduli (6, 10, and 20 kPa) and C) Confocal fluorescent images of magnetically oriented myotubes within  $\mu$ MAC s (GelMA 10%) at different strains (20, 40 and 60%). Adapted with permission.<sup>[117]</sup> Copyright 2016, Springer Nature.

that the content of MCL particles did not affect cell viability of the 3D ring-like constructs, preserving stability of the construct during magnetic stimulation. Furthermore, control samples without intracellular MCLs displayed cell-sheet formation around the magnet due to magnetic forces, forces that subsequently caused the control cells to detach from the ECM. At the completion of the experiment, there were clear myofiber formations on the MCL-labeled cells, arranged parallel within the cylindrical structure.<sup>[96]</sup>

Most of the conducted studies have shown in 2D systems that a minimum magnetic flux density of  $\approx 10$  T is required to boost the myofiber differentiation and subsequent alignment. However,  $\alpha$ -actinin, F-actin and nuclei staining depicted sarcomere formation within aligned myotubes, indicating that distribution of low magnetic fields (0.4 T) through the material, resulted in beneficial results in stimulated cells. Indeed the contractile responses triggered by magnetic fields on developed 3D myotubes confirms the importance of exploring new alternatives in terms of external stimuli. In conclusion, magnetic fields are a powerful tool for the successful regeneration of skeletal muscle for both in vitro and in vivo models, especially as a non-invasive alternative to ES. There has been no report on DNA damages of cells after exposure to different magnetic fields thus far, and the techniques reviewed here have all significantly improved the proliferation and differentiation capabilities of the various muscle fibers. However, the real mechanism of how such magnetic fields can impact the neuronal response within the muscle, and consequently how it will impact self-regenerative processes, is still under investigation. An overview of all important parameters and obtained results for mechanical, electrical and magnetic stimulation of skeletal muscle cells is shown in **Table 1**.

#### 4.4. Chemical Stimuli

In recent years, researchers have attempted to dissect the complex mechanisms involved in the proliferation and differentiation of SMT via chemical stimulation. While the general chemical pathways and the proteins that comprise them have been identified, there is still a lack of knowledge about how these pathways regulate themselves and each other. Additionally, many chemical techniques have been used to probe specific known signaling pathways. Researchers can further elucidate the contribution of each pathway over the myogenic behavior of the skeletal muscle cells. This section will focus on the researches that have used growth factors or other chemical stimulants to activate the robust regulatory pathways that maintain the crucial SMT functions, whether it be via increased proliferation of myoblasts or through the widening of muscle fiber diameters in tissue engineered structure.

Many studies assess the effects of growth factors on myoblasts and differentiated myotubes. Growth factors are signaling molecules that impact most of the tissues in the body.<sup>[119]</sup> In SMT, there are different types of growth factors that appear at different times during skeletal muscle development, such as IGF, fibroblast growth factor (FGF), transforming growth factor (TGF), hepatocyte growth factor (HGF), and platelet-derived growth factor (PDGF).<sup>[119a,120]</sup> Each of these growth factors can have a variety of isoforms with unique impacts on skeletal muscle differentiation; for example, FGF-19 has been shown to cause important muscle hypertrophy alongside increased functional capabilities, whereas FGF-21 has been found to have no direct impact on the proliferation or differentiation of skeletal muscle cells.<sup>[121]</sup> The majority of the work on growth factors and their impact on muscle differentiation has been reviewed elsewhere.<sup>[10,122]</sup>

**Table 1.** Overview on important parameters and obtained results for mechanical, electrical and magnetic stimulation.

Type of Stimuli	Device	Voltage (V)	Frequency (Hz)	Strain (%)	Magnetix Flux (T)	Duration (days)	Type of cells/tissue	Results	Ref.
MS	Externally mounted stimulator with stainless steel electrodes	N/A	10	N/A	N/A	3	Soleus muscle hind limbs (Rabbits)	<ul style="list-style-type: none"> <li>· Rapid activation of myosin heavy chain.</li> <li>· Production of slow, type I and fast oxidative IIA fibers</li> <li>· Loss of tissue mass started to appear for constant stretching</li> </ul>	[91]
MS	Flexercell FX-4000 Tension Plus System	N/A	0.6	-10 (CSDS) 8 h -6 (ALDS) 60 s	N/A	4	NHDF monolayer on Bioflex membrane and C2C12 monolayer on petri dish	<ul style="list-style-type: none"> <li>· Fibroblast layer induces higher expression of different cytokines on C2C12 cells.</li> <li>· higher myogenesis due to the co culture</li> </ul>	[92]
MS	Self-made culture device (Gripper for hydrogel fibers, actuator by stepping motor)	N/A	1	3	N/A	2	C2C12 encapsulated in core-shell collagen hydrogels.	<ul style="list-style-type: none"> <li>· Core-shells hydrogel led to mimicking muscle fibrous structure.</li> <li>· Random alignment on 2D systems was overcome by constant mechanical stretching.</li> <li>· Elongation through the fiber axis due to external stimulation.</li> </ul>	[94]
MS	MagneTissue (Self-made bioreactor)	N/A	N/A	10	N/A	≈10	C2C12 cells encapsulated in fibrin gels.	<ul style="list-style-type: none"> <li>· after 3 days of MS mature tissue was formed</li> <li>· Cell alignment enhanced by strain-effect transmission.</li> <li>· Significant expression of MyoD and Myogenin markers.</li> </ul>	[93]
MS	Self-made bioreactor	N/A	0.5	≈2 (Static vs Constant)	N/A	13	C2C12 cells seeded on microfibrinous DegraPol strips.	<ul style="list-style-type: none"> <li>· Significant reduction in MHC expression for static stimulation in comparison with cyclic models.</li> <li>· Higher alignment and density under cyclic stretching.</li> </ul>	[96]
ES	Self-made battery-powered stimulator	39 ± 14 V	N/A	N/A	N/A	7–10	15 muscle biopsies (vastus lateralis) from 15 old patients.	<ul style="list-style-type: none"> <li>· Higher expression of Ca<sup>2+</sup> proteins.</li> <li>· Muscle restoration achieved on soleus and VL muscle</li> </ul>	[102]
ES	C-Pace Culture Pacer (IonOptix)	4 V cm <sup>-1</sup>	6	N/A	N/A	2–3	3D bioartificial muscle (mBAMs)	<ul style="list-style-type: none"> <li>· Sarcomeric production leading to contraction at given frequency.</li> <li>· No striation achieved on 2D systems in contracts with high striations levels obtained on 3D stimulated scaffolds</li> </ul>	[104]
ES	Self-made electrical stimulator	N/A	1	N/A	N/A	6–10	C2C12 myotubes on top of an atelocollagen membrane	<ul style="list-style-type: none"> <li>· Correlation between contractility and 2-NBDG uptaking.</li> <li>· Higher myogenesis</li> </ul>	[103]
ES	Carbon flat electrodes (BMK Designs)	40 V cm <sup>-1</sup>	N/A	N/A	N/A	8	Human myoblasts on a Matrigel/fibrin solution	<ul style="list-style-type: none"> <li>· Reduction in oxygen consumption due to hydrogel presence.</li> <li>· Significant improvement in muscle cells respiration</li> </ul>	[105]
ES	Pulse stimulator	0.7 V mm <sup>-1</sup>	5, 10 and 20	N/A	N/A	≈10	Muscle skeletal bundles around PEDOT/PU wire films	<ul style="list-style-type: none"> <li>· Sarcomeric expression.</li> <li>· No significant cellular damage.</li> <li>· Monocyte chemoattraction</li> </ul>	[107]
ES	Self-made PDMS chamber for conducting ES using LabView.	N/A	1–10	N/A	N/A	≈20	Myobundles (iSKM)	<ul style="list-style-type: none"> <li>· Significant increase of nuclei and cross sections for 3D constructs in contrast with 2D cell systems.</li> <li>· Rapid sarcomeric development and larger myotube</li> </ul>	[106]
Magnetic	Biocon 2000 W	N/A	10 and 50	N/A	N/A	5	Injury in Quadriceps from C57 mice	<ul style="list-style-type: none"> <li>· Faster restoration of injury (Higher cross-sections formation).</li> <li>· Lack of hypertrophy due to absence of stimulation.</li> <li>· Higher expression of MHC levels</li> </ul>	[112]

**Table 1.** Continued.

Type of Stimuli	Device	Voltage (V)	Frequency (Hz)	Strain (%)	Magnetix Flux (T)	Duration (days)	Type of cells/tissue	Results	Ref.
Magnetic	Custom-made 4 cm × 4 cm Neodymium magnetic plaques	N/A	N/A	N/A	80 mT	5	Static magnetic fields (SMF) on mammal skeletal muscle cells (L6).	· Faster alignment after differentiation for stimulated myotubes in contrast with non-stimulated ones, due to an increase in the number of myoblast fused	[114]
Magnetic	Custom-made 4 cm × 4 cm Neodymium magnetic plaques	N/A	N/A	N/A	80 mT	12	Static magnetic field on myoblasts/mesenchymal stem cells coculture.	· No significant difference among stimulated and non-stimulated cells in the expression of Myf5 marker. · AB confirmed higher proliferation rate for stimulated cells	[115]
Magnetic	Magnet bore (150 mm × 900 mm)	N/A	N/A	N/A	0–10 Gradient: 0–41.7 T m <sup>-1</sup>	6	C2C12 mouse-derived cells	· No effect on cell proliferation or myogenic differentiation. · No myotube orientation at 3 T	[116]
Magnetic	NdFeB permanent magnet	N/A	N/A	10, 20, 40, and 60	N/A	10	Self-fabricated cell-laden hydrogels (μMACs).	· Reduction of cell viability in GelMA 20% strain · Less myotube formation at 60% strain. · Higher expression of mRNA regulators for constructions strained at 40%.	[117]

Growth factors and proteoglycans, such as agrin, are also attractive for use in SMT engineering, as they are capable of activating signaling cascades that are known to regulate the development of mature, functional myotubes. IGF-1 in particular has been well-noted as a promoter of myoblast differentiation and the hypertrophy of differentiated myotubes; in recent years, the exact mechanisms of IGF-1 have been confirmed as operating via the mitogen-activated protein kinase (MAPK) and phosphatidylinositol 3-kinase (PI3K) signaling pathways.<sup>[123]</sup> Both of these pathways are crucial for the successful development of functional myotubes in vitro and in vivo, highlighting IGF-1 as a potentially important growth factor to include as a part of therapies. Other therapies have included agrin in 3D bioengineered artificial muscles (BAMs), in an attempt to create mature AChRs on the periphery of the differentiated myotubes.<sup>[124]</sup> These BAMs were constructed by culturing green fluorescent protein-transduced CH3 mouse myoblasts between two silicone posts, allowing for aligned, 3D tissues to form. After 14 days of culturing, Wang et al. placed 6 μL 1 U mL<sup>-1</sup> of agrin into a solution of differentiation media; agrin is noted in literature as having a positive impact on AChR clustering in myofibers, which is an important physical characteristic of mature, functional muscle fibers. The treatment of agrin caused a 73-fold increase of AChR clustering in the BAM, however these AChRs were notably immature in both size and morphology.<sup>[124]</sup> Likewise, the MHC isoform content of the BAM was primarily perinatal and embryonic. The ever-present issue of immature myofiber phenotypes requires more work to resolve, than these experiments have provided.

Insulin-like growth factors, which include IGF-1, are peptide growth hormones that assist in the formation of mature myotubes during the later stages of embryogenesis as well as in the regeneration of damaged muscle fibers.<sup>[10,123,125]</sup> Recent studies have found that IGF-1 and HGF work via the p38 MAPK and

PI3K pathways to activate satellite cells for muscle repair after an injury, while a daily injection of recombinant FGF-19 over 7 days has been found to promote the phosphorylation of extracellular-signal-regulated protein kinase 1/2 (ERK1/2) in adult murine models.<sup>[10,121b]</sup> ERK1/2 is part of another important cascade mechanism, which can promote either the proliferation of satellite cells or the differentiation of those cells into myotubes, depending on how prolonged the pathway activation is.<sup>[126]</sup> The intricacies of these pathways have been slowly revealed in recent years, allowing increasingly targeted therapies to be attempted on both in vitro and in vivo diseased and atrophied muscle models.

Growth factors affect the expression of key MRFs in different ways, which is important when considering which growth factors to include in specific therapies. While FGF-19 promotes activation of satellite cell populations and induces hypertrophy in adult mice models, it has no impact on the expression of the various MRFs; the same is true for HGF and PDGF.<sup>[10,121b]</sup> IGFBP-6, however, was able to upregulate MyoD, Myogenin, and total MHC levels in pediatric mesenchymal stem cells (PMSCs)<sup>[119b]</sup>, while IGF-1 is likewise known to increase the expression of MHC and tropomyosin, resulting in more mature muscle fibers.<sup>[119a]</sup> By utilizing these growth factors, researchers can use the natural signaling pathways of the body to assist with tissue engineering approaches.

Apart from growth factors, researchers have used other therapies inspired from different chemicals used in natural skeletal muscle development and maintenance in order to potentially build up a portfolio of singular techniques that, although relatively limited in their individual therapeutic potential, can be used in tandem to great effect. Researchers have assessed the impact of specific chemicals already utilized in various natural processes, such as calcium<sup>[14a]</sup>, thyroid hormones,<sup>[16]</sup> and choline<sup>[127]</sup> on muscle development. Various studies in



the past two decades have found success in increasing the muscle mass of both young and old mice models via the use of  $\beta$ -adrenoceptors, specifically the  $\beta_2$ -adrenoceptors found in SMT.<sup>[128]</sup>  $\beta$ -adrenoceptors are a specific type of G-protein coupled receptor that operate in a multitude of signaling pathways throughout the body; in skeletal muscle, the  $\beta$ -adrenoceptor isoform that is most commonly seen is the  $\beta_2$ -adrenoceptor.<sup>[129]</sup>  $\beta_2$ -adrenoceptors use G-proteins to activate the PI3K-Akt signaling pathway, which utilizes an amalgamation of other proteins and signaling molecules in order to activate mTOR and other transcription factors.<sup>[130]</sup> Previously, this isoform has been activated through chemicals such as fenoterol, a  $\beta_2$ -adrenoceptor agonist which has unfortunate protein degradative side effects as well as problematic off-target impacts, both due to the relatively long exposure times required for desired results.<sup>[131]</sup> Hagg et al.<sup>[129]</sup> were able to bypass the usage of agonists such as these, and their side effects, by using recombinant adeno-associated virus-based vectors (rAAV) for  $\beta_2$ -adrenoceptor gene delivery. Through a single injection of  $1 \times 10^{10}$  of the rAAV/ $\beta_2$ -adrenoceptor genomes, the authors were able to induce a 22% increase in the muscle mass of tibialis anterior muscles of adult mice, which maintained for the duration of their 84-day long experiment; this is equivalent to the increase in muscle mass that was seen with 28 days of repeated formoterol treatment.<sup>[129]</sup>

Some researchers have made significant improvements on muscle differentiation by changing standard culturing procedures in vitro, while others have experimented with altering the dosage of known inducers of muscle atrophy in order to promote myotube formation. While the gold standard for differentiation media traditionally contains streptomycin with 25 mM of glucose, Khodabukus and Barr reported on how lowering the glucose levels to 10 mM and removing streptomycin might impact muscle development.<sup>[132]</sup> They found that total MHC decreased with 10 mM glucose levels supplemented with streptomycin, compared to the traditional 25 mM glucose found in control media. However, MyoD levels were higher in conditions where glucose was decreased, while Myogenin was expressed more under the traditional, high glucose conditions, whereas Myf5 and MHC isoforms were not significantly different among any of the groups.<sup>[132]</sup> In fact, streptomycin has been found to decrease force production in bioengineered C2C12 constructs, by causing a fast-to-slow SERCA isoform shift.<sup>[3]</sup> This, combined with streptomycin's abilities as a calcium blocker for muscle cells, creates a narrative where it is difficult to consider including streptomycin in experiments without taking these characteristics into consideration.

Similarly, the effect of the dosage of dexamethasone (DEX) on differentiation of C2C12 mouse myoblasts was investigated as DEX is known to induce muscle atrophy at high doses<sup>[121b,133]</sup> Immunocytochemical analysis showed sarcomere development in samples treated with 10 nM of DEX at day 6 of muscle culture, whereas few sarcomeres were formed in controls without DEX.<sup>[133]</sup>

#### 4.5. Biological Stimuli

In SMT engineering, it has been important to try to use as many tools as possible in order to learn more about what exact

stimuli myoblasts require in order to successfully differentiate into mature, functional myotubes. In vivo, a crucial amount of information is taken by the differentiating myoblasts from the cellular environment around them; this information is derived from the types of cells that constitute that environment, as well as from the materials they extrude into the ECM.<sup>[9,134]</sup> By including different types of cells, such as fibroblasts or MNs, into skeletal muscle stimulation methods, researchers have been able to theorize exactly what effects these cells will have on the proliferation and differentiation of skeletal muscle cells. For example, fibroblasts are cells that act in predominantly supporting roles throughout the body, including in SMT. They have been a target of research by tissue engineers due to the matrix materials, such as collagen, that they frequently lay down following an injury.<sup>[135]</sup> In vitro cocultures of fibroblast and myoblasts are not entirely new concepts, as they have seen success in the creation of 2D and 3D muscle organoids in the past few decades.<sup>[136]</sup> In recent years, however, their role in the development of functional SMT has been further elucidated, due to the dedicated continuation of crucial coculture studies.<sup>[137]</sup>

During the muscle repair process after an injury, the wound site is typically flooded with a variety of cells, including macrophages, fibroblasts, and regenerative satellite cells.<sup>[20b]</sup> These cells have a significant impact on myogenic migration and proliferation in vitro if cultured together, as reported by Venter et al.<sup>[138]</sup> Their experiments investigated the proliferative and migratory effects on myoblasts, compared between three experimental groups: myoblast/macrophage cocultures, myoblast/fibroblast cocultures, and a triple coculture with all three cell types. In individual cocultures, fibroblast cells would promote the migration of myoblasts whereas macrophages could only promote their proliferation. Specifically, the promoted migratory effects seen in the myoblast/fibroblast coculture were not reproducible in the triple coculture, indicating that particular response was inhibited in some way by the presence of the macrophages.<sup>[138]</sup> The exact mechanisms for these responses are as of yet unknown.

Myoblasts are not only impacted by other cell types, but they have been shown to be impactful in their own rights. Fry et al.<sup>[139]</sup> performed an in vivo analysis of fibroblasts and myoblasts in a model of early hypertrophy. Their results indicate that the early presence of myoblasts could lessen the amount of fibrotic collagen produced by fibroblasts, even if those myoblasts are only present for a short period of time.<sup>[139]</sup> If the goal is to replace and repair damaged muscle fibers with functional adult myofibers, then tissue engineers must focus on the techniques that reduce and prevent fibrosis just as they must focus on those that promote healthy myogenesis. Myofibroblasts, however, have been shown to interact with C2C12 cells in 3D cocultures in a positive way; Krieger et al.<sup>[140]</sup> indicated that, when compared to mono-cultures as well as fibroblast/myoblast cocultures, myofibroblast/myoblast cocultures produced myotubes that were distinctly thicker and more multinucleated. This more mature morphological phenotype implies that myofibroblasts promote the differentiation of myoblasts significantly when cultured together, than monoculture.<sup>[140]</sup>

In order to provide the appropriate amount of energy needed for skeletal muscles to function, a highly integrated vascular system is required. Vascular cells, such as endothelial cells,

have a robust relationship with the satellite cells, myoblasts, and myotubes that comprise the muscular system.<sup>[144]</sup> The lack of a vascular network in large, engineered muscle tissues, both *in vitro* and *in vivo*, frequently results in necrosis and tissue failure. Therefore, the diffusion limit of oxygen and other nutrients in the absence of a vascular system is one of the single most important barriers for the development of *in vitro* skeletal muscles, as well as for the field of tissue engineering as a whole.<sup>[142]</sup> Angiogenesis, or the vascularization of bulk tissues, is a complex and multi-faceted process, and is far outside the scope of this review; however, the inclusion of endothelial cells into co-cultures with myoblasts is an ever-evolving part of skeletal muscle tissue engineering, and should be discussed here.

Current knowledge about the exact crosstalk pathways that endothelial cells and myogenic precursors utilize in their synergistic dialogues is, unfortunately, lacking. Researchers have known for decades that the connection between endothelial cells and muscle satellite cells goes beyond their close spatial proximity; these two cell types coordinate to each promote the migration, proliferation, and differentiation of the other.<sup>[141]</sup> In recent years, these cells have been re-introduced to each other *in vitro* to further investigate how far this coordination can potentially go. Gholobova et al.<sup>[61]</sup> introduced human umbilical vein endothelial cells (HUVECs) to their BAM model in 2015, in an attempt to pre-vascularize their muscle constructs. Their results indicated that a 70:30 or 60:40 ratio of human muscle cells to HUVECs promoted the proliferation and alignment of the resultant myofibers significantly more than a simple 50:50 ratio. These myofibers, however, were cultured in endothelial growth media (EGM), in order to maintain both cell populations without rampant cell death. These myofibers had no cross-striations visible after 7 days of co-culture, potentially due to the lack of muscle-specific growth or differentiation media or to the short culturing time frame.<sup>[61]</sup> Latroche et al.<sup>[143]</sup> investigated whether media, conditioned by endothelial cells, could potentially carry some of their benefits when this conditioned media is cultured together with human myoblasts. Their 2017 study found that endothelial cell-conditioned media promoted the proliferation and myogenin expression of human myoblasts; however, no other MRFs were analyzed outside of myogenin, and the overall maturity of the resultant myofibers is not known.<sup>[143]</sup>

Due to the inherent dependency that myofibers have on electrical stimulation, MNSs have also been identified as an important biological factor to consider in skeletal muscle development. MNs taken from the ventral spinal cord in particular have had a history of successful cocultures with skeletal myoblasts.<sup>[144]</sup> As MNs attach to myofibers, they form NMJs, which have been successfully formed in 3D coculture experiments *in vitro* and subsequently used to stimulate myofibers both chemically and electrically.<sup>[98,145]</sup> Unfortunately, these methods of stimulation frequently result in phenotypically immature myofibers, as the neural networks formed between MNs and myoblasts do not provide enough stimulation to promote mature myogenic differentiation.<sup>[146]</sup> Bakooshli et al.<sup>[147]</sup> investigated this with a set of experiments culturing MN clusters onto 3D fibrin/Geltrex hydrogels seeded with human myogenic progenitor cells and human fibroblast-like cell lines. After two weeks of culture, the 3D hydrogel environment had promoted thicker, more functional myotube formation alongside greater

neurite regrowth from the MN clusters than the 2D controls. This triple coculture provided an optimal environment for the formation of aligned myotubes with detected neurite regrowth into AChRs; unfortunately, without data on the specific MHC isoforms, it is unclear whether or not the coculture produced myotubes with mature phenotypes.<sup>[147]</sup>

While traditional coculturing methods have had cell-to-cell contact, the advent of microfluidic devices allows researchers to provide some segregation to their cell populations, mimicking the *in vivo* environment while still retaining the benefits of coculturing two different types of cells together.<sup>[148]</sup> Uzel et al.<sup>[149]</sup> reported on the development of one such microfluidic device that used traditional C2C12 myoblasts along with gene-edited MNs that were susceptible to optical stimulation. By optically stimulating the MNs in one well of their device, the researchers could see a contractile twitch response in the myofibers of the other well. Immunostaining confirmed the presence of striated sarcomeric structures, presumably promoted and enhanced by the presence of the stimulating neural network.<sup>[149]</sup> Zahavi et al.<sup>[150]</sup> performed a similar study with their own microfluidic neuromuscular coculture, and found that the contractile behavior of innervated myotubes is significantly stronger and more frequent than that of non-innervated fibers.<sup>[150–151]</sup>

Monitoring the Ca<sup>2+</sup> fluxes in myofibers in response to stimulation via neural networks is increasingly important to dissect the impact that MNs have on the determination of myofiber phenotype. Juhas et al.<sup>[152]</sup> published a method to analyze these fluxes in real time through the use of a dorsal window implantation in a rat model. They implanted differentiated and undifferentiated skeletal muscle constructs into a dorsal skinfold window, together with the introduction of an intracellular Ca<sup>2+</sup> sensor that could be measured via the window. Post-implantation analysis indicated that previously-differentiated myofibers produced significantly larger myofibers than the un-differentiated samples. Their subsequent significantly higher force production capabilities were attributed to increased Ca<sup>2+</sup> fluxes, along with an ingrowth of new blood vessels from the host.<sup>[98,152]</sup>

#### 4.6. Combinations of Multiple Stimulation Methods

Thus far, in this review, important research has been highlighted that focuses on specific methods of external and internal stimulation of SMT. While each published report helps to clear the way for future research, the ultimate success of these endeavors will not be built on the backs of any individual method; it will be the cumulation of these techniques, rather, that will be the key to developing useful and critical tissue engineering strategies for skeletal muscle regeneration. This next section focuses on the recent work that has found interesting and successful ways of bringing together multiple methods of skeletal muscle stimulation in order to promote appropriate muscle growth *in vitro* and *in vivo*.

##### 4.6.1. Biological and Topographical Co-Stimulation

As discussed previously, the inclusion of different cell types in coculture studies with skeletal muscle progenitors has

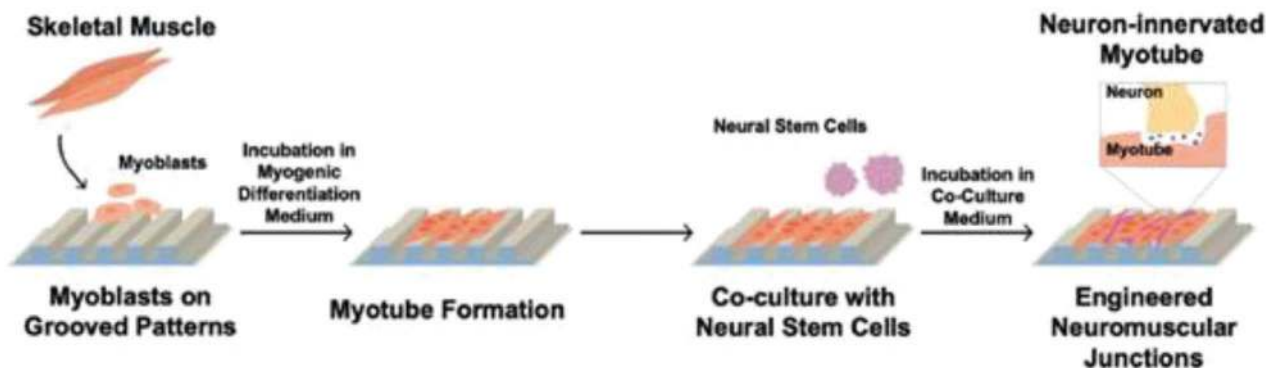


**Figure 17.** Primary myoblasts are plated onto micro-grooved patterns and differentiated. Following differentiation, neural stem cells were cocultured on top of the myotubes and differentiated into neural networks. Adapted under the terms of a Creative Commons Attribution 4.0 International License.<sup>[145]</sup> Copyright 2019, The Authors, published by Wiley-VCH.

shown researchers that biological entities such as fibroblasts, endothelial cells, and chemical growth factors have a positive effect on the proliferative and myogenic properties of myoblasts.<sup>[98,139,148,151,153]</sup> These studies have been carried forward and enhanced using techniques that provide mechanical stimuli in addition to studies with coculture, in an effort to further enhance their promyogenic results. Since the promotion of alignment is such a crucial aspect in mechanical stimulation studies, researchers have used micro-grooved substrates to promote the alignment of various myoblast cocultures.<sup>[2,145,154]</sup> Ko et al.<sup>[145]</sup> advanced neural and muscle cocultures by plating primary myoblasts and neural stem cells together onto a micro-grooved poly(urethane acrylate) (PLA) substrate, which was coated with Matrigel to promote cell attachment, shown in **Figure 17**. The authors found that the 1600 nm grooves in the substrate promoted the anisotropic alignment of the myoblasts, with the additional benefit of parallel axon ingrowth into the subsequently differentiated myotubes. This structure proved to be significantly more sensitive to chemical stimulation than an equivalent coculture plated on a simple flat surface.<sup>[145]</sup>

Similarly, a chitosan-coated surface was used to promote the attachment of fibroblasts and primary myoblasts, in an effort to promote beneficial organization of F-actin and integrin  $\beta$ , both key players in skeletal muscle regeneration.<sup>[155]</sup> The inclusion of chitosan-coated plates in the coculture study promoted the proliferation of myoblasts while simultaneously inhibiting the attachment of fibroblasts, which is the preferred result for applications using 1:1 cocultures of fibroblasts and myoblasts. By slightly inhibiting the attachment of fibroblasts, the chitosan coating inhibits the fibrotic tissue formation which frequently results in nonfunctional scar tissue. Unfortunately, this study did not look at the effects that this substrate had on the differentiation of these myoblasts.<sup>[155b]</sup>

Ito et al.<sup>[156]</sup> also progressed their own previous work that had studied the effects of IGF-1 on myoblast differentiation, through the use of gene-edited myoblasts and the addition of DOX. They attempted to culture the same gene-edited myoblasts onto various cultured surfaces that were each coated with a particular ECM protein, such as fibronectin, type I collagen, laminin, and type IV collagen. In the presence of DOX, these cells had the most improved motility and proliferation on type

IV collagen-coated surfaces; unfortunately, none of the surfaces significantly changed the differentiation rates or myotube structures once the myoblasts were differentiated. However, the promoted proliferative responses do correspond to a more mature phenotype, and the additional over-expression of IGF-1 caused by the addition of DOX was able to still promote differentiation over controls.<sup>[156a]</sup> This work, along with additional work using VEGF-gene edited sheets to promote muscle differentiation, is a promising step to the development of robust in vitro differentiation techniques.<sup>[157]</sup>

In recent work, there has been an influx of skeletal muscle studies done on substrates patterned through a variety of fiber-spinning techniques.<sup>[39,52,154a-d]</sup> In 2018, Ebrahimi et al. used a microfluidic spinning apparatus to create defined, micropatterned substrates using GelMA hydrogel fibers.<sup>[39]</sup> By culturing C2C12 myoblasts onto this micropatterned surface with the addition of 100 ng mL<sup>-1</sup> of agrin, they were able to produce C2C12 with a higher percentage of AChR clusters, regardless of whether the GelMA fibers were extruded with a defined micropatterned surface or as nonpatterned fibers. Interestingly, this experiment also showed that agrin promoted the differentiation of myoblasts into functional myotubes with higher amplitudes of contractions, further confirmed by an increased expression of sarcomeric actin, Myogenin, and fast type IIX MHC.

#### 4.6.2. Electrical and Mechanical Co-Stimulation

Mechanical techniques are particularly applicable in combination with electrical methods, as their stimulation methods are typically on similar timescales and can be done using similar equipment.<sup>[158]</sup> Recent research has pointed to particularly interesting results involving out-of-phase co-stimulation, such as the work done by Kim et al. showing the correct propagation of the impulses and contractility responses exerted by the myotubes.<sup>[158]</sup> They found that engineered 3D fascicle-inspired muscle constructs (C2C12 myoblasts mixed with fibrinogen and Matrigel) had 31% better functional performance after 20 minutes of co-stimulation, where a mechanical cantilever would induce 2.3% strain until an electric potential was administered. The electric potential produced an electric field of 2.5 V mm<sup>-1</sup>

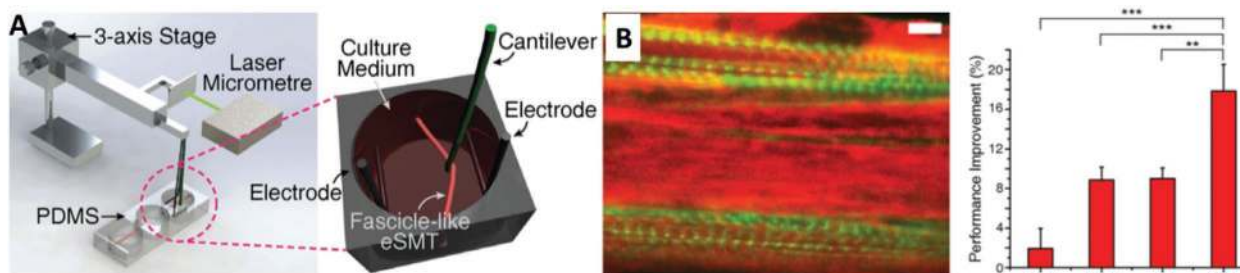


**Figure 18.** A) Schematic representation of co-stimulation of skeletal muscle constructs, consisting of parallel electrodes for applications of electrical potential and cantilever wire moved by a servomotor in order to stretch sideways using the desired strain. B) Fluorescent images of well-aligned collagen (red) and actin (green) fibers obtained after ES (5  $\mu\text{m}$ ) and performance improvement obtained in the levels of contractile forces achieved by individual stimulation in contrast with co-stimulation approach. Adapted with permission.<sup>[158]</sup> Copyright 2019, Nature Springer.

by two platinum wires with bipolar pulse of 1 ms, structured to be combined with the mechanical stimulation at a  $180^\circ$  phase shift.<sup>[158]</sup> (Figure 18A). Immunostaining results depicted that co-stimulation system led to a larger striation of  $\alpha$ -actinin, due to the enhancement in the transmission of external stimuli that triggered internal contraction forces of the myotubes within the 3D-fascicles. Constant muscle stretching produced by the cantilever directed a faster propagation of the electrical pulses. Co-stimulation was applied at different frequencies (0.1, 0.23, and 0.45 Hz) finding that 0.23 Hz showed a better stimulation response. Furthermore, when it was compared with single ES and MS, there was a significant improvement in the way tissue maturation was achieved. Co-stimulated samples showed the production of well-aligned fibers, while single-stimulated 3D constructs showed significantly fewer benefits in the orientation of actin filaments after 3 min (Figure 18B). Overall, alternating applications of MS and ES resulted in higher contractility responses (20%) in contrast with individual stimulation, indicating that the initial mechanical stretching somehow impacted how the electrical current was transferred towards those myofibers enclosed in the Matrigel/fibrin gel.

In recent years, however, the conversation has also begun to include various aspects of nanotechnology, such as nanoparticles and nanotubes.<sup>[159]</sup> Boron nitride nanotubes were used to increase the myogenic differentiation effects in response to ultrasound stimulation in C2C12 myoblasts during an interesting coculture study performed by Ricotti et al.<sup>[154a]</sup> Since boron nitride nanotubes are capable of inducing an electrical stimulus in response to stress, the authors used ultrasound sources at 40 kHz for 10 seconds a day to upregulate MRFs and MHC conversions during differentiation. Moreover, Ostrovidov et al.<sup>[1b]</sup> demonstrated fabrication of aligned electrically conductive hybrid fibers from gelatin and multi-walled carbon nanotubes (MWNTs) to enhance the formation of aligned myotubes with improved contractibility. The improved mechanical properties of the resulting 20% gelatin fibers due to the presence of  $0.5 \text{ mg mL}^{-1}$  and  $5 \text{ mg mL}^{-1}$  MWNTs improved the myotube formation by comparing 20% gelatin fibers and hybrid fibers. Variable mechanical properties and electrical conductivity of fibers resulted in upregulation of the activation of mechanotransduction-related genes. However, this alone was not able to achieve the maturation required for these constructs to resemble native, mature muscle tissue; therefore, the function of the muscle tissue grown on these fibers was further

improved upon by applying additional continuous electrical pulses. Myotube contraction was analyzed after 4 days culture in differentiation medium and 2 additional days accompanied with electrical stimulation (5 V, 1 Hz, 1 ms duration). They observed by increasing the MWNT concentrations myotubes with higher maturation and contractibility were formed and the myotubes which were cultured on 20% gelatin fibers with  $0.5 \text{ mg mL}^{-1}$  MWNTs continuously contracted even after ES was OFF for more than 10 min indicating a high level of maturation.

The inclusion of electrical stimulation and mechanical stimulation, along with advancements in nanotechnology, has already bore important fruit, and it will be a key focus of research in the coming years to deduce specific mechanisms for the MHC isoform conversions that cause these differences in myofiber maturity.

#### 4.6.3. Electrical and Biological Co-Stimulation

Electrical stimulation studies have also been combined with biological co-cultures.<sup>[159f,160]</sup> Takahashi et al. took this work one step further, by using a stepwise experimental design to first induce myotube alignment prior to the use of electrical pulse stimulation (EPS).<sup>[161]</sup> The researchers first cocultured human dermal fibroblasts and human skeletal muscle myoblasts onto a thermoresponsive, micro-patterned acrylamide surface to induce alignment. These cells would then peel off at low temperatures and would be introduced into a Matrigel-containing fibrin gel; after seven days of differentiation in this gel, they would undergo electrical stimulation (10 V, 1 Hz, 3 ms duration) using a commercial C-Dish device (IonOptix) for two weeks post-differentiation. After two weeks of EPS, they found a significant increase of myotube diameter compared to control, with no significant difference between duration times used.<sup>[161]</sup> Confocal microscopy confirmed that contractions responses triggered in Matrigel/cell sheet system led to more aligned myofibers, with expression of laminin and Col IV in contrast with the random alignment of control sample which was a stimulated cell sheet cultured on a nonpatterned surface without Matrigel layer. Their work confirms work done by Ostrovidov et al. in 2014 in a similar experiment.<sup>[146a]</sup> Ostrovidov et al. used a micropatterned GelMA coculture system in combination with EPS, but with C2C12 and PC12 neural cells cocultured instead of fibroblasts and myoblasts. They applied

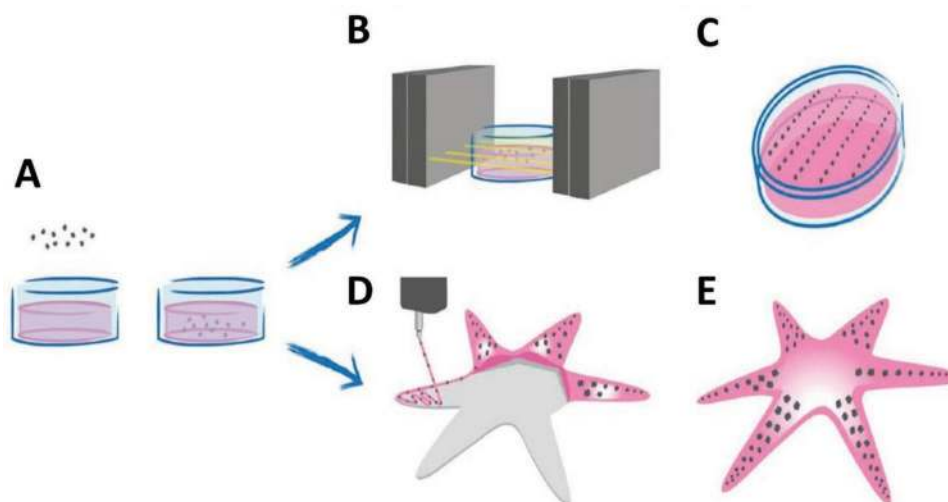


**Figure 19.** Iron oxide nanoparticles are suspended into a GelMA matrix A) and subsequently placed in an external magnetic field B). The magnetic particles form anisotropic lines along the magnetic field lines C) and can be bioprinted D) and crosslinked E) to form the desired substrates. Adapted with permission.<sup>[163]</sup> Copyright 2018, Wiley-VCH.

an electrical pulse (6 V, 1 Hz, 1 ms duration) for two days, and characterized changes in MRF expression due to the combination of enhanced alignment and induced EPS. The authors found that the co-culturing of C2C12 myoblasts with PC12 cells improved myotube formation and upregulated Myf5, MHC-IIx, MHC-IIb, and MHC-neo; they also found that the combined electrical stimulation significantly boosted those results even further.<sup>[146a]</sup>

#### 4.6.4. Magnetic and Mechanical Co-Stimulation

In terms of potential impact, the combination of magnetic particles and SMT engineering strategies seems a perfect match; skeletal muscle is a type of tissue that requires alignment and responds nicely to stimulation methods that provide a direction of force, and magnetic particles are capable of providing such a force via external magnetic fields. Particles, both magnetic and non-magnetic, have been successfully used in skeletal muscle studies to improve differentiation in 3D hydrogel environments.<sup>[159b,162]</sup> Tognato et al.<sup>[163]</sup> published a report that utilized iron oxide nanoparticles in a GelMA hydrogel to enhance myotube alignment and differentiation, as shown in **Figure 19**.<sup>[163]</sup> The iron oxide nanoparticles, once stimulated via an external magnetic field, produced anisotropic lines inside of the hydrogel; these anisotropic formations induced better alignment from the myoblasts embedded inside GelMA.<sup>[163]</sup> Even without differentiation media, the myoblasts were able to differentiate into myotubes with high cell numbers; unfortunately, no MHC isoforms were characterized, and therefore the phenotypes of those resultant fibers are unknown.

As always, the results of these experiments are difficult to compare with one another, due to the wide range of applications, hypotheses, and questions that these authors were attempting to resolve. For SMT engineering, the underlying constraint remains unanswered; the muscle fibers that are

created in vitro and in vivo are still phenotypically immature. These myofibers are still predominantly composed of MHC-neo isoforms, with contractile behaviors that are still orders of magnitude beneath those of native myofibers. Nonetheless, the research that has been completed in recent years has made significant progress towards the potential development of mature phenotypes, through the combined use of mechanical, electric, biological, and magnetic techniques.

## 5. Outlook

Recent years have seen advancement of fabrication and developmental techniques in formation of more complex models of human skeletal muscle with higher similarity in functionality and mimicking the physiological subtleties of native tissue. Applications of these developed models with multicellular structure range from more accurately modelling disease, to generating tissues for transplantation in VML. Mimicking the in vivo conditions in vitro, such as by applying various loadings or electrical impulses, as well as coculturing with supporting cells enables further maturation of the tissue. However, the field is yet in its infancy and there are still unanswered questions about the combinatorial effects of materials, regulators and cells on muscle maturation processes to form more representative human tissue models.

The question of how the muscle tissue will be connected to the native tissue after transplantation has to be faced in future studies. As it has been shown in this review, the progress that has been made mostly is focused on improving the function of the in vitro grown tissue. For medical applications like transplantation there are more factors to be considered. Moreover, to avoid necrosis of the tissue, the provision of nutrition and oxygen to the in vitro grown muscle tissue is essential and can be achieved by vascularization before implantation. Despite the efforts made until now, a permanent connection between native and implanted tissue could not be established.<sup>[164]</sup> Similarly,

the connection of the native nervous system to the transplanted tissue is paramount to achieve simultaneous contraction of both native and transplanted tissue and thus functionality. This issue has not been solved yet, although research shows progress in co-cultivating skeletal muscle cells and neuronal cells.<sup>[165]</sup>

As outlined above, the SMT engineering field has developed greatly in the last 10 years, moving forward to creating ever-increasing complexity and biomimetic tissues. In the next 10 years, we believe research on generating functional SMT research will focus on four major gaps. i) Production of multicellular tissues with similar functionality and contraction-induced forces equivalent to native tissue. Redesign of platforms for combinational stimulation and coculturing will result in maturation of tissue architecture. ii) Development of strategies for vascularization of engineered tissues to enable transport of nutrients, oxygen and soluble factors to cells, and thus facilitate the formation of larger engineered skeletal muscle constructs. iii) Modelling multi-tissue and multi-organ constructs. The development of multilineage organoids which can self-assemble vastly increases the potential of formation of multicellular structure with similar complexity as human muscle tissue. iv) Advancement in application of the SMT models for drug screening purposes which is less advanced than for cardiac and other tissues.<sup>[166]</sup> Further challenges exist to translate the outcomes of research studies to commercial manufacturing and widespread clinical application, including achieving scale-up, reproducibility and regulatory approvals.<sup>[167]</sup>

Apart from the medical applications, which were the main focus of this paper, growing skeletal muscle tissue is also attractive for other industries, particularly in the pharmaceutical and food sectors. Biomimetic engineered tissues open opportunities for high throughput and personalized drug screening to reduce the need to animal testing, accelerate the successful translation of drugs to clinic, and optimize patient outcomes. As skeletal muscle tissue engineering continues to progress with the incorporation of biologically meaningful stimuli, it can be envisaged that improvements in the in vitro–in vivo correlation of drug responses may also improve, and engineered tissues have the potential to reduce and ultimately potentially replace animal testing. Companies like Cytokinetics, Sarpeta Therapeutics and Solid Biosciences are developing approaches for disease and patient specific drugs. The focus is not only on the development of genetic and medical approaches but also on devices for the most common muscular and neuromuscular diseases.

Furthermore, global demand for protein-based foods is growing rapidly and muscle tissue engineering is attracting increasing interest as a source of artificial meat. The production of artificial meat replacements in the laboratory is an emerging industry to provide ethically preferable alternatives to meat from conventional farming. The importance of the production of artificial meat arises not only due to the tremendous increase in demand for animal-derived proteins but also to the major contribution of animal agriculture in  $\approx 10\%$  of production of greenhouse gas emissions in the US alone and  $37\%$  of all methane emissions globally.<sup>[168]</sup> The term artificial meat can refer to meats from various sources such as meat alternatives from plants (tofu, seitan or tempeh) and fungi (e.g., fungal protein product Quorn), cell-based meat and meat from genetically modified animals.<sup>[168–169]</sup> The cell-based meat is ideally

genetically identical to conventional animal meat; however, it is hard to develop due to the structural complexity. Therefore, efforts have been made to mimic the taste and texture of meat from animals by growing different cell types in coculture, on different substrates and in bioreactor systems. For example, the myo satellite or adipose stem cells can be grown in growth medium outside an animal in a bioreactor. These are multipotent cells that can be differentiated, but need to be reharvested from time to time.<sup>[170]</sup> Moreover, mimicking the texture of natural meat remains challenging, and this directly and strongly contributes to the taste and mouthfeel of the products. In fact, replication of ground meat is far simpler and easier than steaks. Stimuli in culture is being investigated as a potential means to address this challenge. The first reported slaughter-free hamburger from laboratory-cultured meat dates back to 2013 by the CSO of Mosa Meat, Professor Mark Post, and it cost at that time  $\approx 250\,000\text{ €}$ .<sup>[171]</sup> However, major hurdles in this field still remain as there is still a need to use animals as an initial source of cells and animal-derived serum is a basic ingredient of the culture media for cell proliferation and differentiation which is difficult and expensive to replace. Furthermore, this option may not satisfy vegetarians and vegans and the amount of meat which can be obtained with these methods cannot yet satisfy a global market.<sup>[168–169,172]</sup>

## Acknowledgements

C.M., M.T.M., and M.M. contributed equally to this work. This work was supported by the Deutsche Forschungsgemeinschaft (DFG, German Research Foundation) – Projektnummer 326998133 – TRR 225 (subproject B03) and SA 3575/1-1. M.M. gratefully acknowledges support from the University of Melbourne and an Australian Government Research Training Program Scholarship. The authors further acknowledge financial support by the German Academic Exchange service (DAAD) through its Thematic Melbourne-Bayreuth Polymer/Colloid Network sponsored from funds of the Federal Ministry of Education and Research (BMBF).

Open access funding enabled and organized by Projekt DEAL.

## Conflict of Interest

The authors declare no conflict of interest.

## Keywords

bioengineering, maturation, skeletal muscle tissue, stimulation, tissue engineering

Received: June 30, 2020

Revised: October 15, 2020

Published online: November 17, 2020

- [1] a) S. Ostrovidov, X. Shi, R. B. Sadeghian, S. Salehi, T. Fujie, H. Bae, M. Ramalingam, A. Khademhosseini, *Stem. Cell Rev. Rep.* **2015**, *11*, 866; b) S. Ostrovidov, V. Hosseini, S. Ahadian, T. Fujie, S. P. Parthiban, M. Ramalingam, H. Bae, H. Kaji, A. Khademhosseini, *Tissue Eng., Part B* **2014**, *20*, 403.  
[2] T. H. Qazi, D. J. Mooney, M. Pumberger, S. Geißler, G. N. Duda, *Biomaterials* **2015**, *53*, 502.

- [3] J. Wang, A. Khodabukus, L. J. Rao, K. Vandusen, N. Abutaleb, N. Bursac, *Biomaterials* **2019**, 221, 119416.
- [4] B. J. Kwee, D. J. Mooney, *Curr. Opin. Biotech.* **2017**, 47, 16.
- [5] R. L. Lieber, *Skeletal Muscle Structure, Function, and Plasticity*, Lippincott Williams & Wilkins, Philadelphia, PA **2002**.
- [6] M. E. Carnes, G. D. Pins, *Bioengineering (Basel)* **2020**, 7, 85.
- [7] M. Cervelli, A. Leonetti, G. Duranti, S. Sabatini, R. Ceci, P. Mariottini, *Med. Sci. (Basel)* **2018**, 6, 14.
- [8] M. Murphy, G. Kardou, *Curr. Top. Dev. Biol.* **2011**, 96, 1.
- [9] G. S. Lynch, in *The Plasticity of Skeletal Muscle: From Molecular Mechanism to Clinical Applications*, (Ed: K. Sakuma), Springer, Singapore **2017**, p. 277.
- [10] B. C. Syverud, K. W. VanDusen, L. M. Larkin, *Cells Tissues Organs* **2016**, 202, 169.
- [11] S. Ebashi, I. Ohtsuki, *Regulatory Mechanisms of Striated Muscle Contraction*, Springer, New York **2007**.
- [12] A. J. Isak, P. C. Pablo, F. Trine, Z. Vladimir, *Tissue Eng. Pt. A* **2018**, 24, 631.
- [13] J. D. Humphrey, E. R. Dufresne, M. A. Schwartz, *Nat. Rev. Mol. Cell Bio.* **2014**, 15, 802.
- [14] a) T. Benavides Damm, M. Egli, *Cell Physiol. Biochem.* **2014**, 33, 249; b) S. M. Somers, A. A. Spector, D. J. DiGirolamo, W. L. Grayson, *Tissue Eng. Part B Rev.* **2017**, 23, 362.
- [15] S. Schiaffino, C. Reggiani, *Physiol. Rev.* **1996**, 76, 371.
- [16] K. M. Baldwin, F. Haddad, *J. Appl. Physiol.* **2001**, 90, 345.
- [17] R. J. Talmadge, *Muscle Nerve* **2000**, 23, 661.
- [18] G. R. Adams, S. A. McCue, M. Zeng, K. M. Baldwin, *Am. J. Physiol. Reg. I.* **1999**, 276, R954.
- [19] A. Grossi, K. Yadav, M. A. Lawson, *J. Biomech.* **2007**, 40, 3354.
- [20] a) B. Moses, J. Orchard, J. Orchard, *Res. Sports Med.* **2012**, 20, 157; b) L. A. Ramos, R. T. de Carvalho, R. J. Abdalla, S. J. M. Ingham, *Current Reviews in Musculoskeletal Medicine* **2015**, 8, 188; c) J. W. Orchard, H. Seward, J. J. Orchard, *Am. J. Sport Med.* **2013**, 41, 734.
- [21] a) K. W. Janssen, J. W. Orchard, T. R. Driscoll, W. van Mechelen, *Scand. J. Med. Sci. Sports* **2012**, 22, 495; b) T. O. Clanton, K. J. Coupe, *J. Am. Acad. Orthop. Surg.* **1998**, 6, 237.
- [22] C. S. Russell, A. Mostafavi, J. P. Quint, A. C. Panayi, K. Baldino, T. J. Williams, J. G. Daubendiek, V. Hugo Sánchez, Z. Bonick, M. Trujillo-Miranda, S. R. Shin, O. Pourquie, S. Salehi, I. Sinha, A. Tamayol, *ACS Appl. Bio. Mater.* **2020**, 3, 1568.
- [23] a) S. K. Powers, G. S. Lynch, K. T. Murphy, M. B. Reid, I. Zijdewind, *Med. Sci. Sport Exer.* **2016**, 48, 2307; b) W. J. Evans, *Am. J. Clin. Nutr.* **2010**, 91, 1123S.
- [24] Z. Aversa, P. Costelli, M. Muscaritoli, *Ther. Adv. Med. Oncol.* **2017**, 9, 369.
- [25] J. P. Hardee, G. S. Lynch, *Expert Opinion on Pharmacotherapy* **2019**, 20, 1645.
- [26] a) B. De Paepe, J. L. De Bleecker, *Mediators Inflammation* **2013**, 2013, 540370; b) Y. Kharraz, J. Guerra, P. Pessina, A. L. Serrano, P. Muñoz-Cánoves, *Biomed. Res. Int.* **2014**, 2014, 965631.
- [27] B. Maleiner, J. Tomasch, P. Heher, O. Spadiut, D. Rünzler, C. Fuchs, *Front. Physiol.* **2018**, 9, 1130.
- [28] R. P. Feynman, *J. Microelectromech. Syst.* **1992**, 1, 60.
- [29] K. E. Drexler, *P. Natl. Acad. Sci. USA* **1981**, 78, 5275.
- [30] a) R. Gauvin, A. Khademhosseini, *ACS Nano* **2011**, 5, 4258; b) Y. A. Du, E. Lo, S. Ali, A. Khademhosseini, *Proc. Natl. Acad. Sci. USA* **2008**, 105, 9522; c) J. W. Nichol, A. Khademhosseini, *Soft Matter* **2009**, 5, 1312; d) Y. C. Zuo, X. L. Liu, D. Wei, J. Sun, W. Q. Xiao, H. Zhao, L. K. Guo, Q. R. Wei, H. S. Fan, X. D. Zhang, *ACS Appl. Mater. Inter.* **2015**, 7, 10386.
- [31] a) S. Jana, S. K. Levegood, M. Zhang, *Adv. Mater.* **2016**, 28, 10588; b) M. Koning, M. C. Harmsen, M. J. A. van Luyn, P. M. N. Werker, *J. Tissue Eng. Regen. M* **2009**, 3, 407.
- [32] Q. P. Hou, P. A. De Bank, K. M. Shakesheff, *J. Mater. Chem.* **2004**, 14, 1915.
- [33] a) K. J. M. Boonen, M. L. P. Langelaan, R. B. Polak, D. W. J. van der Schaft, F. P. T. Baaijens, M. J. Post, *J. Biomech.* **2010**, 43, 1514; b) P. Y. Huri, C. A. Cook, D. L. Hutton, B. C. Goh, J. M. Gimble, D. J. DiGirolamo, W. L. Grayson, *Biochem. Biophys. Res. Co.* **2013**, 438, 180; c) N. F. Huang, R. J. Lee, S. Li, *Am. J. Transl. Res.* **2010**, 2, 43.
- [34] N. L'Heureux, S. Paquet, R. Labbe, L. Germain, F. A. Auger, *FASEB J.* **1998**, 12, 47.
- [35] D. M. Dean, A. P. Napolitano, J. Youssef, J. R. Morgan, *FASEB J.* **2007**, 21, 4005.
- [36] F. Y. Li, V. X. Truong, P. Fisch, C. Levinson, V. Glattauer, M. Zenobi-Wong, H. Thissen, J. S. Forsythe, J. E. Frith, *Acta. Biomater.* **2018**, 77, 48.
- [37] a) V. Mironov, T. Boland, T. Trusk, G. Forgacs, R. R. Markwald, *Trends Biotechnol.* **2003**, 21, 157; b) D. L. Elbert, *Curr. Opin. Biotech.* **2011**, 22, 674.
- [38] S. Salehi, S. Ostrovidov, M. Ebrahimi, R. B. Sadeghian, X. B. Liang, K. Nakajima, H. Bae, T. Fujie, A. Khademhosseini, *ACS Biomater. Sci. Eng.* **2017**, 3, 579.
- [39] M. Ebrahimi, S. Ostrovidov, S. Salehi, S. B. Kim, H. Bae, A. Khademhosseini, *J. Tissue Eng. Regen. M* **2018**, 12, 2151.
- [40] B. Mirani, E. Pagan, S. Shojaei, S. M. H. Dabiri, H. Savoji, M. Mehrali, M. Sam, J. Alsaif, R. B. Bhiladvala, A. Dolatshahi-Pirouz, M. Radisic, M. Akbari, *Acs Appl. Mater. Inter.* **2020**, 12, 9080.
- [41] A. Fallahi, I. K. Yazdi, L. Serex, E. Lesha, N. Faramarzi, F. Tarlan, H. Avci, R. Costa-Almeida, F. Sharifi, C. Rinoldi, M. E. Gomes, S. R. Shin, A. Khademhosseini, M. Akbari, A. Tamayol, *ACS Biomater. Sci. Eng.* **2020**, 6, 1112.
- [42] G. H. Yang, J. Lee, G. Kim, *Biofabrication* **2019**, 11, 025005.
- [43] a) S. Tajbakhsh, D. Rocancourt, M. Buckingham, *Nature* **1996**, 384, 266; b) L. A. Megeney, B. Kablar, K. Garrett, J. E. Anderson, M. A. Rudnicki, *Gene Dev.* **1996**, 10, 1173.
- [44] G. Y. Liu, R. Agarwal, K. R. Ko, M. Ruthven, H. T. Sarhan, J. P. Frampton, *Sci. Rep.-Uk* **2017**, 7, 1.
- [45] a) Y. Sun, R. Duffy, A. Lee, A. W. Feinberg, *Acta Biomater.* **2013**, 9, 7885; b) R. M. Duffy, Y. Sun, A. W. Feinberg, *Ann. Biomed. Eng.* **2016**, 44, 2076; c) R. B. Sadeghian, M. Ebrahimi, S. Salehi, *J. Tissue Eng. Regen. M* **2018**, 12, 912.
- [46] L. T. Denes, L. A. Riley, J. R. Mijares, J. D. Arboleda, K. McKee, K. A. Esser, E. T. Wang, *Skelet Muscle* **2019**, 9, 17.
- [47] T. Fujie, X. T. Shi, S. Ostrovidov, X. B. Liang, K. Nakajima, Y. Chen, H. K. Wu, A. Khademhosseini, *Biomaterials* **2015**, 53, 86.
- [48] a) M. M. Smoak, A. Han, E. Watson, A. Kishan, K. J. Grande-Allen, E. Cosgriff-Hernandez, A. G. Mikos, *Tissue Eng. Part C-Me* **2019**, 25, 276; b) K. H. Nakayama, M. Quarta, P. Paine, C. Alcazar, I. Karakikes, V. Garcia, O. J. Abilez, N. S. Calvo, C. S. Simmons, T. A. Rando, N. F. Huang, *Commun. Biol.* **2019**, 2, 170; c) M. T. Wolf, C. L. Dearth, S. B. Sonnenberg, E. G. Lobo, S. F. Badylak, *Adv. Drug Deliver Rev.* **2015**, 84, 208.
- [49] S. Ostrovidov, M. Ebrahimi, H. Bae, H. K. Nguyen, S. Salehi, S. B. Kim, A. Kumatani, T. Matsue, X. T. Shi, K. Nakajima, S. Hidema, M. Osanai, A. Khademhosseini, *Acs Appl. Mater. Inter.* **2017**, 9, 42444.
- [50] N. Narayanan, C. Jiang, C. Wang, G. Uzunalli, N. Whittern, D. Chen, O. G. Jones, S. Kuang, M. Deng, *Front. Bioeng. Biotechnol.* **2020**, 8, 203.
- [51] K. H. Patel, M. Talovic, A. J. Dunn, A. Patel, S. Vendrell, M. Schwartz, K. Garg, *J. Biomed. Mater. Res. B Appl. Biomater.* **2020**, 108, 2528.
- [52] K. H. Patel, A. J. Dunn, M. Talovic, G. J. Haas, M. Marcinczyk, H. Elmashady, E. G. Kalaf, S. A. Sell, K. Garg, *Biomed. Mater.* **2019**, 14, 035010.
- [53] S. Ostrovidov, M. Ebrahimi, H. Bae, H. K. Nguyen, S. Salehi, S. B. Kim, A. Kumatani, T. Matsue, X. Shi, K. Nakajima, S. Hidema,

- M. Osanai, A. Khademhosseini, *ACS Appl. Mater. Interfaces* **2017**, 9, 42444.
- [54] A. Patel, Y. Xue, S. Mukundan, L. C. Rohan, V. Sant, D. B. Stolz, S. Sant, *Ann. Biomed. Eng.* **2016**, 44, 2036.
- [55] A. Patel, S. Mukundan, W. H. Wang, A. Karumuri, V. Sant, S. M. Mukhopadhyay, S. Sant, *Acta Biomater.* **2016**, 32, 77.
- [56] G. Lalwani, M. D'Agati, A. M. Khan, B. Sitharaman, *Adv. Drug Deliver. Rev.* **2016**, 105, 109.
- [57] B. Fadeel, C. Bussy, S. Merino, E. Vazquez, E. Flahaut, F. Mouchet, L. Evariste, L. Gauthier, A. J. Koivisto, U. Vogel, C. Martin, L. G. Delogu, T. Buerki-Thurnherr, P. Wick, D. Beloin-Saint-Pierre, R. Hischier, M. Pelin, F. C. Carniel, M. Tretiach, F. Cesca, F. Benfenati, D. Scaini, L. Ballerini, K. Kostarelos, M. Prato, A. Bianco, *ACS Nano* **2018**, 12, 10582.
- [58] a) S. Ahadian, R. B. Sadeghian, S. Salehi, S. Ostrovidov, H. Bae, M. Ramalingam, A. Khademhosseini, *Bioconjugate Chem.* **2015**, 26, 1984; b) M. A. Mohamed, A. Fallahi, A. M. A. El-Sokkary, S. Salehi, M. A. Akl, A. Jafari, A. Tamayol, H. Fenniri, A. Khademhosseini, S. T. Andreadis, C. Cheng, *Prog. Polym. Sci.* **2019**, 98, 101147.
- [59] K. M. Fischer, T. E. Scott, D. P. Browe, T. A. McGaughy, C. Wood, M. J. Wolyniak, J. W. Freeman, *Regen. Eng. Transl. Med.* **2020**, <https://doi.org/10.1007/s40883-019-00146-x>.
- [60] B. E. Pollot, C. R. Rathbone, J. C. Wenke, T. Guda, *J. Biomed. Mater. Res. B Appl. Biomater.* **2018**, 106, 672.
- [61] D. Gholobova, M. Gerard, L. Decroix, L. Desender, N. Callewaert, P. Annaert, L. Thorrez, *Sci. Rep.-Uk* **2018**, 8, 12206.
- [62] a) R. Lev, D. Seliktar, *J R Soc Interface* **2018**, 15, 20170380; b) A. S. Salimath, A. J. Garcia, *J. Tissue Eng. Regen. M* **2016**, 10, 967.
- [63] M. Kim, W. Kim, G. Kim, *ACS Appl. Mater. Interfaces* **2017**, 9, 43459.
- [64] W. Kim, M. Kim, G. H. Kim, *Adv. Funct. Mater.* **2018**, 28, 1800405.
- [65] M. Yeo, G. Kim, *ACS Biomater. Sci. Eng.* **2018**, 4, 728.
- [66] A. Urciuolo, E. Serena, R. Ghua, S. Zatti, M. Giomo, N. Mattei, M. Vetralla, G. Selmin, C. Luni, N. Vitulo, G. Valle, L. Vitiello, N. Elvassore, *PLoS One* **2020**, 15, e0232081.
- [67] X. Chen, W. Du, Z. Cai, S. Ji, M. Dwivedi, J. Chen, G. Zhao, J. Chu, *ACS Appl. Mater. Interfaces* **2020**, 12, 2162.
- [68] M. Yeo, H. Lee, G. H. Kim, *Biofabrication* **2016**, 8, 035021.
- [69] H. X. Chen, J. C. Zhong, J. Wang, R. Y. Huang, X. Y. Qiao, H. H. Wang, Z. K. Tan, *Int. J. Nanomed.* **2019**, 14, 937.
- [70] A. Garcia-Lizarribar, X. Fernandez-Garibay, F. Velasco-Mallorqui, A. G. Castano, J. Samitier, J. Ramon-Azcon, *Macromol. Biosci.* **2018**, 18, e1800167.
- [71] Y. Zhang, Z. Zhang, Y. Wang, Y. Su, M. Chen, *Mater. Sci. Eng. C Mater. Biol. Appl.* **2020**, 116, 111070.
- [72] A. Naik, M. Griffin, M. Szarko, P. E. Butler, *Artif. Organs* **2020**, 44, 178.
- [73] W. E. Reyna, R. Pichika, D. Ludvig, E. J. Perreault, *J. Biomech.* **2020**, 110, 109961.
- [74] J. W. Wassenaar, G. R. Boss, K. L. Christman, *Biomaterials* **2015**, 64, 108.
- [75] a) S. F. Badylak, J. L. Dziki, B. M. Sicari, F. Ambrosio, M. L. Boninger, *Biomaterials* **2016**, 103, 128; b) L. N. Wang, J. A. Johnson, D. W. Chang, Q. X. Zhang, *Biomaterials* **2013**, 34, 2641.
- [76] H. Lee, Y. M. Ju, I. Kim, E. Elsangeedy, J. H. Lee, J. J. Yoo, A. Atala, S. J. Lee, *Methods* **2020**, 171, 77.
- [77] Z. Q. Wan, P. Zhang, Y. S. Liu, L. W. Lv, Y. S. Zhou, *Acta Biomater.* **2020**, 101, 26.
- [78] I. Apsite, J. M. Uribe, A. F. Posada, S. Rosenfeldt, S. Salehi, L. Ionov, *Biofabrication* **2020**, 12, 015016.
- [79] L. Vannozzi, I. C. Yasa, H. Ceylan, A. Menciasci, L. Ricotti, M. Sitti, *Macromol. Biosci.* **2018**, 18, e1700377.
- [80] S. D. Miao, M. Nowicki, H. T. Cui, S. J. Lee, X. Zhou, D. K. Mills, L. J. G. Zhang, *Biofabrication* **2019**, 11, 035030.
- [81] a) A. Khodabukus, N. Prabhu, J. Wang, N. Bursac, *Adv. Health-care Mater.* **2018**, 7, 1701498; b) Q. A. Soltow, E. H. Zeanah, V. A. Lira, D. S. Criswell, *Biochem. Bioph. Res. Co.* **2013**, 434, 316; c) C. Handschin, A. Mortezaei, J. Plock, D. Eberli, *Adv. Drug Deliver. Rev.* **2015**, 82-83, 168; d) K. Bilodeau, D. Mantovani, *Tissue Eng.* **2006**, 12, 2367; e) R. Balint, N. J. Cassidy, S. H. Cartmell, *Tissue Eng. Part B-Re* **2013**, 19, 48.
- [82] S. Oh, H. Chung, S. Chang, S. H. Lee, S. H. Seok, H. Lee, *Sci. Rep.* **2019**, 9, 5156.
- [83] S. Park, Y. Choi, N. Jung, Y. Yu, K. H. Ryu, H. S. Kim, I. Jo, B. O. Choi, S. C. Jung, *Int. J. Mol. Med.* **2016**, 37, 1209.
- [84] W. Klomjai, A. Lackmy-Vallee, N. Roche, P. Pradat-Diehl, V. Marchand-Pauvert, R. Katz, *Ann. Phys. Rehabil. Med.* **2015**, 58, 220.
- [85] I. Herreros, A. Giovannucci, A. H. Taub, R. Hogri, A. Magal, S. Bamford, R. Prueckl, P. F. Verschure, *Front. Bioeng. Biotechnol.* **2014**, 2, 14.
- [86] C. A. Powell, B. L. Smiley, J. Mills, H. H. Vandenberg, *Am. J. Physiol.-Cell Ph.* **2002**, 283, C1557.
- [87] R. Tatsumi, *Anim. Sci. J.* **2010**, 81, 11.
- [88] a) J. G. Tidball, E. Lavergne, K. S. Lau, M. J. Spencer, J. T. Stull, M. Wehling, *Am. J. Physiol.-Cell Ph.* **1998**, 275, C260; b) H. H. Vandenberg, *Med. Sci. Sport Exer.* **1987**, 19, S142; c) L. E. Freed, F. Guilak, X. E. Guo, M. L. Gray, R. Tranquillo, J. W. Holmes, M. Radisic, M. V. Sefton, D. Kaplan, G. Vunjak-Novakovic, *Tissue Eng.* **2006**, 12, 3285; d) M. M. Smoak, A. G. Mikos, *Mater. Today Bio.* **2020**, 7, 100069.
- [89] D. E. Jaalouk, J. Lammerding, *Nat. Rev. Mol. Cell Bio.* **2009**, 10, 63.
- [90] J. Eyckmans, T. Boudou, X. Yu, C. S. Chen, *Dev. Cell* **2011**, 21, 35.
- [91] D. F. Goldspink, J. Easton, S. K. Winterburn, P. E. Williams, G. E. Goldspink, *J. Cardiac. Surg.* **1991**, 6, 218.
- [92] M. R. Hicks, T. V. Cao, D. H. Campbell, P. R. Standley, *J. Appl. Physiol.* (1985) **2012**, 113, 465.
- [93] P. Heher, B. Maleiner, J. Pruller, A. H. Teuschl, J. Kollmitzer, X. Monforte, S. Wolbank, H. Redl, D. Runzler, C. Fuchs, *Acta Biomater.* **2015**, 24, 251.
- [94] S. Bansai, T. Morikura, H. Onoe, S. Miyata, *Micromachines (Basel)* **2019**, 10, 10.
- [95] G. Cittadella Vigodarzere, S. Mantero, *Front. Physiol.* **2014**, 5, 362.
- [96] G. Candiani, S. A. Riboldi, N. Sadr, S. Lorenzoni, P. Neuenschwander, F. M. Montevecchi, S. Mantero, **2010**, 8, 68.
- [97] J. Miyakoshi, *Prog. Biophys. Mol. Bio.* **2005**, 87, 213.
- [98] Y. Morimoto, M. Kato-Negishi, H. Onoe, S. Takeuchi, *Biomaterials* **2013**, 34, 9413.
- [99] R. D. Keynes, D. J. Aidley, C. L. H. Huang, *Nerve and Muscle*, Cambridge University Press, Cambridge **2011**.
- [100] S. Ribeiro, A. C. Gomes, I. Etxebarria, S. Lanceros-Méndez, C. Ribeiro, *Mater. Sci. Eng., C* **2018**, 92, 868.
- [101] a) O. F. Vila, S. G. M. Uzel, S. P. Ma, D. Williams, J. Pak, R. D. Kamm, G. Vunjak-Novakovic, *Theranostics* **2019**, 9, 1232; b) R. Maidhof, N. Tandon, E. J. Lee, J. W. Luo, Y. Duan, K. Yeager, E. Konofagou, G. Vunjak-Novakovic, *J. Tissue Eng. Regen. M* **2012**, 6, e12.
- [102] S. Mosole, S. Zampieri, S. Furlan, U. Carraro, S. Loeffler, H. Kern, P. Volpe, A. Nori, *Gerontol. Geriatr. Med.* **2018**, 4, 2333721418768998.
- [103] H. Kaji, T. Ishibashi, K. Nagamine, M. Kanzaki, M. Nishizawa, *Biomaterials* **2010**, 31, 6981.
- [104] M. L. P. Langelaan, K. J. M. Boonen, K. Y. Rosaria-Chak, D. W. J. van der Schaft, M. J. Post, F. P. T. Baaijens, **2011**, 5, 529.
- [105] B. N. Davis, R. G. Yen, V. Prasad, G. A. Truskey, *APL Bioeng.* **2019**, 3, 026103.
- [106] A. Khodabukus, L. Madden, N. K. Prabhu, T. R. Koves, C. P. Jackman, D. M. Muoio, N. Bursac, *Biomaterials* **2019**, 198, 259.
- [107] K. Nagamine, H. Sato, H. Kai, H. Kaji, M. Kanzaki, M. Nishizawa, *Sci. Rep.-Uk* **2018**, 8, 2253.
- [108] B. K. Pedersen, M. A. Febbraio, *Nat. Rev. Endocrinol.* **2012**, 8, 457.
- [109] W. D. C. Man, J. Moxham, M. I. Polkey, *Eur. Respir. J* **2004**, 24, 846.



- [110] R. G. Bickford, M. Guidi, P. Fortesque, M. Swenson, *Neurosurgery* **1987**, 20, 110.
- [111] J. L. Taylor, *J. Appl. Physiol.* (1985) **2007**, 103, 733.
- [112] M. N. L. Stolting, A. S. Arnold, D. Haralampieva, C. Handschin, T. Sulser, D. Eberli, *Muscle Nerve* **2016**, 53, 598.
- [113] R. R. Raylman, A. C. Clavo, R. L. Wahl, *Bioelectromagnetics* **1996**, 17, 358.
- [114] D. Coletti, L. Teodori, M. C. Albertini, M. Rocchi, A. Pristera, M. Fini, M. Molinaro, S. Adamo, *Cytom. Part A* **2007**, 71A, 846.
- [115] C. E. Mueller, R. Birk, H. Kramer, A. Wenzel, J. U. Sommer, K. Hormann, J. Stern-Straeter, C. Weilbach, *Mol. Med. Rep.* **2018**, 17, 3813.
- [116] T. Sakurai, A. Hashimoto, T. Kiyokawa, K. Kikuchi, J. Miyakoshi, **2012**, 33, 421.
- [117] Y. H. Li, G. Y. Huang, B. Gao, M. X. Li, G. M. Genin, T. J. Lu, F. Xu, *NPG Asia Mater.* **2016**, 8, e238.
- [118] Y. Yamamoto, A. Ito, H. Fujita, E. Nagamori, Y. Kawabe, M. Kamihira, *Tissue Eng. Part A* **2011**, 17, 107.
- [119] a) I. Husmann, L. Soulet, J. Gautron, I. Martelly, D. Barritault, *Cytokine Growth Factor Rev.* **1996**, 7, 249; b) D. Aboalola, V. K. Han, *Stem cells international* **2019**, 2019, 9245938; c) A. L. Serrano, C. J. Mann, B. Vidal, E. Arditte, E. Perdiguero, P. Munoz-Canoves, *Curr. Top. Dev. Biol.* **2011**, 96, 167.
- [120] H. D. Kollias, J. C. McDermott, *J. Appl. Physiol.* (1985) **2008**, 104, 579.
- [121] a) C. S. Kim, Y. Joe, H. S. Choi, S. H. Back, J. W. Park, H. T. Chung, E. Roh, M. S. Kim, T. Y. Ha, R. Yu, *J. Inflamm. (Lond)* **2019**, 16, 17; b) B. Benoit, E. Meugnier, M. Castelli, S. Chanon, A. Vieille-Marchiset, C. Durand, N. Bendridi, S. Pesenti, P. A. Monternier, A. C. Durieux, D. Freyssenet, J. Rieusset, E. Lefai, H. Vidal, J. Ruzzin, *Nat. Med.* **2017**, 23, 990.
- [122] a) C. Borselli, H. Storrie, F. Benesch-Lee, D. Shvartsman, C. Cezar, J. W. Lichtman, H. H. Vandenburgh, D. J. Mooney, *Proc. Natl. Acad. Sci. USA* **2010**, 107, 3287; b) T. Nicholson, C. Church, D. J. Baker, S. W. Jones, *Journal of Inflammation* **2018**, 15, 9.
- [123] S. B. Charge, M. A. Rudnicki, *Physiol. Rev.* **2004**, 84, 209.
- [124] L. Wang, J. Shansky, H. Vandenburgh, *Mol. Neurobiol.* **2013**, 48, 397.
- [125] J. Suzuki, Y. Yamazaki, L. Guang, Y. Kaziro, H. Koide, *Mol. Cell Biol.* **2000**, 20, 4658.
- [126] C. J. Marshall, *Cell* **1995**, 80, 179.
- [127] F. M. Alves, M. K. Caldwell, J. Trieu, T. Naim, M. K. Montgomery, M. J. Watt, G. S. Lynch, R. Koopman, *Clinical Nutrition Experimental* **2019**, 24, 83.
- [128] a) D. A. P. Goncalves, E. C. Lira, A. M. Baviera, P. R. Cao, N. M. Zanon, Z. Arany, N. Bedard, P. Tanksale, S. S. Wing, S. H. Lecker, I. C. Kettelhut, L. C. C. Navegantes, *Endocrinology* **2009**, 150, 5395; b) J. G. Ryall, D. R. Plant, P. Gregorevic, M. N. Sillence, G. S. Lynch, *The Journal of Physiology* **2004**, 555, 175.
- [129] A. Hagg, T. D. Colgan, R. E. Thomson, H. Qian, G. S. Lynch, P. Gregorevic, *Sci. Rep.-Uk* **2016**, 6, 23042.
- [130] a) O. R. Joassard, A. Amirouche, Y. S. Gallot, M. M. Desgeorges, J. Castells, A. C. Durieux, P. Berthon, D. G. Freyssenet, *Int. J. Biochem. Cell Biol.* **2013**, 45, 2444; b) M. Toledo, J. Springer, S. Busquets, A. Tschirner, F. J. López-Soriano, S. D. Anker, J. M. Argilés, *Journal of Cachexia, Sarcopenia and Muscle* **2014**, 5, 315.
- [131] a) J. G. Ryall, J. E. Church, G. S. Lynch, *Clin. Exp. Pharmacol. Physiol.* **2010**, 37, 397; b) N. D. Duncan, D. A. Williams, G. S. Lynch, *Clinical science (London, England: 1979)* **2000**, 98, 339; c) J. G. Burniston, Y. Ng, W. A. Clark, J. Colyer, L.-B. Tan, D. F. Goldspink, *J. Appl. Physiol.* **2002**, 93, 1824.
- [132] A. Khodabukus, K. Baar, *J. Cell Physiol.* **2015**, 230, 1226.
- [133] B. C. Syverud, K. W. VanDusen, L. M. Larkin, *Tissue Eng. Part A* **2016**, 22, 480.
- [134] a) M. Murphy, G. Kardon, in *Current Topics in Developmental Biology*, Vol. 96 (Ed: G. k. Pavlath), Academic Press, Cambridge, MA **2011**, p. 1; b) J. Prüller, I. Mannhardt, T. Eschenhagen, P. S. Zammit, N. Figeac, *PLoS One* **2018**, 13, e0202574.
- [135] P. Bainbridge, *Journal of wound care* **2013**, 22.
- [136] a) R. G. Dennis, P. E. Kosnik, M. E. Gilbert, J. A. Faulkner, *Am J. Physiol.-Cell Ph.* **2001**, 280, C288; b) C. S. Fry, J. D. Lee, J. R. Jackson, T. J. Kirby, S. A. Stasko, H. Liu, E. E. Dupont-Versteegden, J. J. McCarthy, C. A. Peterson, *FASEB J.* **2014**, 28, 1654.
- [137] M. N. Wosczyzna, T. A. Rando, *Dev. Cell* **2018**, 46, 135.
- [138] C. Venter, C. Niesler, *BioTechniques* **2018**, 64, 52.
- [139] C. S. Fry, T. J. Kirby, K. Kosmac, J. J. McCarthy, C. A. Peterson, *Cell Stem Cell* **2017**, 20, 56.
- [140] J. Krieger, B.-W. Park, C. R. Lambert, C. Malcuit, *PeerJ* **2018**, 6, e4939.
- [141] C. Christov, F. Chrétien, R. Abou-Khalil, G. Bassez, G. Vallet, F.-J. Authier, Y. Bassaglia, V. Shinin, S. Tajbakhsh, B. Chazaud, R. K. Gherardi, *Mol. Biol. Cell* **2007**, 18, 1397.
- [142] M. W. Laschke, M. D. Menger, *Biotechnol. Adv.* **2016**, 34, 112.
- [143] C. Latroche, M. Weiss-Gayet, L. Muller, C. Gitiaux, P. Leblanc, S. Liot, S. Ben-Larbi, R. Abou-Khalil, N. Verger, P. Bardot, M. Magnan, F. Chrétien, R. Mounier, S. Germain, B. Chazaud, *Stem Cell Rep.* **2017**, 9, 2018.
- [144] a) M. P. Daniels, B. T. Lowe, S. Shah, J. Ma, S. J. Samuelsson, B. Lugo, T. Parakh, C.-S. Uhm, *Microscopy Research and Technique* **2000**, 49, 26; b) J. A. Umbach, K. L. Adams, C. B. Gundersen, B. G. Novitch, *PLoS One* **2012**, 7, e36049.
- [145] E. Ko, S. J. Yu, G. J. Pagan-Diaz, Z. Mahmassani, M. D. Boppart, S. G. Im, R. Bashir, H. Kong, *Adv. Sci. (Weinh)* **2019**, 6, 1801521.
- [146] a) S. Ostrovidov, S. Ahadian, J. Ramon-Azcon, V. Hosseini, T. Fujie, S. P. Parthiban, H. Shiku, T. Matsue, H. Kaji, M. Ramalingam, H. Bae, A. Khademhosseini, *J. Tissue Eng. Regen. M* **2017**, 11, 582; b) M. L. Williams, T. Y. Kostrominova, E. M. Arruda, L. M. Larkin, *J. Tissue Eng. Regen. M* **2013**, 7, 434.
- [147] M. Afshar Bakooshli, E. S. Lippmann, B. Mulcahy, N. Iyer, C. T. Nguyen, K. Tung, B. A. Stewart, H. van den Dorpel, T. Fuehrmann, M. Shoichet, A. Bigot, E. Pegoraro, H. Ahn, H. Ginsberg, M. Zhen, R. S. Ashton, P. M. Gilbert, *eLife* **2019**, 8, e44530.
- [148] a) Z. Tong, O. Seira, C. Casas, D. Reginensi, A. Homs-Corbera, J. Samitier, J. A. Del Río, *RSC Adv.* **2014**, 4, 54788; b) M. Das, J. W. Rumsey, C. A. Gregory, N. Bhargava, J. F. Kang, P. Molnar, L. Riedel, X. Guo, J. J. Hickman, *Neuroscience* **2007**, 146, 481.
- [149] S. G. M. Uzel, R. J. Platt, V. Subramanian, T. M. Pearl, C. J. Rowlands, V. Chan, L. A. Boyer, P. T. C. So, R. D. Kamm, *Sci. Adv.* **2016**, 2, e1501429.
- [150] E. E. Zahavi, A. Ionescu, S. Gluska, T. Gradus, K. Ben-Yaakov, E. Perlson, *J. Cell Sci.* **2015**, 128, 1241.
- [151] A. Ionescu, E. E. Zahavi, T. Gradus, K. Ben-Yaakov, E. Perlson, *Eur. J. Cell Biol.* **2016**, 95, 69.
- [152] M. Juhas, G. C. Engelmayr, A. N. Fontanella, G. M. Palmer, N. Bursac, *Proc. Natl. Acad. Sci. USA* **2014**, 111, 5508.
- [153] L. M. Larkin, J. H. van der Meulen, R. G. Dennis, J. B. Kennedy, *In Vitro Cellular & Developmental Biology – Animal* **2006**, 42, 75.
- [154] a) L. Ricotti, T. Fujie, H. Vazão, G. Ciofani, R. Marotta, R. Brescia, C. Filippeschi, I. Corradini, M. Matteoli, V. Mattoli, L. Ferreira, A. Mencias, *PLoS One* **2013**, 8, e71707; b) P. Molnar, W. Wang, A. Natarajan, J. W. Rumsey, J. J. Hickman, *Biotechnol. Prog.* **2007**, 23, 265; c) E. M. Cronin, F. A. Thurmond, R. Bassel-Duby, R. S. Williams, W. E. Wright, K. D. Nelson, H. R. Garner, *J. Biomed. Mater. Res. A* **2004**, 69A, 373; d) J. L. Charest, A. J. Garcia, W. P. King, *Biomaterials* **2007**, 28, 2202; e) P.-Y. Wang, W.-T. Li, J. Yu, W.-B. Tsai, *J. Mater. Sci.: Mater. Med.* **2012**, 23, 3015.
- [155] a) S. R. Iyer, N. Udpa, Y. X. Gao, *J. Biomed. Mater. Res. A* **2015**, 103, 1899; b) S. R. Iyer, N. Udpa, Y. Gao, *J. Biomed. Mater. Res. A* **2015**, 103, 1899.

- [156] a) A. Ito, M. Yamamoto, K. Ikeda, M. Sato, Y. Kawabe, M. Kamihira, *J. Biosci. Bioeng.* **2015**, *119*, 596; b) M. Sato, A. Ito, Y. Kawabe, E. Nagamori, M. Kamihira, *J. Biosci. Bioeng.* **2011**, *112*, 273.
- [157] A. Ito, Y. Yamamoto, M. Sato, K. Ikeda, M. Yamamoto, H. Fujita, E. Nagamori, Y. Kawabe, M. Kamihira, *Sci. Rep.-Uk* **2015**, *4*, 4781.
- [158] H. Kim, M.-C. Kim, H. H. Asada, *Sci. Rep.-Uk* **2019**, *9*, 2732.
- [159] a) I. C. Liao, J. B. Liu, N. Bursac, K. W. Leong, *Cell Mol. Bioeng.* **2008**, *1*, 133; b) A. Ito, M. Kamihira, *Prog. Mol. Biol. Transl.* **2011**, *104*, 355; c) J. Ramón-Azcón, S. Ahadian, M. Estili, X. Liang, S. Ostrovidov, H. Kaji, H. Shiku, M. Ramalingam, K. Nakajima, Y. Sakka, A. Khademhosseini, T. Matsue, *Adv. Mater.* **2013**, *25*, 4028; d) X. Zan, S. Feng, E. Balizan, Y. Lin, Q. Wang, *ACS Nano* **2013**, *7*, 8385; e) A. F. Quigley, J. M. Razal, M. Kita, R. Jalili, A. Gelmi, A. Penington, R. Ovalle-Robles, R. H. Baughman, G. M. Clark, G. G. Wallace, R. M. I. Kapsa, *Adv. Healthcare Mater.* **2012**, *1*, 801; f) Z.-M. Huang, Y. Z. Zhang, M. Kotaki, S. Ramakrishna, *Compos. Sci. Technol.* **2003**, *63*, 2223; g) I. Jun, S. Jeong, H. Shin, *Biomaterials* **2009**, *30*, 2038.
- [160] a) S. T. Cooper, A. L. Maxwell, E. Kizana, M. Ghoddsu, E. C. Hardeman, I. E. Alexander, D. G. Allen, K. N. North, *Cell Motility* **2004**, *58*, 200; b) L. Ricotti, A. Menciassi, *Biomed. Microdevices* **2012**, *14*, 987; c) A. W. Feinberg, A. Feigel, S. S. Shevkoplyas, S. Sheehy, G. M. Whitesides, K. K. Parker, *Science* **2007**, *317*, 1366.
- [161] H. Takahashi, T. Shimizu, T. Okano, *Sci. Rep.-Uk* **2018**, *8*, 13932.
- [162] a) J. Ge, K. Liu, W. Niu, M. Chen, M. Wang, Y. Xue, C. Gao, P. X. Ma, B. Lei, *Biomaterials* **2018**, *175*, 19; b) A. Grossi, A. H. Karlsson, M. A. Lawson, *Cell Biol. Int.* **2008**, *32*, 615.
- [163] R. Tognato, A. R. Armiento, V. Bonfrate, R. Levato, J. Malda, M. Alini, D. Eglin, G. Giancane, T. Serra, *Adv. Funct. Mater.* **2019**, *29*, 1804647.
- [164] a) S. Levenberg, J. Rouwkema, M. Macdonald, E. S. Garfein, D. S. Kohane, D. C. Darland, R. Marini, C. A. van Blitterswijk, R. C. Mulligan, P. A. D'Amore, R. Langer, *Nat. Biotechnol.* **2005**, *23*, 879; b) L. Perry, S. Landau, M. Y. Flugelman, S. Levenberg, *Commun. Biol.* **2018**, *1*, 161.
- [165] a) J. M. F. Martins, C. Fischer, A. Urzi, R. Vidal, S. Kunz, P. L. Ruffault, L. Kabuss, I. Hube, E. Gazzero, C. Birchmeier, S. Spuler, S. Sauer, M. Gouti, *Cell Stem Cell* **2020**, *26*, 172; b) C. R. Slater, *Int. J. Mol. Sci.* **2017**, *18*, 2183.
- [166] L. A. Moyle, E. Jacques, P. M. Gilbert, *Curr. Opin. Biomed. Eng.* **2020**, *16*, 9.
- [167] T. Hoffman, A. Khademhosseini, R. Langer, *Tissue Eng. Part A* **2019**, *25*, 679.
- [168] H. Rischer, G. R. Szilvay, K. M. Oksman-Caldentey, *Curr. Opin. Biotech.* **2020**, *61*, 128.
- [169] N. Stephens, L. Di Silvio, I. Dunsford, M. Ellis, A. Glencross, A. Sexton, *Trends Food Sci. Tech.* **2018**, *78*, 155.
- [170] M. Pandurangan, D. H. Kim, *Appl. Microbiol. Biot.* **2015**, *99*, 5391.
- [171] M. J. Post, *Ann. Ny. Acad. Sci.* **2014**, *1328*, 29.
- [172] a) A. Listrat, B. Leuret, I. Louveau, T. Astruc, M. Bonnet, L. Lefaucheur, J. Bugeon, *Inra. Prod. Anim.* **2015**, *28*, 125; b) L. A. MacQueen, C. G. Alver, C. O. Chantre, S. Ahn, L. Cera, G. M. Gonzalez, B. B. O'Connor, D. J. Drennan, M. M. Peters, S. E. Motta, J. F. Zimmerman, K. K. Parker, *NPJ Sci. Food* **2019**, *3*, 20.



**Claudia Mueller** received her Bioengineering Diploma from University of Bayreuth in 2018. She is currently a Ph.D. student at the Department of Biomaterials, University of Bayreuth, under the supervision of Dr. Sahar Salehi. Her research focuses on the application of bioprinting for bifabrication and engineering of skeletal muscle tissue.



**Mairon Trujillo Miranda** received his Bachelor's degree in biomedical engineering from Instituto Tecnológico Metropolitano (Colombia) in 2016 and Master's degree in Biofabrication from University of Bayreuth (Germany) in 2020. He is currently a Ph.D. student at University of Bayreuth (Germany) under the supervision of Prof. Leonid Ionov and his current research focuses on fibrous shape-morphing materials for fabrication of vascular networks.



**Michael Maier** is a Ph.D. student at the University of Melbourne, Australia. His current thesis focuses primarily on promoting the development and maturation of skeletal muscle tissues *in vitro* via the implementation of indirect magnetic forces.



**Daniel E. Heath** is a Senior Lecturer of Biomedical Engineering at the University of Melbourne. He completed his Ph.D. degree in chemical and biomolecular engineering at The Ohio State University in 2010. He then undertook postdoctoral research at the Singapore-MIT Alliance for Research and Technology (SMART) Centre and at MIT. He began as a Lecturer at the University of Melbourne in 2014. His lab focuses on the design of next-generation biomaterials, with a particular interest in blood contacting biomaterials and stem cell expansion.



**Andrea O'Connor**, FIChemE, is the Head of the Department of Biomedical Engineering and leads the Tissue Engineering Group at the University of Melbourne. Her research is focused on design, synthesis and fabrication of biomaterials, porous materials and antimicrobial nanomaterials. She is particularly interested in strategies for scale-up of tissue engineering including vascularization, and design of antimicrobial materials for medical implants. She collaborates with a range of hospitals, medical research institutes, and medical device companies to improve existing products, develop new devices and solve clinical problems.



**Sahar Salehi** is a leader of the research group "Biomaterials for Tissue Regeneration" at the Department of Biomaterials, University of Bayreuth (UBT), Germany. She received her Bachelor's and Master's degree in Materials Engineering and Ph.D. in Biomaterials. After her postdoc at Tohoku University, she established her research group at UBT. Her research is focused on biomaterials and micro/nanoengineering technologies for tissue engineering of musculoskeletal tissues and she is interested in engineering the tissue-like constructs with gradient structures.



Minerva Access is the Institutional Repository of The University of Melbourne

**Author/s:**

Mueller, C;Trujillo-Miranda, M;Maier, M;Heath, DE;O'Connor, AJ;Salehi, S

**Title:**

Effects of External Stimulators on Engineered Skeletal Muscle Tissue Maturation

**Date:**

2020-11-17

**Citation:**

Mueller, C., Trujillo-Miranda, M., Maier, M., Heath, D. E., O'Connor, A. J. & Salehi, S. (2020). Effects of External Stimulators on Engineered Skeletal Muscle Tissue Maturation. *ADVANCED MATERIALS INTERFACES*, 8 (1), <https://doi.org/10.1002/admi.202001167>.

**Persistent Link:**

<http://hdl.handle.net/11343/274069>

**License:**

[CC BY](#)